



Volume 9, Issue Suppl_1, June 2019
ISSN 2158-0510

IJB

International Journal

M

BIO MEDICINE

Abstracts

**from the Second Russian
International Conference "Cryo-
Electron Microscopy 2019:
Achievements and Prospects"**

June 2-5, 2019 • Moscow • Russia

www.ijbm.org

IJBM

International Journal of
BIOMEDICINE



ISSN 2158-0510

Available online at
www.ijbm.org

INTERNATIONAL JOURNAL OF BIOMEDICINE

Aims and Scope: *International Journal of Biomedicine (IJBM)* publishes peer-reviewed articles on the topics of basic, applied, and translational research on biology and medicine. Original research studies, reviews, hypotheses, editorial commentary, and special reports spanning the spectrum of human and experimental and tissue research will be considered. All research studies involving animals must have been conducted following animal welfare guidelines such as the National Institutes of Health (NIH) Guide for the Care and Use of Laboratory Animals, or equivalent documents. Studies involving human subjects or tissues must adhere to the Declaration of Helsinki and Title 45, US Code of Federal Regulations, Part 46, Protection of Human Subjects, and must have received approval of the appropriate institutional committee charged with oversight of human studies. Informed consent must be obtained.

International Journal of Biomedicine endorses and behaves in accordance with the codes of conduct and international standards established by the Committee on Publication Ethics (COPE).

International Journal of Biomedicine (ISSN 2158-0510) is published four times a year by International Medical Research and Development Corp. (IMRDC), 6308, 12 Avenue, Brooklyn, NY 11219 USA

Customer Service: International Journal of Biomedicine, 6308, 12 Avenue, Brooklyn, NY 11219 USA; Tel: 1-917-740-3053; E-mail: editor@ijbm.org

Photocopying and Permissions: Published papers appear electronically and are freely available from our website. Authors may also use their published .pdf's for any non-commercial use on their personal or non-commercial institution's website. Users are free to read, download, copy, print, search, or link to the full texts of these articles for any non-commercial purpose. Articles from IJBM website may be reproduced, in any media or format, or linked to for any commercial purpose, subject to a selected user license.

Notice: No responsibility is assumed by the Publisher, Corporation or Editors for any injury and/or damage to persons or property as a matter of products liability, negligence, or otherwise, or from any use or operation of any methods, products, instructions, or ideas contained in the material herein. Because of rapid advances in the medical and biological sciences, in particular, independent verification of diagnoses, drug dosages, and devices recommended should be made. Although all advertising material is expected to conform to ethical (medical) standards, inclusion in this publication does not constitute a guarantee or endorsement of the quality or value of such product or of the claims made of it by its manufacturer.

Manuscript Submission: Original works will be accepted with the understanding that they are contributed solely to the Journal, are not under review by another publication, and have not previously been published except in abstract form. Accepted manuscripts become the sole property of the Journal and may not be published elsewhere without the consent of the Journal. A form stating that the authors transfer all copyright ownership to the Journal will be sent from the Publisher when the manuscript is accepted; this form must be signed by all authors of the article. All manuscripts must be submitted through the International Journal of Biomedicine's online submission and review website. Authors who are unable to provide an electronic version or have other circumstances that prevent online submission must contact the Editorial Office prior to submission to discuss alternate options (editor@ijbm.org).

IJB M

INTERNATIONAL JOURNAL OF BIOMEDICINE

Editor-in-Chief
Marietta Eliseyeva
New York, USA

Founding Editor
Simon Edelstein
Detroit, MI, USA

EDITORIAL BOARD

Mary Ann Lila
*North Carolina State University
Kannapolis, NC, USA*

Ilya Raskin
*Rutgers University
New Brunswick, NJ, USA*

Yue Wang
*National Institute for Viral Disease
Control and Prevention, CCDC
Beijing, China*

Nigora Srojidinova
*National Center of Cardiology
Tashkent, Uzbekistan*

Dmitriy Labunskiy
*Lincoln University
Oakland, CA, USA*

Randy Lieberman
*Detroit Medical Center
Detroit, MI, USA*

Victoria Garib
*The Medical University of Vienna
Vienna, Austria*

Seung H. Kim
*Hanyang University Medical Center
Seoul, South Korea*

Alexander Dreval
*M. Vladimirsky Moscow Regional
Research Clinical Institute, Russia*

Shaoling Wu
*Qingdao University, Qingdao
Shandong, China*

Roy Beran
*Griffith University, Queensland
UNSW, Sydney, Australia*

Biao Xu
*Nanjing University
Nanjing, China*
Said Ismailov
*Republican Specialized Scientific-
Practical Medical Center of
Endocrinology, Tashkent, Uzbekistan*

Karunakaran Rohini
*AIMST University
Bedong, Malaysia*

Luka Tomašević
*University of Split
Split, Croatia*

Lev Zhivotovsky
*Vavilov Institute of General Genetics
Moscow, Russia*

Bhaskar Behera
*Agharkar Research Institute
Pune, India*

Srdan Poštić
*University School of Dental Medicine
Belgrade, Serbia*

Gayrat Kiyakbayev
*RUDN University
Moscow Russia*

Timur Melkumyan
*Tashkent State Dental Institute
Tashkent, Uzbekistan*

Hesham Abdel-Hady
*University of Mansoura
Mansoura, Egypt*

Nikolay Soroka
*Belarusian State Medical University
Minsk, Belarus*

Boris Mankovsky
*National Medical Academy for
Postgraduate Education
Kiev, Ukraine*

Tetsuya Sugiyama
*Nakano Eye Clinic
Nakagyo-ku, Kyoto, Japan*

Alireza Heidari
*California South University
Irvine, California, USA*

Rupert Fawdry
*University Hospitals of Coventry &
Warwickshire Coventry, UK*

Igor Kireev
*AN Belozersky Inst of Physico-Chemical
Biology, Moscow State University, Russia*

Sergey Popov
*Scientific Research Institute of
Cardiology, Tomsk, Russia*

Bruna Scaggiante
*University of Trieste
Trieste, Italy*

Igor Kvetnoy
*D.O. Ott Research Institute of Obstetrics
and Gynecology, St. Petersburg, Russia*

Editorial Staff

Paul Edelstein (*Managing Editor*)

Dmitriy Eliseyev (*Statistical Editor*)

Arita Muhaxhery (*Editorial Assistant*)

2017 NOBEL PRIZE IN CHEMISTRY

Jacques Dubochet
Joachim Frank
Richard Henderson

*"for developing cryo-electron microscopy for the high-resolution
structure determination of biomolecules in solution"*



IJB M

INTERNATIONAL JOURNAL OF BIOMEDICINE

www.ijbm.org

June 2019 - Volume 9, Issue Suppl_1

CONTENTS

Abstracts From the Second Russian International Conference "Cryo-electron microscopy 2019: achievements and prospects"

ORAL ABSTRACT PRESENTATIONS

Structure of Membrane Proteins	6
Structure and Functions of the Transcription and Translation Apparatus of the Cell	6
Molecular Organization of Cells and Organelles.....	7
Structure of Viruses and Chaperonins.....	9
Applications of Cryo-EM in Medicine	10
New Methods of Sample Preparation and Data Processing for Cryo-Electron Microscopy	12
Complex and Emerging Techniques in Structural Biology.....	13

POSTER ABSTRACT PRESENTATIONS

Structure of Membrane Proteins	16
Structure and Functions of the Transcription and Translation Apparatus of the Cell	22
Molecular Organization of Cells and Organelles.....	26
Structure of Viruses and Chaperonins.....	29
Applications of Cryo-EM in Medicine	31
New Methods of Sample Preparation and Data Processing for Cryo-Electron Microscopy	34
Complex and Emerging Techniques in Structural Biology.....	35

STRUCTURE OF MEMBRANE PROTEINS

OR-1

http://dx.doi.org/10.21103/IJBM.9.Suppl_1.OR1

NMR Spectroscopy: Alternative Method for Structural Studies of Highly Dynamic Membrane Proteins and Ion Channels

Mikhail Yu. Myshkin, Dmitrii S. Kulbatskii, Anton O. Chugunov, Atonina A. Berkut, Alexander S. Paramonov, Alexander A. Vassilevski, Ekaterina N. Lyukmanova, Zakhar O. Shenkarev
Shemyakin-Ovchinnikov Institute of Bioorganic Chemistry, Moscow, Russia

Background: Integral membrane proteins (IMPs) play key roles in a variety of biological processes essential for living cells and multicellular organisms. Despite the intensive studies, the molecular mechanisms of IMPs functioning are not very well established. IMPs frequently possess high-amplitude intramolecular mobility, which is essential for their function, but hampers structure-function studies. High-resolution NMR spectroscopy is complementary to crystallographic and electron microscopy methods and permits simultaneous characterization of the structure and dynamics of moderately sized (up to 30 kDa) IMPs.

Methods: First and second isolated voltage-sensing domains (VSD, ~150 a.a., four transmembrane helices, S1-S4) of human skeletal muscle sodium channel Nav1.4 were produced by cell-free expression. The structure, dynamics, and interaction of VSDs with gating modifier toxin Hm-3 (crab spider *Heriades mellotei*) were studied by heteronuclear ($^1\text{H}/^{13}\text{C}/^{15}\text{N}$) NMR spectroscopy.

Results: The VSDs samples demonstrated limited stability in lipid- and detergent-based membrane mimetics due to aggregation (half-life time ~24 h). Nevertheless, the use of combinatorial selective $^{13}\text{C},^{15}\text{N}$ -labeling permitted to assign ~50% of VSDs backbone. The secondary structure of VSDs showed similarity with the known structures of other K^+ and Na^+ channels. Paramagnetic relaxation enhancement and PELDOR EPR data obtained for the spin-labeled domains confirmed the native-like tertiary structure of isolated VSDs. ^{15}N relaxation data revealed significant mobility of both VSDs at ps-ns time scale. The instability of the domain structure associated with these motions is probably responsible for the observed protein aggregation. Hm-3 has similar affinities to both VSDs, but binds to the different sites on their surface. At VSD-I the toxin interacts with the S3-S4 extracellular loop forming salt bridges with conserved E208 and D211 residues, while at VSD-II the toxin binds to the S1-S2 extracellular loop interacting with E604 and D606 residues. In the both cases, the toxin binding to these charged groups probably inhibits voltage sensor transition to the activated state and blocks the channel opening.

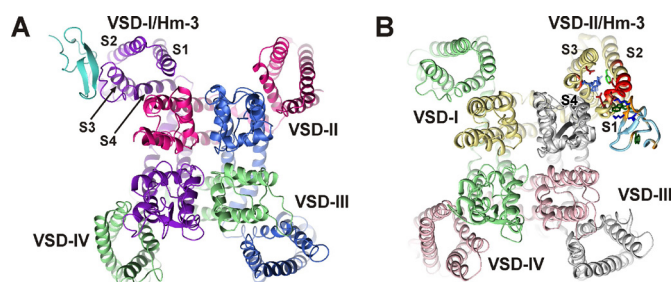


Fig. 1. Obtained models of Hm-3 complexes with Nav1.4 channel.

Conclusion: Obtained results validate the use of NMR spectroscopy for the ligand-receptor interactions in the conformationally flexible domains of ion channels.

Key Words: sodium channel, gating modifier, combinatorial selective labeling, ligand-receptor interactions

This work was supported by the Russian Science Foundation (Project № 16-14-10338).

STRUCTURE AND FUNCTIONS OF THE TRANSCRIPTION AND TRANSLATION APPARATUS OF THE CELL

OR-2

http://dx.doi.org/10.21103/IJBM.9.Suppl_1.OR2

Investigating Interaction of Pioneering Transcription Factors with Nucleosomes Using Cryo-Electron Microscopy

Svetlana Dodonova, Patrick Cramer

Max Planck Institute for Biophysical Chemistry, Göttingen, Germany

Background: Specific regulation of gene expression determines cellular life and fate. Hundreds of transcription factor proteins (TFs) play critical role in this process. Typically, TFs bind short DNA motifs and then alter expression of their target genes. Majority of cellular DNA is associated with histones, as nucleosomes and higher order arrays, which occlude binding of most TFs. Only a minority of TFs (the pioneering TFs) are able to bind compact chromatin, and thus play a major role in altering gene expression and changing developmental programs. For instance, Oct4, Sox2, Klf4, c-Myc are highly expressed in embryonic stem cells and are able to drive differentiated somatic cells into pluripotent state. A recent study systematically explored interactions between the nucleosome and 220 TFs, and showed that most TFs preferably bind free DNA, and very few are able to bind nucleosomes in vitro. This study has also provided a selection of DNA-templates selected for ability to form nucleosomes and promote binding of a TF of interest.

Results and Methods: Currently our mechanistic understanding of how pioneer TFs interact with chromatin is rather poor. Our structural knowledge in that area is limited to individual TFs or TFs bound to short DNA fragments. Thus, we aimed at structural characterization of pioneer TFs in the context of a nucleosome. We have formed a complex of a nucleosome on a DNA template from with a pioneer TF from purified individual components and have solved the structure by cryo-EM. We have confirmed the binding of a pioneer TF to the nucleosome by electrophoretic mobility shift assays.

Conclusions: We report the first structure of a nucleosome and a pioneer TF. Our structural and biochemical results illustrate a possible role of a pioneer TF in nucleosome destabilization and shed light on how such TFs can interact with chromatin.

Key Words: nucleosome, pioneer factors, cryo-EM.

OR-3

http://dx.doi.org/10.21103/IJBM.9.Suppl_1.OR3

Fleeting Ensembles: Transient Protein-Protein Interactions in DNA Repair

Dmitry O. Zharkov

Novosibirsk State University, Novosibirsk, Russia

Background: DNA repair is a vitally important process that protects the cell's genome from ongoing damage. Six DNA repair pathways are commonly outlined: direct reversal, base excision repair, nucleotide excision repair, mismatch repair, recombination repair, and non-homologous end joining. Of these, base excision repair that deals with small non-bulky lesions removes the greatest number of damaged nucleotides daily. Unlike many other cellular pathways, base excision repair is not carried out by multienzyme complexes but rather involves many DNA-mediated transient protein-protein interactions that pass the damaged DNA between consecutive participants of the pathway.

Methods: Direct structural characterization of such DNA substrate channeling remains elusive, and most of what is known about it was obtained through enzyme kinetics and modeling.

Results: DNA glycosylases, the enzymes that initiate base excision repair, are actively displaced from their enzyme-product complexes by abasic site (AP) endonucleases, the next enzyme in the pathway. Several accessory proteins, such as XRCC1, PCNA, and PARP1, guide the dynamic assembly and disassembly of DNA repair complexes providing regulatory modifications and scaffolding. Interestingly, eukaryotic and bacterial DNA repair proteins are often homologous but the eukaryotic proteins carry additional extended intrinsically disordered domains, which are believed either to be involved into dynamic protein-protein interactions or provide additional DNA-binding capabilities outside the well-defined DNA binding domains.

Conclusion: Overall, DNA repair, and especially base excision DNA repair, relies on extensive conformational rearrangements of the participating proteins, which is necessary both for damage recognition and for progress along the repair pathway. As such, they represent a promising target for studies with cryo-EM techniques.

Key Words: DNA damage, DNA repair, conformational ensembles, protein-protein interactions.

This work was supported by the Russian State Foundation (Grant 17-14-01190).

OR-4

http://dx.doi.org/10.21103/IJBM.9.Suppl_1.OR4

Molecular Mechanism of Antibiotics Inhibiting Prokaryotic Translation

Andrey Konevga^{1,2,3}, Evgeny Pichkur^{1,2,4}, Alena Paleskava^{2,3}, Pavel Kasatsky², Elena Maksimova², Daria Vinogradova², Yuri Polikanov⁵, Alexander Myasnikov^{2,6}

¹NRC "Kurchatov Institute", Moscow, Russia; ²NRC "Kurchatov Institute" - PNPI, Gatchina, Russia; ³Peter the Great St. Petersburg Polytechnic University, St. Petersburg, Russia; ⁴FSRC "Crystallography and Photonics", Moscow, Russia; ⁵Department of Biological Sciences, University of Illinois at Chicago, Chicago, USA; ⁶St. Jude Children's Research Hospital, Memphis, USA and Centre for Integrative Biology (CBI), IGBMC, CNRS, Inserm, Université de Strasbourg, Illkirch, France

Background: About 50% of antibiotics used in the therapy of infectious diseases target bacterial 70S ribosomes. High resolution X-ray crystallographic studies allow us for determination of position of drug on the ribosome, but to elucidate the detailed molecular mechanism of inhibition it is necessary to study the dynamics of

partial reactions of protein biosynthesis. Majority of high resolution structures were obtained on ribosomes from thermophilic bacteria *T. thermophilus*, whereas most of the functional studies were performed on reconstituted in vitro translation system from mesophilic organism *E. coli*. Despite of high homology among bacterial ribosomes, in many cases particular contacts observed are specific to thermophilic organism and is not allowing us to generalize the molecular mechanism of inhibition.

Methods: Functional ribosomal pre-translocation complexes containing deacylated tRNA^{fMet} in the P site and fMetPhe-tRNA^{Phe} or fMetVal-tRNA^{Val} in the A site were incubated with specific inhibitors: spectinomycin, amicoumacin, dirithromycin. Functional and structural studies were performed by using pre-steady state stopped-flow fluorescent spectroscopy and time-resolved cryo-electron microscopy. Kinetic studies of partial reactions of elongation were performed with thermophilic elongation factors and mesophilic reconstituted translation system.

Results: Combination of structural data and pre-steady state kinetics reveals the details of molecular mechanism of inhibition of EF-G catalysed translocation and shows the intermediate conformations of ribosome-tRNA complexes during forward translocation. Heterologous translation system with substituted thermophilic elongation factors allows for differential studies of elongation cycle.

Conclusion: Time-resolved high-resolution cryo-electron microscopy is a method of choice for structural characterization of active complexes in physiological conditions in the process of functioning. Reconstituted in vitro translation system from *E. coli* can be used both for structural and functional studies, allowing merging of two types of data for extensive characterization of bacterial protein synthesis apparatus.

Key Words: ribosome, antibiotics, structure, cryo-EM.

This work was supported by Russian Science Foundation Grant #17-14-01416. The authors acknowledge the support and the use of resources of the Resource Center for Probe and Electron Microscopy at the NRC "Kurchatov Institute".

MOLECULAR ORGANIZATION OF CELLS AND ORGANELLES

OR-5

http://dx.doi.org/10.21103/IJBM.9.Suppl_1.OR5

Prediction of Relaxed Conformations for Tubulin Dimers: From Cryo-Electron Microscopy to Molecular Dynamics

Vladimir A. Fedorov¹, Philipp S. Orekhov^{1,2}, Ekaterina G. Kholina¹, Ilya B. Kovalenko^{1,3,4}, Nikita B. Gudimchuk⁵

¹Department of Biology and ⁵Department of Physics, Lomonosov Moscow State University, Moscow, Russia; ²Moscow Institute of Physics and Technology, Dolgoprudny, Russia; ³Federal Research and Clinical Center of Specialized Medical Care and Medical Technologies, Federal Medical and Biological Agency of Russia, Moscow, Russia; ⁴Astrakhan State University, Astrakhan, Russia; ⁵Center for Theoretical Problems of Physicochemical Pharmacology, Russian Academy of Sciences, Moscow, Russia

Background: Tubulin microtubules are essential cytoskeletal filaments, with diverse and critical functions at all stages of the cell cycle. Tubulin dimers, which serve as main building blocks for microtubules, can self-assemble and disassemble, depending on the phosphorylation state of associated nucleotide. Tubulins bound to guanosine triphosphate (GTP) make stable microtubule lattice, but when the GTP molecules lose their γ -phosphates,

microtubules become prone to depolymerization. The relationship between tubulin conformation and GTP hydrolysis is still poorly understood. Recent progress in cryo-electron microscopy and related data analysis methods have brought new critical insights into the nucleotide-dependent structure of microtubule lattice (Alushin et al., Cell, 2014; Manka et al., Nat. Struct. Mol. Biol., 2018; Zhang et al., PNAS, 2018). However, supplementary methods are needed to bridge static cryo-electron microscopy-based structures with microtubule dynamic instability. Here we use all-atom molecular dynamics (MD) simulations to examine relaxed conformations and mechanical properties of tubulin dimers, extracted from cryo-electron microscopy-based tubulin structures of different generations. This analysis enables us to draw conclusions about the mechanism for microtubule dynamic instability.

Methods: Molecular models of straight GDP-bound tubulin and Mg-GTP-bound tubulin structures (dimers and tetramers) were based on 3j6f, 6dpv and 3j6e, 6dpu PDB structures of tubulin lattice (Alushin et al., Cell, 2014; Zhang et al., PNAS, 2018). 3j6e and 6dpu structures contained non-hydrolyzable GTP analog (GMPCPP) in the exchangeable site of β -tubulin. GMPCPP was converted into GTP by replacing the carbon atom between α - and β -phosphate with an oxygen atom, and the new bond lengths and angle relaxed to their equilibrium values during minimization. Simulations were performed using the GROMACS 5 software package, which allowed parallel computing on hybrid architecture, with the CHARMM27 force field (Abraham et al., SoftwareX, 2015). Parameters for MD-preparation and simulations were set according to our previous work (Fedorov et al., Supercomput. Front. Innov., 2018).

Results: Tubulins were extracted from cryo-electron microscopy-based structures of microtubule lattice and subjected to one-microsecond-long MD simulations. Overall, we carried out 12 MD simulation runs, covering total simulation time of six 6 microseconds for each nucleotide. Relaxed conformations of tubulins were twisted and non-radially bent at the intradimer interfaces, regardless of the bound nucleotide type. Both low (Alushin et al., Cell, 2014) and high (Manka et al., Nat. Struct. Mol. Biol., 2018) resolution cryo electron microscopy-based model structures converged to similar shapes, which closely resembled structures, obtained with X-ray crystallography method (Ravelli et al., Nature, 2004).

Conclusion: A combination of cryo-electron microscopy and molecular dynamics data suggest that the GTP hydrolysis does not change the conformation of the intradimer tubulin interface, implying that microtubule dynamic instability may rather be explained by the modulation of lateral bonds or interfaces between adjacent tubulin dimers.

Key Words: microtubules, tubulin, cryo-electron microscopy, conformation.

This work was supported by the Russian Science Foundation grant #17-74-20152 to N.G. The research was carried out using the equipment of the shared research facilities of HPC computing resources at Lomonosov Moscow State University.

OR-6

http://dx.doi.org/10.21103/IJBM.9.Suppl_1.OR6

Looking for an order in chaos: approaches to mapping chromosomal loci for cryo-EM studies

Igor I. Kireev, Amir N. Zakirov, Sophia Yu. Sosnovskaya, Olga S. Strelkova, Oxana A. Zhironkina

A.N.Belozersky Institute of Physico-chemical biology, Lomonosov Moscow State University, Moscow, Russia

Background: Chromatin higher order structure has been for decades a matter of debate, mainly due to its mesoscale nature, which precluded its accurate analysis by optical microscopy, while electron microscopy studies rendered controversial results reflecting highly dynamic and heterogeneous DNA folding prone to sample preparation artifacts. On the other hand, lack of adequate tools for nondestructive yet selective staining of DNA as a whole, and specific chromosomal loci in particular, added another layer of uncertainty to the fuzzy picture of how DNA is organized in the cell nucleus.

Methods: Here we propose an approach for specific labeling of endogenous chromosomal loci compatible with the direct visualization of DNA folding motifs at near native conditions by cryo-electron tomography. The approach is based on use of tagged DNA-binding proteins for mapping chromosomal loci, with subsequent introduction of Nanogold-conjugated ligands into the cell nuclei by microinjection (Fig.1).

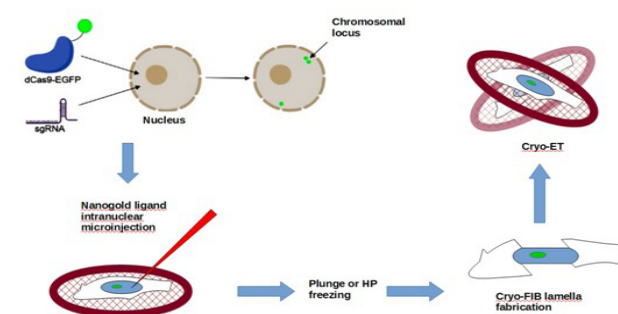


Fig.1. Flowchart of in vivo Nanogold labeling of endogenous chromosomal loci for cryo-ET.

Results: Our preliminary data demonstrated feasibility of above-mentioned approach with a set of DNA-binding tools (LacO-lac-rep system, TALEs, dCas) tagged with GFP, 6His and subsequent detection with anti-GFP antibodies, GBP, or Ni-NTA, conjugated with 1.4-nm gold. The passage to the cryo-ET would require further development of robust 3D-CLEM tools for location of target loci and lamella preparation with cryo-FIB.

Conclusion: A combination of nondestructive in vivo labeling of endogenous chromosomal loci with correlative cryo-FIB – cryo-ET would open new perspectives to our efforts to understand how genome is organized and functions in living cells.

Key Words: chromatin, in vivo gold labeling, cryo-ET

This work was supported by the Russian Science Foundation (grant #17-15-0129) and RFBR (grant #19-015-00273)

OR-7

http://dx.doi.org/10.21103/IJBM.9.Suppl_1.OR7

Condensation of Nucleoid in Bacteria as a Result of Starvation

Yurii Krupyanski¹, Natalia Loiko², Andrey Moiseenko³, Kseniya Tereshkina¹, Olga Sokolova³

¹Semenov Institute of Chemical Physics RAS, Moscow, Russia; ²FR Center "Fundamentals of Biotechnology" RAS, Moscow, Russia; ³Biological Faculty, Lomonosov Moscow State University, Moscow, Russia.

Background: Living organisms survive in constantly changing environmental conditions due to universal strategies of adaptation to various stresses based on structural, biochemical,

and genetic rearrangements. One of adaptive strategies utilized in bacterial cells involves the protection of the nucleoid from unfavorable factors via binding of DNA to specific histone-like proteins. This strategy leads to the condensation of DNA in complexes with Dps (DNA-binding protein from starved cells), which has been discovered in starved for up to 48 hrs cells of the *E. coli* bacterium

Methods: Electron microscopy and X-ray diffraction of synchrotron radiation studies were used to reveal distinct forms of nucleoid condensation in dormant *E. coli* cells that were starving for longer period – up to 7 months.

Results: We have found and described not only previously detected forms of nucleoid condensation: quasi-nanocrystalline, quasi-liquid crystalline and spore-like, but also observed a new type of nucleoid condensation in dormant cells - folded nucleosome-like.

Conclusion: According to the recognized concept of a bacterial population as a multicellular organism, their heterogeneity allows to respond flexibly to the environmental changes and to survive in stressful situations. Heterogeneity is the reason why we observed several types of nucleoid condensation in dormant *E. coli* cells. Heterogeneity of dormant cells increases the ability of the whole population to survive under various stress conditions. Results, observed here, shed a new light both on the phenomenon of nucleoid condensation in prokaryotic cells and on the general problem of developing a response to the stress.

Key Words: stress, nucleoid, condensation, structure.

Research was performed within frameworks of the state tasks for ICP RAS 0082-2014-0001 and 0104-2018-0029

OR-8

http://dx.doi.org/10.21103/IJBM.9.Suppl_1.OR8

High-Resolution Structures of Microtubule-Drug Complexes Revealed by Cryo-EM

Kushal Sejwal¹, Thorsten B. Blum^{1,2}, Joseph Atherton³, Ashwani Sharma¹, Natacha Olieric¹, Andrea E. Prota³, Carolyn A. Moores³, Michel O. Steinmetz^{1,2}

¹Laboratory of Biomolecular Research, Division of Biology and chemistry, Paul Scherrer Institut, Villigen, Switzerland;

²University of Basel, Biozentrum, Basel, Switzerland; ³Institute of Structural and Molecular Biology, Birkbeck, University of London, London, United Kingdom

Background: Microtubules are dynamic protein filaments that are crucial for cell division and constitute key elements of the cytoskeleton. They are assembled from $\alpha\beta$ -tubulin heterodimers that form hollow cylindrical structures. There is a large number of naturally occurring compounds that are known to interact with tubulin, including alkaloids, macrolides and peptides, which are collectively called microtubule-targeting agents (MTAs). Based on their activities, MTAs can be classified as microtubule-stabilizing agents (MSAs) that enhance MT assembly, and microtubule-destabilizing agents (MDAs) that suppress MT assembly. The chemical structure of these drugs and their binding mode to microtubules varies greatly amongst each other and confer the ability to act either synergistically or competitively on microtubules. Owing to their effects on microtubule dynamics, MTAs are of great interest and widely used in a variety of medical applications as antiparasitic agents, herbicides and, most importantly, as chemotherapeutic drugs used for the treatment of cancer.

In the past years, we and others solved the structures of a large number of different MTAs bound to tubulin to high resolution using X-ray crystallography. Very recently, however, with the advent of the “Resolution Revolution” in cryo-electron microscopy (cryo-EM), atomic structures of known MSAs bound to microtubules have also been obtained. These cryo-EM structures confirmed that the sites and modes of binding described in the previous X-ray crystallographic studies are similar in the context of the assembled microtubule but additionally explain the effects of MTAs on lattice parameters in microtubules and the lateral contacts between protofilaments, especially at the microtubule seam.

Methods: Cryo-EM and model building.

Results: We solved several high-resolution structures of microtubules bound to novel MSAs and identified differential binding modes in comparison to that revealed by X-ray crystallography.

Conclusion: Cryo-EM and X-ray crystallography can be used in a complementary manner to investigate the molecular mechanism of action of MSAs in detail.

Key Words: cryo-EM, microtubule, microtubule-stabilizing agents.

STRUCTURE OF VIRUSES AND CHAPERONINS

OR-9

http://dx.doi.org/10.21103/IJBM.9.Suppl_1.OR9

Cryo-Electron Microscopy Studies of Flaviviruses

Victor A. Kostyuchenko, Guntur Fibriansah, Shuijun Zhang, Thiam-Seng Ng, Shee-Mei Lok

Virus structure and function group, Program in Emerging Infectious Diseases, Duke-NUS Medical School, Singapore

Background: Flaviviruses cause human disease such as dengue fever, West Nile fever, and Zika fever with high degree of severity. There are almost no licensed vaccines and treatment except symptomatic for these diseases. Our group studies the virus structure and interactions with ligands such as receptors and antibodies in order to understand the virus' life cycle with the aim to find possible preventive or curative drugs.

Methods: For structural biology work, we employ mostly cryo-EM such as single particle analysis and cryo-electron tomography to study complexes of the virus with antibody fragments.

Results: We obtained subnanometer and near-atomic resolution cryo-EM structures for immature and mature forms of dengue virus serotype 1, dengue virus serotype 4, and Zika virus. We described a possible maturation pathway based on the higher resolution structures. We also described a temperature-dependent structural change that occurs in some strains of the flaviviruses, important for vaccine development. In addition, we described a cryo-EM structure of a complex of a dengue virus and antibody fragment that demonstrates that in some cases cryo-EM is superior to X-ray crystallography as providing a fuller picture of the virus and antibody interaction.

Conclusion: Modern cryo-EM allows us a better and more detailed look at the viruses, their life cycle and help the development of a better vaccines and therapeutics.

Key Words: Dengue virus, Zika virus, Flavivirus, Cryo-EM

This work was supported by grants from Singapore Ministry of Education and National Medical Research Council to Prof. Lok

OR-10

http://dx.doi.org/10.21103/IJBM.9.Suppl_1.OR10

The Structure of Human Echovirus 30

Liya Mukhamedova, Tibor Füzik, David Buchta, Pavel Plevka

CEITEC, Masaryk University, Brno, Czech Republic

Background: Human Echovirus 30 (E30) is one of the most frequently isolated Enteroviruses in temperate climates. E30 affects the central nervous system, causing aseptic meningitis, encephalitis in newborns and immunocompromised hosts. Last year EU/EEA public health institutes observed an upsurge in the number of positive enterovirus detections, including E30 cases. The strain - E30 Bastianni shows distinct infection progress. It infects epithelial cells of human choroid plexus leading to alteration of its barrier function. The virus is able to disrupt the contacts between the brain choroid plexus cells and can rapidly replicate and transmit among the host cells.

Method: We solved the structure of E30 strain Bastianni virion with the resolution of 3,5 Å.

Results: The particle is built from three major capsid proteins VP1-VP3 and genome, packed inside of the capsid. The VP4 – minor capsid protein was not detected and the 54 residues of N-terminus of the VP1 subunit also lack on the electron density map. Such organization of a capsid is typical for the A-particle - the genome release intermediate state. Together with the A-particle, virions missing one pentamer were detected. Similar particles were observed for Echovirus 18. This discovery enabled to propose a novel genome release mechanism for enteroviruses, where opening of the capsid with the release of one or few pentamers enables genome release without the need to unwind its putative double-stranded RNA segments.

Conclusion: Obtaining detailed information about both the structure and the infection process of the Echovirus 30 may facilitate the development of new antiviral compounds and prevent its outbreaks worldwide.

Key Words: CryoTEM, Single-particle reconstruction, Picornavirus infections

OR-11

http://dx.doi.org/10.21103/IJBM.9.Suppl_1.OR11

Conformations of a viral chaperonin in different nucleotide-bound states

Tatiana B. Stanishneva-Konovalova¹, Pavel I. Semenyuk¹, Evgeny B. Pichkur², Lidia P. Kurochkina¹, Olga S. Sokolova¹

¹Lomonosov Moscow State University, Moscow, Russia;

²National Research Center "Kurchatov Institute", Moscow, Russia

Background: Chaperonins are protein complexes which assist nascent or misfolded proteins in attaining their native conformation. Several viral chaperonins have recently been found in the genomes of bacteriophages. In this study cryo-EM structures of a viral chaperonin from the phage OBP in different nucleotide-bound states were obtained.

Methods: The recombinant OBP chaperonin was expressed in *E. coli* and purified using chromatography on Q-sepharose. Chaperonin complexes with nucleotides were vitrified in Vitrobot Mark IV (FEI). Images were collected in cryo-

TEM Titan Krios (Thermo-Fisher) equipped with Schottky FEG electron source and direct electron detector Falcon II. Image processing and model generation was performed using Warp, CryoSPARC and Relion.

Results: 4.5-Å-resolution structure of the apo-form of the OBP chaperonin is a single ring composed of 7 identical subunits with a surprising degree of asymmetry at the upper part of the complex. Because of two sets of nucleotide-binding sites in chaperonin revealed by isothermal titration calorimetry, there are two structurally different subunit conformations. Therefore, subunits are arranged in the ring into three pairs stabilized by a number of salt bridges. The unpaired subunit lacks these contacts, which leads to a higher mobility and the fact that its intermediate and apical domains were not resolved in our reconstruction.

To study the effects of nucleotide binding on the OBP conformations, we obtained reconstructions at 4-6 Å of the OBP with ADP, ATPγS (a non-hydrolysable ATP analogue) and ATP. In the case of ATPγS, the conformation was the same as for the ADP-bound chaperonin. In all these structures only one or two pairs of subunits were resolved above the intermediate domains, which indicates that nucleotide binding results in the partial breakage of inter-subunit salt bridges and a higher structural mobility. Importantly, none of the tested nucleotides cause rotation of the apical domains typical for GroEL. The rotation, which provides cis/trans switching in GroEL, is enabled by the "hinge" residues, Gly192 and Gly375, between the intermediate and apical domains. In the OBP chaperonin they are replaced by the large polar residues Glu191 and Asn376 thus fixing the position of the apical domains relative to intermediate.

Conclusion: Phage OBP chaperonin possesses a unique asymmetric single-ring structure and a different ATP-dependent protein folding cycle compared to its presumable ancestor GroEL.

Key Words: chaperonin, phage OBP, cryo-EM

This work was supported by RFBR grants #19-04-00605 (to O.S.S.) and #18-04-01281 (to L.P.K.) and RSF grant #18-41-06001 (in part of the cryo-EM data processing). The authors acknowledge the support and the use of resources of the Resource Center for Probe and Electron Microscopy at the NRC "Kurchatov Institute".

APPLICATIONS OF CRYO-EM IN MEDICINE

OR-12

http://dx.doi.org/10.21103/IJBM.9.Suppl_1.OR12

Cryo-EM of Human and Parasite Proteasomes for Structure-Based Drug Design

Pavel Afanasyev¹, Euna Yoo², Matthew Bogoy^{2,3}, Paula C.A. da Fonseca¹

¹MRC Laboratory of Molecular Biology, Cambridge, UK;

²Department of Pathology and ³Department of Microbiology and Immunology, Stanford University School of Medicine, Stanford, USA

Background: The increasing spread of *Plasmodium falciparum* resistance to current antimalarials, including the frontline artemisinin and its derivatives, represents a major global threat to human health and urges the development of novel medicaments. For many years, proteasomal inhibition by specific chemical compounds has been considered for use

in medicine. Using cryo-electron microscopy (cryo-EM), we previously demonstrated functional and structural differences between the human and the *Plasmodium* proteasomes that are sufficient to allow specific inhibition, particularly by the vinyl sulfone compound WLW-vs (H. Li, et al. Nature 530(7589): 233-236 2016). However, a detailed description of the molecular basis for the parasite proteasome specific targeting is still missing.

Methods and Results: Here we present a structural cryo-EM analysis of the *Plasmodium* 20S proteasome in the presence of the novel EY-3-123 *Plasmodium* proteasome inhibitor (compound 21 in E. Yoo, et al. J. Am. Chem. Soc. 140, 36, 11424-11437 (2018)). This compound has been shown to be the most potent *Plasmodium* specific inhibitor within a library of novel vinyl-sulfone compounds. Single-particle analysis of this sample by extensive image classification allowed solving two high resolution proteasome structures, at about 3 Å, corresponding to *Plasmodium* and human complexes with inhibitor bound. Direct comparison of the active sites in these proteasome structures reveals the molecular basis for the *Plasmodium* proteasome specific inhibition.

Conclusion: The new structural information can be directly used for further development of proteasome inhibitors as potential antimalarials. This work demonstrates the high potential of cryo-EM in modern structure-based drug design.

Key words: proteasome inhibition, cryo-EM, *Plasmodium falciparum*, structure-based drug design

OR-13

http://dx.doi.org/10.21103/IJBM.9.Suppl_1.OR13

Functional and structural studies on human ASCT2 transporter — a promising drug target

Albert Guskov^{1,2}, Alisa Garaeva¹, Cornelius Gati³, Cristina Paulino¹, Dirk Slotboom¹

¹Groningen Biomolecular Sciences and Biotechnology Institute, University of Groningen, the Netherlands; ²Moscow Institute of Physics and Technology, Dolgoprudny, Russia; ³Stanford University, Department of Structural Biology, Stanford, CA, USA

Background: ASCT2 protein belongs to Solute Carrier Family 1 (SLC1A) transporters and is a promising target for the development of anticancer and antiretroviral drugs. It is upregulated and linked to poor survival in melanoma, lung, breast, prostate, pancreatic, thyroid and colon cancer and serves as a receptor for simian retrovirus 4, feline endogenous virus, human endogenous retrovirus type W and baboon M7 endogenous virus. However, there is a lack of structural and functional characterization of this protein.

Methods: We used single particle cryo-electron microscopy to obtain three-dimensional models of ASCT2 in two distinct conformations – inward-occluded and inward-open at resolutions of 3.85 and 3.6 Å respectively.

Results: The structural comparison of ASCT2 in inward-occluded and inward-open states revealed the different positions of mobile HP2 loop. It has moved 8 Å away from the substrate binding site towards the scaffold domain, thus allowing direct access to the binding site from the cytoplasm. Apart from that the conformation of the transport domain is very similar in both structures, however in the inward-open state it is slightly further tilted towards the cytoplasm, away from the scaffold domain.

The analysis of densities revealed possible positions of several lipids / cholesterol molecules. The most peculiar position is at the HP1 / HP2 interface, where a lipid could play a regulatory role of the loop closure / opening. Other positions are between the scaffold and transport domains; intriguingly one such position coincides well with the previously described allosteric inhibitor binding site in EAAT1 transporter.

Conclusion: The reported structures of an inward-open state of ASCT2 transporter confirmed an earlier hypothesis of one-gate elevator mechanism, which is different from any other secondary-active transport mechanism described to date. The observed several lipid densities in the vicinity of the binding site and around scaffold might represent potential inhibitor sites for rational drug design.

Key Words: cryo-EM, membrane proteins, SLC1A transporters, cancer, retroviruses

OR-14

http://dx.doi.org/10.21103/IJBM.9.Suppl_1.OR14

Fibril structure and interface polymorphism of amyloid-β(1-42)

Gunnar F. Schröder

Forschungszentrum Jülich, Jülich, Germany

Background: Amyloids are associated with many diseases. The recent breakthrough in the cryo-EM technique has made it possible to study the structure of amyloid fibrils by cryo-EM to high resolution. The technique will be introduced and applications to different amyloid structures presented, in particular the structure of the amyloid-β fibril (Aβ1-42), which is involved in Alzheimer's disease. Furthermore, new image processing methods will be presented to reconstruct macromolecular motions from single-particle image data.

Methods: Single-particle cryo-EM was used to determine helical reconstructions of different fibrillar structures. Furthermore, an approach is presented to determine the principal motions of macromolecules from single-particle data.

Typical classification methods aim for maximizing density differences between different models. However, density variance is not the same as conformational variance (i.e. variance of atomic model coordinates), and for interpreting molecular motions, conformational variance is most relevant. We present an approach to determine this conformational variance.

Results: The structure of an amyloid-β fibril (Aβ1-42) and polymorphs of it were determined. In addition, the structure of an SH3 amyloid fibril is presented, which has been extensively studied as a model system for amyloid formation.

Conclusion: Cryo-EM reveals high-resolution structural details of amyloid fibrils.

Key Words: amyloid fibrils, helical reconstruction, Alzheimer disease

OR-15

http://dx.doi.org/10.21103/IJBM.9.Suppl_1.OR15

Structural and functional studies of the *Staphylococcus aureus* ribosome hibernation

Konstantin Usachev¹, Iskander Khusainov^{1,2}, Bulat Fatkhullin^{1,3}, Shamil Validov¹, Marat Yusupov^{1,2}

¹Institute of Fundamental Medicine and Biology, Kazan Federal University, Kazan, Russia; ²Institut de Génétique et de Biologie Moléculaire et Cellulaire, Université de Strasbourg, Illkirch, France; ³Institute of Protein Research, Russian Academy of Sciences, Puschino, Russian Federation

Background: In bacteria, diminishing of protein synthesis is often accompanied with the formation of ribosomal dimers (or disomes). This process might be particularly important for pathogenic bacteria whose successful survival is a key factor for successful infection. Ribosome hibernation is driven by the binding of small stress-induced protein(s) to 70S ribosomes forming stable 100S ribosomal dimers. In contrast with *E. coli* where ribosome dimerization occurs in the presence of two proteins: hibernation promoting factor (HPF, 95 aa residues) and ribosome modulation factor (RMF, 55 aa residues) in *Staphylococcus aureus* only one protein (long version of HPF) is responsible for the formation of hibernating ribosome dimers, which in turn play a role in survival of this pathogen under unfavorable conditions.

Methods: By cryo-electron microscopy we obtained a high-resolution structure of the 100S ribosome dimer and by NMR spectroscopy and X-ray crystallography solved a NTD and CTD of SaHPF protein structures.

Results: Our recent cryo-EM studies demonstrated that integrity of 100S disomes is maintained primarily by interactions between C-terminal domains (CTD) of SaHPF with each other. N-terminal domain (NTD) of SaHPF binds to the 30S subunit at the P-site and A-site and may inhibit protein synthesis as observed for shorter variants of HPF in other species. By NMR spectroscopy we have determined the solution structure of SaHPF-NTD and analyzed its binding with *S. aureus* 70S ribosome.

Conclusion: Based on NMR and crystal structures of SaHPF-CTD we predicted the key amino acids residues stabilizing dimer interface and made several single amino acid substitutions which allows us to abolish the ribosome hibernation. Obtained information about crucial for dimerization residues in long HPF may be used as a potential target for combating *S. aureus*.

Key Words: ribosome, translation, hibernation, NMR

NEW METHODS OF SAMPLE PREPARATION AND DATA PROCESSING FOR CRYO-ELECTRON MICROSCOPY

OR-16

http://dx.doi.org/10.21103/IJBM.9.Suppl_1.OR16

High resolution cryo-electron microscopy and new direct electron detector from Gatan - K3

Alexander Myasnikov^{1,3,4,5}, Shawn Zheng¹, David Bulkley¹, Yifan Cheng^{1,2}, David Agard^{1,2}

¹Department of Biochemistry and Biophysics, University of California San Francisco, USA; ²Howard Hughes Medical Institute, University of California San Francisco, CA, USA; ³Department of Structural Biology, St. Jude Children's Research Hospital, Memphis, USA; ⁴Centre for Integrative Biology (CBI), Department of Integrated Structural Biology, IGBMC, CNRS, Inserm, Université de Strasbourg, Illkirch, France; ⁵Petersburg Nuclear Physics Institute named by B.P. Konstantinov of NRC "Kurchatov Institute", Gatchina, Russia

Background: Much of the success of modern cryo-Electron microscopy is the result of advances in electron

detector, specifically the advent of direct electron detectors [Kuhlbrandt, 2014, Biochemistry]. Of particular utility has been the Gatan K2 camera that was the first camera to provide single electron detection at practical dose rates, resulting in dramatic improvements in DQE and reduction in noise. The K2 also introduced the concept of super-resolution where the electrons can be registered to sub-pixel resolution. Despite the very high internal readout rate of the K2 camera (400 frames/sec), electron coincidence loss reduces DQE at doses above 3-5 e-/pixel/second, requiring prolonged exposures [Li, 2013, J Struct Biol]. The high frame rate does not only increase the DQE, but also allows to correct for beam-induced sample motion by making an alignment of the individual frames before averaging [Li, 2013, Nat Methods], [Zheng, 2017, Nat Methods].

Results: Here at UCSF Mission Bay, we have the opportunity to make some tests on a prototype of the K3, the next generation CMOS camera from Gatan. This camera increases the pixel count from 14Mpixels to 24 megapixels (5,760×4,092), resulting in a significantly increased field of view (1.6 X). Moreover, it also has a much higher internal readout rate, reducing both coincidence losses and exposure. Together, these promise to substantially improve data collection throughput. The performance and our initial experiences with this new camera will be described during the presentation.

Key Words: cryo electron microscopy (cryo-EM), CMOS detectors, high resolution

OR-17

http://dx.doi.org/10.21103/IJBM.9.Suppl_1.OR17

High resolution studies of biocomplexes by cryo-electron microscopy, basis for high throughput studies

Elena Orlova

Institute of Structural and Molecular Biology, University College London and Birkbeck, London, UK

Background: The last decade has witnessed an extremely impressive rise in the role of cryo-electron microscopy (cryo-EM) for structural studies of biocomplexes. For many years, EM was not considered as a structural method and was mainly used for visualisation of shapes of large biocomplexes or organelles in cells. However, the decades of laborious efforts of many scientists to fulfil theoretical promises in usage of electrons for imaging of biological molecules at the level of atomic resolution were not in vain and the best representatives of the EM community were recognised in 2017 by the Nobel prize awarded to J. Dubochet, J. Frank, and R. Henderson (Henderson R. Angew Chem Int Ed Engl. 2018 Aug 20;57(34):10804-10825. doi: 10.1002/anie.201802731; Dubochet J. Angew Chem Int Ed Engl. 2018 Aug 20;57(34):10842-10846. doi: 10.1002/anie.201804280. Frank J. Angew Chem Int Ed Engl. 2018 Aug 20;57(34):10826-10841. doi: 10.1002/anie.201802770).

Methods: Cryo electron microscopy, cryo sample preparations, direct detectors, computational methods (Dubochet J. 2012 Mar;245(3):221-4; McMullan G, Faruqi AR, Henderson R. Methods Enzymol. 2016;579:1-17. doi: 10.1016/bs.mie.2016.05.056; Kaledhonkar S, Fu Z, White H, Frank J. Methods Mol Biol. 2018;1764:59-71. doi: 10.1007/978-1-4939-7759-84),

Results: The last five years in EM were manifested by crucial technical advances in micro technology, improving the electron sources and systems for digital registration of images. It is important to acknowledge the role of improvements in sample preparation where they allowed the retrieval of high-resolution structural information from two-dimensional images. The progress in technology was accompanied by the development of mathematical approaches describing image formation in microscopes, algorithms for the fast and efficient processing of recorded images and automation of processing, where subsequent analysis facilitated the determination of structures at near-atomic resolution. During the last years success of cryo EM was highlighted by a large number of structures resolved at a resolution better than 4Å, where one can recognise the interface of protein-protein interactions, reveal different conformations of complexes and understand their function through their dynamic properties, and now we witness new achievements such as structures at a resolution better as 2 Å.

Now we need to fully automate the data collection on electron microscopes, increase the dimensions of digital detectors (whilst reducing at the same time the sizes of individual sensors) and to get powerful computers that will allow us to do statistical analysis of data to distinguish variations in structures. The next important step would be to resolve functional changes of complexes in time.

Key Words: cryo-EM, biological complexes, structure, image processing

OR-18

http://dx.doi.org/10.21103/IJBM.9.Suppl_1.OR18

Entry of Hantavirus into the innate immune cell

Natalia. G. Plekhova¹, Evgeniy. V. Pustovalov²

¹Pacific State Medical University, Vladivostok, Russia; ²Far Eastern Federal University. Vladivostok, Russia

Background: Hantaviruses cause hemorrhagic fever with renal syndrome and hantavirus cardiopulmonary syndrome, which infects more than 200,000 people worldwide with case fatality ratios of 30%–40%. There are no specific therapies or vaccines for these diseases. Hantaviruses (HV) are enveloped, negative-strand RNA viruses of the family Bunyaviridae. Monocytes/macrophages have an important role in the spread of virus from the primary site of infection. However, the site and detailed mechanism of entry of HV in cells have not yet been defined. Therefore, this study focused on the entry of the pathogenic hantaviruses Hantaan into African green monkey kidney epithelial cells (Vero E6) and macrophages.

Methods: The cellular culture Vero E6, the human monocytic cell line THP-1, obtained from the Korean Cell Line Bank (KCLB) (Seoul, Korea) and cells of mice peritoneal exudate were used. The extracellular liquid of infected culture Vero E6 by strain pathogenic virus Hantaan PM-T79-95 included not less 100 infectious units on the macrophage was used. Mouse monoclonal [5E11] to HV nucleocapsid protein and caveolin-1 (Abcam, USA) at 1:200 dilution were used for immunohistochemical detection of localization in macrophages. Goat polyclonal Anti-Mouse IgG H&L (10 nm Gold) and Alexa Fluor® 488 (Abcam, USA) were used as secondary antibodies. Thin sections were examined in Jeol 100 S electron microscope. Series of optical sections were taken with a confocal scanning

laser microscope LSM510META (Carl Zeiss, Germany). JEOL 100S, transmission electron microscopy, was used to obtain the images, which were acquired at 50,000X magnification.

Results: Using electron microscopy, we found that during the first 5 min of contact, the HV penetrates into the cytoplasm of macrophages by fusing with the plasma membrane. During this process, loosening and thickening of HV supercapsid were noted. The viruses with morphological signs deproteinization of the genome were predominantly detected in the perinuclear space of macrophage cytoplasm, as well as near the cisterns of the granular endoplasmic reticulum (2-3 hours of incubation). The space between the shell and the dense osmiophilic nucleoid, the thinning of the shell and an increase of viral size due to the nucleoid loosening and was determined. At the same time, the number of HV antigen-positive cells was noted minimum. The multichannel scanning of infected cells determined the co-localization HV-antigen and caveolin 1 positive sites. A significant difference of the indicators intensity fluorescence at the sites of co-localization was definitude.

Conclusion: Thus, during the penetration into macrophages HV use the plasma membrane fusion mechanism associated with caveolin 1. In addition to this caveolin mediated endocytosis the HV can also penetrate in another way, which is the aim of further studies.

Key Words: Hantavirus, macrophages, ultrastructure, electron microscope

COMPLEX AND EMERGING TECHNIQUES IN STRUCTURAL BIOLOGY

OR-19

http://dx.doi.org/10.21103/IJBM.9.Suppl_1.OR19

Integrative approach on nucleosome complexes modeling

Grigoriy A. Armeev¹, Anna Panchenko², Alexey K. Shaytan¹

¹Faculty of Biology, Lomonosov Moscow State University, Moscow, Russia; ²National Institutes of Health, National Center for Biotechnology Information, Moscow, Russia

Background: Nucleosomes are the key structural elements of chromatin in all higher organisms. While X-ray crystallography studies of nucleosomes have consistently yielded similar atomistic structures, many biophysical and biochemical techniques suggest that nucleosomes and nucleosome complexes exhibit substantial conformational polymorphism, which is functionally important. The interpretation of such experimental data with such sufficient details is often a tedious task, thus a set of molecular modeling tools is required.

Methods: We performed full-atom molecular dynamics of nucleosomes and DNA fluorescent labels to sample the conformations used for single particle Förster Resonance Energy Transfer (spFRET) measurements. We developed an approach for donor and acceptor quantum yield estimation, during spFRET measurements in a single laser excitation setup. We also implemented a set of methods for the integrative modeling of nucleosome structures based on spFRET constraints.

Results: Using these approaches, we have constructed atomistic models of nucleosomes structural reorganization induced by histone chaperones or histone H1. Besides the distances derived from corrected spFRET efficiencies, histone - DNA contacts are crucial for nucleosome formation and function. We used hydroxyl DNA footprinting data, in conjunction with atomistic structures

of nucleosomes enhanced by molecular dynamics simulations, to develop a computational method for the precise determination of DNA positioning in nucleosomes with single base pair resolution.

Conclusion: We have developed a set of techniques for chromatin modeling on the nucleosomal level. Such approaches tightly integrate various experimental data (mainly corrected spFRET efficiencies and hydroxyl DNA footprints) into molecular modeling pipelines.

Key Words: nucleosome, chromatin, integrative modeling

The part of this work involving spFRET measurements and modeling was supported by the Russian Science Foundation grant #19-74-30003 and the part involving hydroxyl DNA footprinting was supported by the Intramural research program of the national library of medicine, NIH.

OR-20

http://dx.doi.org/10.21103/IJBM.9.Suppl_1.OR20

Visualization of exosomes using transmission electron microscopy and immunogold labelling

Dmitry Bagrov, Anna Vnukova, Evgeniy Evtushenko, Svetlana Semina

Faculty of Biology, Lomonosov Moscow State University, Moscow, Russian Federation

Background: Extracellular vesicles are small membrane particles which are produced by the cells and released into the surrounding space. They can transfer biomolecules into recipient cells. The typical vesicle size is 100-1000 nm, so transmission electron microscopy (TEM) is the most suitable tool for their visualization. This is especially true for the smallest vesicles – the exosomes with the size below 200 nm.

Methods: We isolated exosomes produced by MCF-7 cancer cells and the two drug-resistant MCF-7 sublines (Semina et.al., *Molecules*, 2018). The exosomes were isolated from the conditioned medium by ultracentrifugation, and their size was measured by nanotracking analysis (NTA) and TEM. Immunogold labelling was carried out on exosomes deposited onto carbon TEM grids. It involved the following principal steps: the vesicle deposition, sample treatment by the anti-CD9 antibodies, sample treatment by the 10 nm colloidal gold nanoparticles conjugated with protein A, staining with uranyl acetate. Washing and blocking steps were done between the principal ones. The samples were imaged using a JEM-1011 microscope at 80 kV.

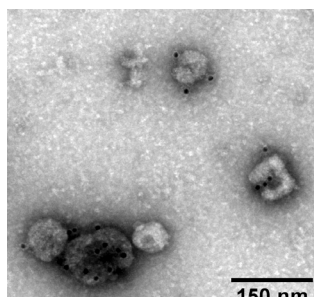


Fig. 1. Exosomes produced by the MCF-7 cells, labelled with colloidal gold.

Results: NTA and TEM yielded similar results – the exosomes produced by the three studied cell lines had the almost equal size in the range from 50 to 200 nm. When

imaged by TEM, most exosomes demonstrated the typical cup-shaped morphology. We used immunogold labelling to verify that the exosomes carried the CD9 marker on them (Fig. 1). We achieved the labelling specificity in the range of 8-10; this value was calculated as the ratio of the surface densities of the exosome-bound labels (colloidal gold nanoparticles) and the non-specific background ones.

Conclusion: We hope that the sample preparation and imaging procedures that we used could be useful for the investigation of other extracellular vesicles.

Key Words: exosomes, nanotracking analysis, transmission electron microscopy, immunogold labelling

The TEM measurements were performed at the User Facilities Center “Electron microscopy in life sciences” at Lomonosov Moscow State University. The work was supported by RFBR (project 18-504-12045).

OR-21

http://dx.doi.org/10.21103/IJBM.9.Suppl_1.OR21

3D structure of the natural tetrameric form of human butyrylcholinesterase as revealed by cryo-EM, MD and SAXS

Konstantin M. Boyko¹, Timur N. Baymukhametov², Yury M. Chesnokov², Michael Hons³, Sofya V. Lushchekina⁴, Alexey V. Lipkin¹, Vladimir O. Popov^{1,2}, Michail V. Kovalchuk²

¹Bach Institute of Biochemistry, Research Center of Biotechnology of the Russian Academy of Sciences, Moscow, Russia; ²National Research Center «Kurchatov Institute», Moscow, Russia; ³EMBL Grenoble, Grenoble, France; ⁴Emanuel Institute of Biochemical Physics, Russian Academy of Sciences, Moscow, Russian Federation

Background: Human plasma butyrylcholinesterase (hBChE, EC 3.1.1.8) is an endogenous bioscavenger that hydrolyzes numerous medicamentous and poisonous esters and scavenges potent organophosphorus nerve agents. Thus, the hBChE can be used to protect acetylcholinesterase as well as a marker for diagnosis of OP poisoning. It is also considered as a therapeutic target against Alzheimer's disease. Though the X-ray structure of a partially deglycosylated monomer of human hBChE was solved 15 years ago, all attempts to determine the 3D structure of the natural full-length glycosylated tetrameric human hBChE were unsuccessful so far.

Methods: A combination of three complementary structural methods – single particle cryo-electron microscopy, molecular dynamic simulations and small-angle X-ray scattering were implemented to elucidate the overall structural and spatial organization of the natural tetrameric human plasma hBChE.

Results: A 7.6 Å cryo-EM map clearly shows the structural organization of the enzyme: a dimer of dimers with a non-planar monomer arrangement in which the interconnecting super helix complex PRAD-(WAT)4-peptide C-terminal tail is located in the center of the tetramer, nearly perpendicular to its plane and deeply plunged between the four subunits. Time-averaged molecular dynamics trajectories allowed to optimize the geometry of the molecule and to reconstruct structural features obscured in the cryoEM density, e.g glycan chains and glycan inter-dimer contact areas as well as inter-monomer disulfide bridges at the C-terminal tail. Finally, SAXS data confirmed the consistency of the obtained model with the experimental data.

Conclusion: The 3D structure of human tetrameric butyrylcholinesterase, obtained for the first time using a combination of complementary structural methods, revealed unique quaternary organization distinct from the model proposed previously.

Key Words: butyrylcholinesterase; tetramer; cryo-EM; bioscavenger

This work was supported by the Russian Science Foundation projects - #19-14-00164 (in part of the data collection and analysis), #18-41-06001 (in part of image processing) and #17-14-01097 (in part of the sample preparation) as well as by Russian Foundation for Basic Research project #19-03-00043 (in part of molecular dynamics simulation).

OR-22

http://dx.doi.org/10.21103/IJBM.9.Suppl_1.OR22

In Vitro Cryo Electron Tomography study of protective Dps-DNA co-crystallization

Roman Kamyshinsky^{1,2}, Yuri Chesnokov^{1,2}, Liubov Dadinova², Andrey Mozhaev^{2,4}, Anton Orekhov^{1,2}, Eleonora Shtykova^{2,3}, Alexander Vasiliev^{1,2}

¹National Research Center "Kurchatov Institute", Moscow, Russia;

²Shubnikov Institute of Crystallography of Federal Scientific Research Centre "Crystallography and Photonics", Russian Academy of Sciences, Moscow, Russia; ³Semenov Institute of Chemical Physics of Russian Academy of Sciences, Moscow, Russia; ⁴Shemyakin-Ovchinnikov Institute of bioorganic chemistry of Russian Academy of Sciences, Moscow, Russia

Background: It was shown that when exposed to extreme environment Dps-DNA co-crystallization takes place in *Escherichia coli* as a protective mechanism. However, to this date most of the proposed models of co-crystals were not backed up with any direct methods. Recent developments in Cryo Electron Tomography allow to visualize co-crystals with high spacial resolution in nearly native state.

Methods: The investigations were carried out in a Titan Krios 60-300 TEM/STEM (FEI, USA) CryoEM, equipped with direct electron detector Falcon II (FEI, USA) and Cs image corrector (CEOS, Germany), at accelerating voltage of 300 kV. Tilt series were collected automatically using FEI Tomography software in low-dose mode which allowed to minimize the radiation damage. Subtomogram averaging was performed in Relion2 software package. Data processing and 3D reconstruction were carried out using computing resources of the Federal Collective Usage Center Complex for Simulation and Data Processing for Mega-Science Facilities at NRC "Kurchatov Institute".

Results: In this study, different types of Dps-DNA co-crystals were observed in vitro. Structural characteristics of the co-crystals were revealed for the first time by Cryo Electron Tomography. Subtomogram averaging allowed the direct visualization of Dps and DNA molecules in co-crystals. It was shown that the first type of co-crystals exhibits lamellar morphology and is formed by Dps layers alternating with DNA strands. The co-crystals adopt central symmetric triclinic crystal structure. The second type adopts body-centered cubic crystal lattice with mutually perpendicular DNA strands packed between Dps molecules. We assume that co-crystals' structure could be dependent on the parameters of the utilized Dps and DNA solutions.

Conclusion: In this study, we established structural

characteristics of different types of Dps-DNA co-crystals. The obtained results are a vital step towards understanding the mechanism of protective Dps-DNA co-crystallization process.

Key Words: biocrystallization, Dps, DNA, nanocrystals.

This work was supported by the Russian Science Foundation (project № 18-74-10071).

OR-23

http://dx.doi.org/10.21103/IJBM.9.Suppl_1.OR23

Current status of biomolecules imaging by X-ray Free Electron Laser without crystallization

Aleksandr V. Kudriavtsev^{1,2}, Anna V. Vakhrusheva¹, Valery N. Novoseletsky¹, Grigoriy A. Armeev¹, Mikhail A. Lozhnikov¹, Alexey K. Shaitan¹, Georgy M. Kobelkov¹, Konstantin V. Shaitan¹

¹Faculty of Biology, Lomonosov Moscow State University, Moscow, Russia; ²Emanuel Institute of Biochemical Physics, Russian Academy of Sciences, Moscow, Russia

Background: X-ray free-electron lasers (XFELs) in structural biology field opened a new opportunity for studying the structural dynamics of biomolecules. Structural dynamics analysis of single protein molecules by XFEL is based on the "diffraction-before-destruction" principle. The obtaining of the diffraction without sample crystallization is a complicated. Despite this fact, there are works about studying of single biomolecules without crystallization by XFEL.

Methods: We have analyzed some works from the Coherent X-ray Imaging Data Bank (<http://www.cxidb.org>). Among all presented structures the works, that contained biological object and did not include crystallization methods for its preparing, were selected. Only the following methods Single Particle Flash X-ray Imaging (SP-XDI), Serial Fiber Diffraction (SFD), Fluctuation X-ray Scattering (FXS) met the chosen criteria. Studies with different objects were considered as different works.

Results: In total, 20 non-recurring studies about studying of various biological objects without usage of crystallization were found. Among them there were two works with usage of FXS method, three works about SFD method and the remaining 15 works – with SP-XDI method. The works were also classified by objects: three studies were about cell structure of yeast and cyanobacteria; in two cases the structures of fibrils (bombesin and endorphin) were investigated by SFD method; in two other papers – the structures of protein complexes (RNA Polymerase II and Carboxysomes); and in the remaining 13 articles the viruses of various size were studied. Based on the analysis of works the potential problems of this field were elucidated, such as processing of diffraction patterns and 3D-reconstruction of structures, preparation of small size objects (single proteins less than 500 kDa), and low ratio between successful and error hits.

Conclusion: Currently, the field of structural biology has gained necessary conditions for the analysis of single biological molecules. It was noted in the recent study (Pietrini, 2018), in case of solution of such problems as reducing electrospray aerosol droplet size, will allow to get the 5 Å resolution. Thus, it makes the problem of 3D-reconstruction from XFEL diffraction patterns is extremely important area for future studies.

Key Words: XFEL, single molecules, diffraction.

This work was supported by the Russian Foundation for Basic Research No. 18-02-40010.

OR-24

http://dx.doi.org/10.21103/IJBM.9.Suppl_1.OR24

Detection and Characterization of Extracellular Vesicles in Transmission Electron Microscopy by Convolutional Neural Network

Igor Nikishin, Dmitry Bagrov, Elena Tchevkina, Gleb Skryabin, Ruslan Dulimov

Department of Biology, Lomonosov Moscow State University, Moscow, Russia

Background: Extracellular vesicles (EVs) are produced by almost all known organisms and released or secreted from cells. EVs particles are lipid-based particles with size ranging from 30 to 1000 nm. Transmission Electron Microscopy (TEM) is the most convenient method for imaging of EVs. The size measurement of the EVs on the TEM images can be automated and accelerated using convolutional neural networks (CNN). Our approach is to use a CNN that transforms a TEM image to a probabilistic map that indicates where extracellular vesicles particles are located. Our method is based on supervised learning that requires both the input images and their corresponding annotations.

Methods: We used EVs isolated from ascitic fluids from ovarian cancer patients by ultracentrifugation. The TEM images were obtained using negative staining. The software development included four steps: data augmentation and marking datasets using VGG Image Annotator (VIA) software (Oxford, England); neural network education; particle detection and features extractions. Mask R-CNN was chosen as the core CNN for object detection and instance segmentation using Keras and TensorFlow.

Results: Mask RCNN Neural Network was educated using more than 2000 particles. The EVs were counted, and their size was measured (area, effective diameter, square). We added the option of manual checking the results. After processing, the software calculates the key parameters of each EV and provides the results as a table for further statistical analysis.

Conclusion: Our approach helps to analyze each TEM image of vesicles approximately 10 times faster than by handpicking of single EVs. Since the CNN method is highly flexible, similar convolutional networks could be adapted to detect other particles by learning from annotated datasets.

Key Words: extracellular vesicles, TEM, neural networks

This work was supported by the Russian Fund for Basic Research, project № 17-00-00166. The electron micrographs were made at User Facilities Center of Lomonosov Moscow State University under financial support of Ministry of Education and Science of Russian Federation.

OR-25

http://dx.doi.org/10.21103/IJBM.9.Suppl_1.OR25

Fitting structural fragments into electron microscopy density maps using spectral shape descriptors

Amihai Holzer¹, Dina Schneidman-Duhovny^{1,2}

¹School of Computer Science and Engineering, The Hebrew University of Jerusalem, Jerusalem, Israel; ²Department of Biological Chemistry, Institute of Life Sciences, The Hebrew University of Jerusalem, Jerusalem, Israel

Background: Macromolecular assemblies play a major role in cellular processes. Atomic resolution structural characterization of these machineries is necessary for understanding and modulating their function. The resolution revolution in cryo-EM paved a way for solving structures that for years resisted X-ray crystallography. This progress introduced a need for a new generation of computational methods for automatic structure determination with high and medium resolution cryo-EM density maps.

Methods: We present a novel method for rapid fitting of structural fragments into high and medium resolution density maps. The fragments can range in size from peptides to large proteins. The method utilizes spectral Heat Kernel Signature (HKS) shape descriptors, that are used in 3D shape recognition in Computer Vision. The fragment descriptors are fitted to the descriptors of the density map using the Geometric Hashing approach.

Results: We benchmark the method on a set of maps with resolved atomistic structures in the 3.4-6Å resolution range (Fig. 1).

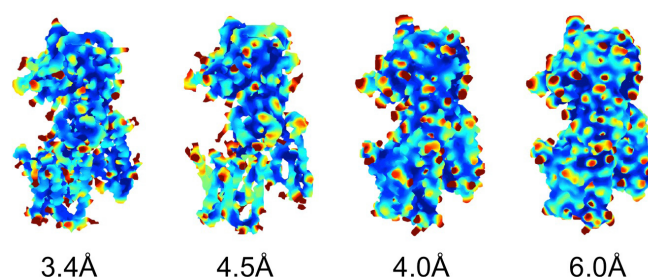


Fig. 1. HKS descriptors of experimental (resolutions 3.4 and 4.5Å) and simulated maps (resolutions 4 and 6Å) of γ -secretase. The coloring is according to the sum of HKS descriptors computed at 27 different time points.

Conclusion: The method is an important building block towards automated ab initio structure modeling.

Key Words: Atomic resolution structure modeling, EM density map fitting

STRUCTURE OF MEMBRANE PROTEINS

P-1

http://dx.doi.org/10.21103/IJBM.9.Suppl_1.P1

Analysis of the structure of serotonin 5-HT₃ receptor by X-Ray, CryoEM and MD methods: identification of conformational state

Popinako A.V.

A.N. Bach Institute of Biochemistry, Federal Research Center of Biotechnology of the Russian Academy of Sciences, Moscow, Russia

Background: Ion channels form a varied class of integral membrane proteins involved in the regulation of fundamental cellular processes. The structural and functional diversity of ion channels, as well as their participation in the vital systems of the body causes an increased interest in their study. The importance of research of channels' structures is underscored by the identification of numerous "channelopathies", caused by ion channel mutations. However, the complex molecular architecture of eukaryotic ion channels, which include large non-membrane domains, is often an obstacle to structural

studies by experimental methods. Thus, only epy atomic X-ray structure of the pentameric ligand-dependent mammalian channel of the serotonin 5-HT₃ receptor (pdb id 4PIR) and the Cryo-EM structure (pdb id 6BE1) are known at the present. Based on the available experimental data on this channel, the conformational state of this channel cannot be determined. In this regard, the aim of this study was to compare and analyze the structure of serotonin 5-HT₃ receptor and its models, built by modeling homology.

Methods: Structures with pdb id 2BG9, 4AQ9 for modeling 5-HT₃ receptor closed and open conformations respectively were used as templates for modeling. We used the model of water TIP4P/2005 which sufficiently well describes the liquid and crystal states. The cutoff radius for nonvalent interaction was 1.8 nm. The calculations ran as an NPT ensemble. To maintain constant temperature and pressure, we used the stochastic dynamics thermostat and Berendsen barostat. We placed the ion channels molecules at the nodes of a hexagonal lattice and rotated them about their axes through random angles. The simulations ran in the software package Gromacs 4.6.7. We specified the initial velocities of atoms using a random number generator with the Maxwell distribution.

Results: The obtained models of open and closed channels of 5-HT₃ receptor differ in the area of the internal threshold: the pore radius in this area is greater in open conformation models, compared with the closed conformation model and the structure of 5-HT₃ receptor (4PIR). In the membrane part of the 5-HT₃ receptor and the model of the closed conformation, the oxygen of the hydroxyl groups of threonine in the M2 helices form the area of the minimum radius of the pores.

Conclusion: According to the molecular dynamics data obtained by us, hydrated sodium ions are unable to pass through this section of the channel 5-HT₃ of the receptor. Thus, the data obtained suggest that the structure of the 5-HT₃ receptor (pdb id 4PIR) is more consistent with the closed conformation. The work was carried out with the financial support of the Russian Foundation for basic research, agreement № 16-34-60252. The MD research has been carried out using the equipment of the shared research facilities of HPC computing resources at Lomonosov Moscow State University. This work structural analysis has been carried out using computing resources of the federal collective usage center Complex for Simulation and Data Processing for Mega-science Facilities at NRC "Kurchatov Institute" (ministry subvention under agreement RFMEFI62117X0016), <http://ckp.nrcki.ru/>.

Key Words: Ion channels, conformational state, modeling

P-2

http://dx.doi.org/10.21103/IJBM.9.Suppl_1.P2

Modeling encapsulated lipid molecules in CryoEM maps of membrane complexes

Olga Novitskaia, Pavel Buslaev, Ivan Gushchin

Moscow Institute of Physics and Technology, Dolgoprudny, Russia

Background: Membrane complexes are of great importance for cell functioning. Among the best studied complexes are rotor ATPases which create ATP from ADP, or vice versa (J.E. Walker, Biochem. Soc. Trans. 41, pp. 1-16, 2013). Generally, rotor ATPases consist of a soluble part and a membrane-embedded part. The membrane part includes a c-ring – a

symmetric oligomer of subunits c, which is rotating in the membrane during the protein operation. The inside pore of the c-rings in some cases is plugged by phospholipids.

While the protein components are well ordered in the structures, the surrounding lipid molecules, including those trapped inside the c-ring, usually are not resolved. Most probably this is due to the great flexibility of lipids (P. Buslaev et al., J. Chem. Theory Comput. 12, pp. 1019-1028, 2017) and lack of specific lipid-protein interactions, or due to techniques used for sample preparation.

Recently, a CryoEM structure of spinach chloroplast ATPase with recognizable densities in the membrane region has become available, providing an opportunity to compare the modeled lipid positions with the experimental data (A. Hahn et al., Science eaat4318, 2018).

Methods: We introduce nature-inspired approach to model the lipids inside the c-ring. It uses a biasing force to assemble the whole ring, essentially by incorporating experimental restraints into the coarse grained (CG) molecular dynamics (MD) simulation. The numerical comparison of modeled lipid densities with the EM maps was performed using the real space correlation coefficient (RSCC).

Results: The structures converged into an assembled ring. The numbers of lipids trapped at the loop side and the NC-side were consistent in different runs: 9 to 11 and 13 to 15, respectively. However, RSCC of modeled lipid densities with the EM map was poor. Thus, we conducted short CG simulations where lipids were removed one-by-one to maximize RSCC (Fig. 1). The best fit (RSCC > 0.8) was observed for a system with 6 lipids at the loop side and 9 lipids at the NC side. The obtained systems were converted to atomistic models and were stable for several hundreds of nanoseconds. The atomistic models also correlated with experimental data well (RSCC > 0.8) and showed the same trend as densities for coarse grained simulations.

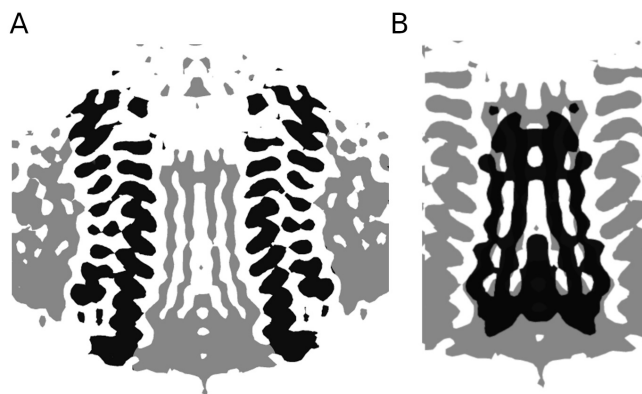


Fig. 1. (A) Experimental densities for c-ring of rotor ATPase. Lipid densities are shown in grey, protein densities in black. (B) Comparison of experimental and modeled densities. Experimental densities are shown in grey; modeled densities for 6 lipids at the loop side and 9 lipids at the NC side are shown in black.

Conclusion: We expect that the approach will be helpful for modelling of the lipids encapsulated within membrane protein and for studies of assembly of membrane complexes.

Key Words: molecular dynamics simulations, rotor ATPase, CryoEM

This work was supported by RFBR according to the research project №18-34-00986

P-3

http://dx.doi.org/10.21103/IJBM.9.Suppl_1.P3**Nanoparticles with ion channels: solubilization and purification of membrane proteins**

Julia Kacher, Grigory Glukhov, Olga Sokolova

Lomonosov Moscow State University, Moscow, Russia

Background: Now there are several approaches to isolate membrane proteins without detergents. Such approaches are promising as they guarantee the preservation of the lipid environment of the target proteins. One of such novel methods is based on the usage of a copolymer of styrene and maleic acid (SMA). Particles with small membrane fragments containing transmembrane proteins bounded by a polymer are called nanodisks (SMALPs).

Methods: We chose HEAG2 with affine 1d4 tag at the C-terminus as an object of interest. Channels were expressed in COS-1 eukaryotic cell line (African green monkey kidney fibroblast-like cell line). The potassium channels were integrated into SMALPs during the solubilization and then purified via affinity chromatography. The embedding of the channel into the particles with SMA was confirmed by immunoblotting. Dynamic light scattering was used to confirm the formation of SMALPs with channel protein. Obtained samples were subjected to negative stain electron microscopy.

Results: We have succeeded to extract voltage-gated potassium channels from the membrane fractions directly. The hydrodynamic diameter of the formed particles was 15.5 nm. The analysis of EM images also confirmed the formation of nanoparticles.

Conclusion: The technique for solubilizing and purifying ion channels from eukaryotic cells using SMA allows to make three-dimensional reconstruction of the particles.

Key words: ion channels, detergent-free solubilization methods, membrane proteins.

This work was supported by the grant of the Russian Science Foundation for young scientists (18-74-00087). Electron microscopy was performed on the basis of the CCP of the Faculty of Biology MSU "Electron microscopy in the science of life" using the 3D-EMC.

P-4

http://dx.doi.org/10.21103/IJBM.9.Suppl_1.P4**Cryo-electron microscopy of G-protein coupled receptors complexes for drug discovery approaches**

Anastasiia Gusach, Aleksandra Luginina, Valentin Borshchevskiy, Alexey Mishin

Research Center for Molecular Mechanisms of Aging and Age-Related Diseases, Moscow Institute of Physics and Technology, Dolgoprudny, Russia

Background: Seven helical transmembrane G-protein coupled receptors (GPCRs) involved in various extracellular ligand recognition and signal transduction processes are prominent targets of about a third of existing drugs (Sriram and Insel, 2018). The study summarizes current advances and opportunities in the field of structural biology of GPCRs using cryo-electron microscopy and its applications for the target-based drug discovery.

Results: An atomic resolution structural information about receptors is of extreme value for predicting novel compounds, binding modes and resolving receptor selectivity issues, in general (Ceska et al., 2019). Obtaining this information is not straightforward though: the established crystallization pipeline requires considerable time and much efforts in expression systems testing, protein purification adjustment, crystallization conditions screening and diffraction data processing.

One of the ways to bypass the crystallization step is the use of cryo-electron microscopy for receptor structure determination (Ceska et al., 2019). Due to the size limitation of about 100 kDa for the single-particle Cryo-EM approach, wild type receptors with a typical size of 40 kDa are not suitable for this method (Ishchenko, Gati and Cherezov, 2018). A large spectrum of possible conformational states and the absence of preferred orientation make single particle classification even more challenging. As GPCRs perform their functions in cells via interaction with heteromeric G-proteins and arrestins, it appears the most natural way to use these complexes for overcoming the size barrier (García-Nafria and Tate, 2019). An active receptor state can also be achieved by having the complexes with synthetic smaller analogues of G-proteins - mini G-proteins (García-Nafria and Tate, 2019). Up to date 9 complexes with 8 unique receptors are published encompassing Gs-bound, G0-bound and Gi-bound states and mini-Gs in case of A2a receptor structure (García-Nafria and Tate, 2019).

Conclusion: Cryo-electron microscopy is an emerging tool for obtaining high resolution structures of GPCRs with the potential in the drug discovery field. A number of ways are developed to stabilize the receptor and to overcome the Cryo-EM size limitation.

Key words: GPCR - g-protein complexes, Cryo-EM, target-based drug design

The work was supported by the Russian President Grant for Governmental support of Young Scientists (project no. MK-5184.2018.4)

P-5

http://dx.doi.org/10.21103/IJBM.9.Suppl_1.P5**Modern membrane mimetic systems for Cryo-EM based structural analysis**

Egor S. Kolesnikov, Polina A. Khorn, Anastasiia U. Gusach, Aleksandra P. Luginina, Alexey V. Mishin

Research Center for Molecular Mechanisms of Aging and Age-Related Diseases, Moscow Institute of Physics and Technology, Dolgoprudny, Russia

Background: Single particle approach that is used to image the sample by an electron beam requires receptors to be extracted from the cell membrane and placed into the sample grid in the solubilized form. Conventional use of detergents for GPCR solubilization often leads to poor stability of the receptor removed from its natural lipid environment. Therefore, scientists use membrane mimetic systems (MMS) such as amphipols and various types of nanodisks, including styrene maleic acid (SMA) derivatives - SMALP and DISMALP. The last one are among the most prospective and interesting MMS and could be used as a tool in Cryo-EM studies. SMALP and DISMALP have better thermal stability than other types

of nanodiscs. SMA could negatively affect the order of phospholipids but DIBMA has a weaker hydrophilic part that is thought to be a reason of weaker impact on phospholipids.

Methods: Thermal stability of the nanodiscs was tested using microscale thermophoresis and thermal shift assay.

Results: In this work adenosine A2a GPCR was solubilized into SMALP and DIBMALP. Then its stability was tested.

Conclusion: SMALP and DIBMALP are useful in Cryo-EM studies. It's better to stabilise membrane proteins in SMALP and DIBMALP for structural analysis because of their high thermal stability.

Key Words: nanodiscs, SMALP, DIBMALP, Cryo-EM

This work was supported by the Russian President Grant for Governmental support of Young Scientists (project no. MK-5184.2018.4)

P-6

http://dx.doi.org/10.21103/IJBM.9.Suppl_1.P6

G-protein coupled receptors engineering for structural analysis

Aleksandra Luginina, Anastasiia Gusach, Valentin Borshchevskiy, Alexey Mishin

Research Center for Molecular Mechanisms of Aging and Age-Related Diseases, Moscow Institute of Physics and Technology, Dolgoprudny, Russia

Background: G-protein coupled receptors (GPCR) are drug targets of great current interest, being meanwhile a challenging object for structural research.

Methods and Results: The protein of interest needs to be expressed in necessary amounts. To obtain folded and functionally active receptor, usually eukaryotic systems are used, and the protein is located on the cytoplasmic membrane (Lv et al. 2016). To deliver a GPCR to the cell surface signaling peptides and their combinations are used (Shepard et al. 2013), however successful combination varies for each GPCR in a particular cell type.

A GPCR must be stable in the membrane-mimetic systems like micelles or nanodiscs, as well as lipidic cubic phase in case of X-ray crystallography. To stabilize a GPCR, fusion partners are put on the protein N-terminus or into the 3rd intracellular loop (ICL-3) (Chun et al. 2012). This helps to fix a receptor in one conformational state, as well as helps to form crystal contacts. ICL-3 insertions are inapplicable for the complexes with G-proteins that are popular for the Cryo-EM structures. Several software tools are used, that help to predict stabilizing point mutations and fusion partner position (Popov et al. 2018; Pándy-Szekeres et al. 2018).

To enhance particular GPCR parameters, like expression, stability or diffraction resolution, N- or C-terminal fragments as well as transmembrane region parts are borrowed from those receptors that are known to be on the top of those parameters, the nearest homologues are preferred. Thus A1 adenosine receptor was crystallized with the parts from muscarinic 4 and adenosine A2A receptors (Glukhova et al. 2017), and for the better β 2AR-arrestin binding GPCR C-terminal region was replaced for the one from AVPR2 (Shukla et al. 2014).

Conclusions: GPCR construct engineering is an inherent tool for structural biology, it requires deep preliminary analysis, hard searching effort, and a bit of luck.

Key Words: gene modifications, stabilization, GPCR

The work was supported by the Russian President Grant for Governmental support of Young Scientists (project no. MK-5184.2018.4).

P-7

http://dx.doi.org/10.21103/IJBM.9.Suppl_1.P7

Cryoelectron microscopy study of water-soluble extracellular domain of $\alpha 7$ nicotinic acetylcholine receptor

Andrey V. Tsarev^{1,2}, Roman A. Kamyshinskiy³, Vasilii I. Mikirtumov⁴, Dmitriy S. Kulbatskii¹, Eugene O. Yablokov⁵, Zakhar O. Shenkarev^{1,2}, Olga S. Sokolova⁴, Ekaterina N. Lyukmanova^{1,2}

¹Shemyakin-Ovchinnikov Institute of Bioorganic Chemistry, Moscow, Russia; ²Moscow Institute of Physics and Technology, Dolgoprudny, Moscow Region, Russian Federation; ³National Research Center, Kurchatov Institute, Moscow, Russia; ⁴Lomonosov Moscow State University, Moscow, Russia; ⁵Institute of Biomedical Chemistry, Moscow, Russia

Background: Nicotinic acetylcholine receptor (nAChR) is a ligand-gated ion channel, which is widely distributed both in the central and peripheral nervous system, and in some of the non-neuronal tissues, including epithelium and immune cells. The pathophysiology of a number of diseases is associated with dysfunctions of this receptor, including neurodegenerative and mental disorders like Alzheimer disease (AD) and schizophrenia. The nicotinic receptor of $\alpha 7$ type ($\alpha 7$ -nAChR) plays important role in the memory and learning processes and is inhibited by soluble aggregates of β -amyloid peptide (A β). A β 1-42 is the most toxic form of the amyloid peptide.

Methods: The water-soluble analogue of the ligand-binding extracellular domain of $\alpha 7$ -nAChR was produced in *Pichia pastoris* and purified from a culture medium by Ni-NTA and size-exclusion chromatography. The equilibrium dissociation constant (K_d) of the complex of the recombinant domain with α -bungarotoxin was measured on the optical SPR biosensor Biacore 3000. Structures of the $\alpha 7$ domain alone and in the complex with oligomeric A β 1-42 peptide were studied by cryoelectron microscopy (cryo-EM).

Results: The $\alpha 7$ ligand-binding domain has an increased stability in solution, and demonstrates ligand-binding characteristics similar to those of the native receptor (K_d of the domain/ α -bungarotoxin complex 28 \pm 2 nM). Statistical analysis of the cryo-EM images of the individual domain particles revealed the presence of a pentameric structure, confirming intact subunit assembly. Unfortunately, the domain demonstrated the preferable orientation on grids with the top view. Nevertheless, the 3D structure of the domain with a height \sim 7 nm, external diameter of \sim 9 nm, and the pore diameter of \sim 2 nm was reconstructed at 8.5 Å resolution. 2D classification of the cryo-EM images of the domain particles in the complex with A β 1-42 revealed the conformational changes appeared due to interaction with the amyloid peptide.

Conclusion: Obtained results open new perspectives for structural studies of the nAChR ligand-binding domains in complex with the ligands which escape crystallization.

Key Words: cryoelectron microscopy, $\alpha 7$ -nAChR, beta-amyloid peptide

This work was supported by the Russian Science Foundation (project # 19-74-20163).

P-8

http://dx.doi.org/10.21103/IJBM.9.Suppl_1.P8

Properties of light-driven proton pump from *Exiguobacterium sibiricum* with amphipathic polymers

Anatolii E. Mikhailov¹, Pavel K. Kuzmichev¹, Lada E. Petrovskaya², Dmitro V. Soloviov^{1,3}, Vladimir V. Chupin¹

¹Research Center for Molecular Mechanisms of Aging and Age-Related Diseases, Moscow Institute of Physics and Technology (National Research University), Dolgoprudnyi, Moscow Region, Russia; ²M. M. Shemyakin–Yu. A. Ovchinnikov Institute of Bioorganic Chemistry, Russian Academy of Sciences, Moscow, Russia; ³Joint Institute for Nuclear Research, Dubna, Moscow Region, Russia

Background: Rhodopsins are chromoproteins, which contain retinal, with various necessary functions for energy or photoreception of a cell. Many homologues of rhodopsins were found in the microorganisms of different taxa. Siberian permafrost is a unique biological community, unifying microorganisms adapted to long-term frosts, high osmolarity and lack of light. *Exiguobacterium sibiricum* is one of the microorganisms that can withstand a wide range of growth conditions. For a long time, the possible role of the found rhodopsin remained unclear in adaptation to extreme environmental conditions.

Methods: In this work, we studied complexes of rhodopsin ESR (*Exiguobacterium sibiricum* rhodopsin - ESR) solubilized in amphipathic polymers (amphipols) A8-35 and PMAL-C12. ESR was expressed in *E. coli*, purified and inserted in amphipols by standard protocols. The complexes were characterized using the dynamic light scattering method and flash-photolysis, which was the author's designed device for measuring photocycles.

Results: Diameters were 4.8 and 5.4 nanometers, all samples were monodisperse and stable for long period. This size indicates the monomericity of the protein. The photocycle of ESR in amphipols was about 150 milliseconds, which was 1.5 times longer than the photocycle of ESR in DDM micelles. This difference could be accounted for by decreasing the conformational mobility of rhodopsin solubilized with into amphipols, rather than detergent micelles.

Conclusion: According to this study, the amphipols is a good membrane mimetic for ESR. The protein is stable and functionally active as a light-driven proton pump, which makes it a good candidate for an optogenetic tool. This method could be used for other retinal proteins and lead to the understanding of the physiological necessity of rhodopsin ESR expression by the microorganism *E. sibiricum*.

Key Words: bacteriorhodopsin, amphipol, photocycle, proton transport

This work was supported in part by the Russian Foundation for Basic Research (Grant No. 17-00-00164, komfi) and the Ministry of Education and Science of the Russian Federation (grant no. 6.3157.2017).

P-9

http://dx.doi.org/10.21103/IJBM.9.Suppl_1.P9

Immobilization of membrane proteins for single-molecule microscopy studies

Aizada Nurdinova, Ivan Maslov, Polina Khorn, Nadezhda Safronova, Nickolay Ilyinsky, Pavel Kuzmichev, Valentin Borshchevskiy

Moscow Institute of Physics and Technology, Dolgoprudny, Russia

Background: Single-molecule fluorescence microscopy studies can reveal conformational changes in proteins, help to find their stable states and to investigate transitions kinetics. The major advantage of this method is the possibility to show the heterogeneity of the properties within the ensemble.

Single molecules can be observed in two different ways: in solution, where they can freely diffuse, and immobilized on the surface. The latter allows to significantly increase the observation time of the molecule.

Methods: Single-molecule fluorescence measurements were performed using microscope LSM780, Carl Zeiss at MIPT. Quartz slides were cleaned, passivated with polyethylene glycol (PEG), and coated with streptavidin. Biotin conjugated samples were introduced into the sample chamber and allowed to bind to the streptavidin-coated surface, after which unbound molecules were washed away with PBS. The two membrane systems were sampled in this work: nanodiscs and liposomes.

Results: In this work, the immobilization protocol have been developed and thoroughly tested. Each layer of the immobilization system has been checked sequentially on specificity. It turned out that streptavidin attaches to the surface covered with 3% biotin-PEG and has free binding sites for biotin-conjugated molecules. Nonspecificity observed when the nanodiscs containing 5% of biotinylated lipids are added to the system. Moreover, the usage of longer biotinylated lipids in nanodiscs does not help. Tests made with liposomes containing 5% of biotinylated lipids showed specific binding. Single-molecule measurements are possible at a concentration about 10pMol.

Conclusion: Attempts to catch a membrane protein were made in this experiment. Unfortunately, nanodiscs immobilization did not show the desired specificity. However, the liposomes look very promising in this context.

Key Words: single-molecule microscopy, immobilization, membrane systems

The work was performed in the framework of governmental task of Ministry of Education and Science of the Russian Federation, project № 6.9909.2017/6.7

P-10

http://dx.doi.org/10.21103/IJBM.9.Suppl_1.P10

Comparison of ion coordination in similar selectivity filters of bacterial sodium and eukaryotic calcium voltage-gated channels

Ivan N. Terterov¹, Alexey A. Bogdanov¹, Ilya A. Pozdnyakov²

¹Saint-Petersburg Clinical Scientific and Practical Center of Specialized Types of Medical Care (Oncological), St. Petersburg, Russia; ²Institute of Cytology RAS, St. Petersburg, Russia

Background: Prokaryotic voltage-gated sodium channels (Navs) and eukaryotic voltage-gated calcium channels (Cavs) are the members of the same superfamily. Bacterial Navs are homotetramers with a selectivity filter formed by four segments given form a P-loop of each monomer. In contrast, eukaryotic Cavs are pseudotetramers with four asymmetric but

homologous P-loops and probably evolved from prokaryotic Navs by two rounds of duplication. Nevertheless, selectivity filters of bacterial Navs and eukaryotic Caves are very similar, and surprisingly, they have identical E/E/E/E high-field-strength (HFS) site. Since HFS site was considered to be responsible for ion selectivity, the mechanism of different Na/Ca discrimination of these channels is still unclear.

From a comparison of the new cryo-EM structure of mammalian Cav1.1 channel with X-ray structure of bacterial Nav, it is clear that backbone positions of Glu residues of HFS sites are identical in these two channels but the side chains have different geometries. However, it is unclear whether these side chain structures are just a distinct conformers from the same ensemble, or their difference is functional and defines dissimilar channel selectivity.

Methods: In order to explore conformational motions of the HFS site residues we conducted molecular dynamics simulations of NavMs channel (PDB: 5BZB) and Cav1.1 channel (PDB: 6BYO) in the same conditions with single ion coordinated in the selectivity filter.

Results: We found that carboxylate groups of Glu residues of HFS site coordinate partially hydrated cation in the pore lumen, as was demonstrated before. A closer look shows that during ion coordination Glu side chains notably alter their conformations from symmetric geometry of X-ray NavMs structure towards asymmetric one observed for Cav1.1 with cryo-EM.

Conclusion: Each published channel structure captures only one Glu side chain geometry in HFS site, while it is thought that these groups sample multiple conformation when ion path through the pore. Results of our simulations suggest that side chains of E/E/E/E HFS sites of NavMs and Cav1.1 channels are flexible and may adopt similar conformations when coordinate the same cation.

Key words: Voltage-gated ion channels, Caves, Navs

This work was supported by RFBR grant No 18-34-00992.

P-11

http://dx.doi.org/10.21103/IJBM.9.Suppl_1.P11

Conformational Study of an Archaeal Photoreceptor/Transducer Complex from *Natronomonas pharaonis* Assembled in Styrene-Maleic Acid Lipid Particles Using Electron Paramagnetic Resonance Spectroscopy

Natalia Voskoboinikova¹, Wageiha Mosslehy¹, Alexandr Colbasevici¹, Dmitry V. Bagrov², Armen Y. Mulkidjanian¹, Konstantin V. Shaitan², Johann P. Klare¹, Heinz-Jürgen Steinhoff¹

¹Department of Physics, University of Osnabrueck, Osnabrueck, Germany; ²Department of Biology, Lomonosov Moscow State University, Moscow, Russia

Background: The membrane-embedded 2:2 sensory rhodopsin II/transducer complex, NpSRII/NpHtrII, plays a key role in the photophobic response of the halophilic archaeon *Natronomonas pharaonis*. Photon absorption induces transient structural changes in the transmembrane part of NpSRII, which are conducted to the transducer NpHtrII. The subsequent signal propagates along the cytoplasmic part of NpHtrII to the intracellular signaling pathway, which modulates the rotation of the flagellum. Here, we studied

the conformation and dynamics of the NpSRII/NpHtrII complex after reconstitution into cell membrane-mimicking nanoparticles, namely, styrene maleic acid lipoprotein particles (SMALPs) (Fig. 1), and in comparison with those of NpSRII/NpHtrII reconstituted in liposomes and nanodiscs.

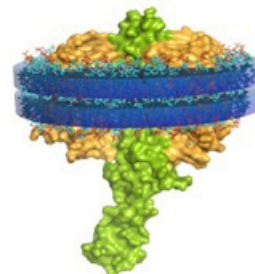


Fig. 1. Schematic SRII/HtrII complex in SMALPs.

Methods: We utilized the SMA copolymer with a 3:1 styrene-to-maleic acid molar ratio (3:1 SMA) to isolate, in a detergent-free manner, the NpSRII/NpHtrII complex from preformed proteoliposomes. We characterized the resulting NpSRII/NpHtrII-SMALPs using a set of optical and electron paramagnetic resonance (EPR, DEER) spectroscopy methods as well as dynamic light scattering (DLS) and transmission electron microscopy (TEM).

Results: The cw-EPR data show unaffected spin-label dynamics of the L159R1 side chain in the interior of NpSRII reconstituted into SMALPs. The DEER data indicate that NpSRII/NpHtrII incorporates into SMALPs as a native-like 2:2 dimer with the distances between L159R1 sites corresponding to the "V"-shaped conformation. Time-resolved optical and EPR spectroscopy data reveal light-induced spectral and conformational changes for NpSRII/NpHtrII reconstituted in SMALPs. The DLS data indicate the monodispersity of SMALP preparations. TEM images reveal well-defined individual particles of 12–14 nm in diameter.

Conclusion: We showed that the NpSRII/NpHtrII complex retains its integrity and functionality upon reconstitution into SMALPs although with restricted dynamics. We conclude that the SMALP approach could be suitable for preparation of stable membrane protein samples for further structural and functional studies.

Key Words: photoreceptor/transducer complex, detergent-free reconstitution, nanolipoprotein particles

This work was supported by German Research Foundation (DFG, STE640/15); Russian Foundation for Basic Research (RFBR, 18-504-12045).

P-12

http://dx.doi.org/10.21103/IJBM.9.Suppl_1.P12

Structure of RyR1 in native membranes

Wenbo Chen^{1,2}, Mikhail Kudryashev^{1,2}

¹Max Planck Institute for Biophysics, Frankfurt am Main, Germany; ²Buchmann Institute for Molecular Life Sciences, Goethe University Frankfurt, Frankfurt am Main, Germany

Background: Ryanodine receptor 1 (RyR1) mediates excitation-contraction coupling by releasing Ca²⁺ from the lumen of sarcoplasmic reticulum (SR) to the cytoplasm of

skeletal muscle cells. RyR1 activity regulation is complicated and modulated by numerous molecules, including several regulatory proteins from both the cytoplasmic and luminal sides of the SR, and cation ions such as Ca^{2+} and Mg^{2+} , and chemicals such as caffeine and ryanodine. The activity regulation mechanism of RyR1 is not fully elucidated, though high resolution structures of purified RyR1 in detergent solved by single particle cryo-EM have been reported.

Methods: We isolated the SR from rabbit skeletal muscle and imaged RyR1 in native SR membrane with cryo-electron tomography. The structures of RyR1 in closed and open states were solved by sub-tomogram averaging, respectively.

Results: Compared to the reported structures of purified RyR1, our structure reveals the occupied competitive binding site of the regulatory proteins calmodulin and S100A1 on RyR1, helix-like densities traversing the bilayer approximately 5 nm from the RyR1 which are speculated to be triadin or junctin, and sarcoplasmic extensions linking RyR1 to the putative calsequestrin network. We document the major conformation or RyR1 in situ and its structural variations. Activation of RyR1 leads to significant changes of membrane curvature and sarcoplasmic extensions movement.

Conclusion: Our structures of RyR1 in situ show novel densities in cytoplasmic region and transmembrane region and SR lumen, respectively. Activation of RyR1 in situ reveals new conformational changes in the SR membrane and SR lumen. The results provide structural insights for mechanistic understanding of RyR1 in native environment.

Key words: ryanodine receptor, sarcoplasmic reticulum, in situ, sub-tomogram averaging

This work was supported by the Sofia Kovalevskaja Award from the Alexander von Humboldt Foundation to Mikhail Kudryashev and by a fellowship from the China Scholarship Council to Wenbo Chen

STRUCTURE AND FUNCTIONS OF THE TRANSCRIPTION AND TRANSLATION APPARATUS OF THE CELL

P-13

http://dx.doi.org/10.21103/IJBM.9.Suppl_1.P13

Cryo-ET structural analysis of polyribosomes from HeLa cells

Zhanna A. Afonina¹, Timur N. Baymukhametov², Dmitry N. Lyabin¹, Yuri M. Chesnokov², Alexander L. Vasiliev^{2,3}, Vladimir A. Shirokov¹

¹Institute of Protein Research RAS, Pushchino, Russia; ²National Research Center «Kurchatov Institute», Moscow, Russia; ³Shubnikov Institute of Crystallography of FSRC «Crystallography and Photonics» RAS, Moscow, Russia

Background: Polyribosomes are complexes consisting of several ribosomes simultaneously translating a single mRNA molecule. In early electron microscopy studies, it was shown that eukaryotic polyribosomes in cells can have various shapes – rings, double rows, and a shape interpreted as helical, based on 2D-images and cross-sections.

Methods: Modern methods of cryo-electron microscopy and tomography (cryo-EM and cryo-ET) allows to analyze the 3D organization of polyribosomes in close to native conditions. We used the cryo-ET approach to investigate the structural organization of cytoplasmic polyribosomes in the lysates of HeLa cells.

Results: Cryo-EM confirmed the presence of ring and double-row structures of polyribosomes in the lysates. Using cryo-ET and averaging of polysomal ribosomes (subtomogram averaging), we determined the relative orientations of the ribosomes in the polyribosomes and traced the deduced mRNA path within every individual polyribosome. Thus, the circular path of the mRNA chain was for the first time demonstrated for ring-shaped polyribosomes from eukaryotic cells. A linear zigzag mRNA chain pathway was found for double row polyribosomes. Besides, relaxed helical and helical-like polyribosomes were detected in lysate. In addition, the structure of polyribosomes in lysate of HeLa cells growing in stressful (heat shock) conditions was analyzed. When the polyribosome profile resumed after heat shock, the ratio of different polyribosome conformations was found similar to that in normal conditions. A densely-packed helical configuration, which is characteristic of polyribosomes with reduced translational activity (Myasnikov et al., Nat. Commun., 2014, 5:5294), was not detected in lysates from cells grown in both normal and stressful conditions.

Conclusion: The structural organization of polyribosomes in lysates of HeLa cells growing in normal and stressful conditions was analyzed by cryo-ET. The revealed linear configurations of polyribosomes are in agreement with helical, helical-like, flat zigzag configurations of polyribosomes found in situ in human glioma cells (Brandt et al., Mol. Cell, 2010, 39:560-569). The circular topology of ring-shaped polyribosomes derived from eukaryotic cells was confirmed by cryo-ET method for the first time.

Key Words: structural organization of polyribosomes, cryo-electron tomography, HeLa

This work was supported by RFBR grant 16-34-60148; cryo-EM data processing part was supported by RSF grant 18-41-06001.

P-14

http://dx.doi.org/10.21103/IJBM.9.Suppl_1.P14

Cryo-electron tomography pipeline on the example of structural analysis of polyribosomes

Timur N. Baymukhametov¹, Yuri M. Chesnokov¹, Zhanna A. Afonina², Alexander L. Vasiliev^{1,3}

¹National Research Center «Kurchatov Institute», Moscow, Russia; ²Institute of Protein Research RAS, Pushchino, Russia; ³Shubnikov Institute of Crystallography of FSRC «Crystallography and Photonics» RAS, Moscow, Russia

Background: Cryo-electron tomography (cryo-ET) is currently the only technique that can be used for quaternary structure determination of polyribosomal complexes under near physiological conditions. Here we describe, in more detail, the cryo-ET pipeline from a sample preparation for data processing from the poster talk “Cryo-ET structural analysis of polyribosomes from HeLa cells” by Zhanna A. Afonina.

Methods: The investigations were carried out in a Titan Krios 60-300 TEM/STEM (FEI, USA), equipped with Falcon II DED (FEI, USA) and Cs-image corrector (CEOS, Germany). Data acquisition were done automatically using FEI Tomography software. All data processing stages including sub-tomogram averaging after tomographic reconstruction using IMOD were carried out using computing resources of the Federal Collective Usage Center Complex for Simulation

and Data Processing for Mega-Science Facilities at NRC "Kurchatov Institute".

Results: Cryo-ET with sub-tomogram averaging was allowed us to determine spatial structure of polyribosomes with 17.5Å resolution. The relative orientations of ribosomes in polyribosomes and the mRNA pathways in each individual polyribosome were determined.

Conclusion: Cryo-ET in combination with sub-tomographic averaging is the most promising technique in cryo-electron microscopy. This approach in comparison of single particle analysis imposes additional requirements both at the stages of data acquisition and data processing. On the example of this work we demonstrated all the stages of the Cryo-ET pipeline. Taking into account the experimental equipment used, bottlenecks and possible solutions were shown.

Key Words: cryo-EM, cryo-ET, polyribosomes

This work was supported by RFBR grant 16-34-60148; cryo-EM data processing part was supported by RSF grant 18-41-06001.

P-15

http://dx.doi.org/10.21103/IJBM.9.Suppl_1.P15

Structural insights of dirithromycin binding to the bacterial ribosome

Evgeny Pichkur^{1,2,5}, Pavel Kasatsky², Alena Paleskava^{2,3}, Alexander Myasnikov^{2,6,7}, Yuri Polikanov⁸, Ilya A. Osterman^{4,9}, Andrey Konevega^{1,2,3}

¹NRC "Kurchatov Institute", Moscow, Russia; ²NRC "Kurchatov Institute"-PNPI, Gatchina, Russia; ³Peter the Great St.-Petersburg Polytechnic University, St. Petersburg, Russia; ⁴Lomonosov Moscow State University, Department of Chemistry and A.N. Belozersky Institute of Physico-Chemical Biology, Moscow, Russia; ⁵FSRC "Crystallography and Photonics", Moscow, Russia; ⁶St. Jude Children's Research Hospital, Memphis, US; ⁷Centre for Integrative Biology (CBI), IGBMC, CNRS, Inserm, Université de Strasbourg, Illkirch, France; ⁸Department of Biological Sciences, University of Illinois, Chicago, USA; ⁹Skolkovo Institute of Science and Technology, Skolkovo, Russia

Background: Macrolide antibiotics bind in the nascent peptide exit tunnel (NPET) of the bacterial ribosome near the peptidyl transferase center. One of the second-generation macrolides, dirithromycin (DIR), differs from the parent erythromycin (ERY) by the presence of a hydrophobic (2-methoxyethoxy)-methyl side chain that has significantly increased the delivery of this antibiotic to tissues due to better lipophilicity. In this work we present a cryo-EM structure of DIR bound to the functional complex of 70S ribosome from *E. coli*.

Methods: Ribosomal complexes containing deacylated tRNA^{fMet} in the P site and fMet-Phe-tRNA^{Phe} in the A site were incubated with 30 mM DIR for 10 min before application onto carbon coated grids (Quantifoil R 2/2) and freezing. Cryo-EM data was collected using cryo-TEM Titan Krios and processed using Warp, Relion 3.0 and CisTEM. Model building was performed in Phenix.real_space_refine and Coot.

Results: Preliminary analysis failed to reveal any significant differences in location of macrolactone ring of DIR (current work) and ERY (pdb: 4v7u). In both structures only one hydrogen bond is formed between antibiotic and residue A2058. However, in comparison to the crystal structure of the ribosomal complex with ERY, our cryo-EM map demonstrates additional

rotation of A2062 of 23S rRNA towards desosamine of DIR.

Conclusion: Structural peculiarities of DIR binding to the *E. coli* ribosome determined by high resolution cryo-EM overall coincide with the mode of ERY interaction with the *E. coli* ribosome revealed by X-ray crystallography. Our results suggest a conformational lability of the (2-methoxyethoxy)-methyl side-chain of DIR, which is directed towards tunnel cavity and doesn't form any additional contacts with its walls.

Key Words: ribosome, antibiotics, structure, cryo-EM

This work was supported by RSF #17-14-01416. The authors acknowledge the support and the use of resources of the Resource Center for Probe and Electron Microscopy at the NRC "Kurchatov Institute".

P-16

http://dx.doi.org/10.21103/IJBM.9.Suppl_1.P16

Interaction of poly(ADP-ribose)polymerase1 and poly(ADP-ribose)polymerase2 with nucleosome during base excision repair

Mikhail M. Kutuzov^{1,2}, Ekaterina A. Belousova^{1,2}, Olga I. Lavrik^{1,2}, Svetlana N. Khodyreva¹

¹Institute of Chemical Biology and Fundamental Medicine, Novosibirsk, Russia; ²Novosibirsk State University, Novosibirsk, Russia

Background: The genome is always exposed to different kinds of DNA damaging agents. DNA repair systems in cells are responsible for the genome integrity. The damages, which do not make strong disturbance of double stranded DNA structure, are normally processed by the base excision repair (BER) system. To the moment, this system is well characterized, but the details of regulation are still under investigation. DNA compaction additionally complicates the functioning of repair systems. For successful DNA repair, BER stages, as well as the degree of DNA compaction, should be regulated. Poly(ADP-ribose)polymerase1 (PARP1) and poly(ADP-ribose)polymerase2 (PARP2) are key BER regulatory members, which are also known to participate in the regulation of chromatin remodeling.

Methods: Polyacrylamide gel electrophoresis.

Results: In our study, we focused on the investigation of the influence of PARPs on the activity of major enzymes of the BER system - APE1 and DNA polymerase beta, using both reconstituted nucleosomes and naked DNAs. We obtained the inhibitory effect of PARP1 and PARP2 on the activity of both APE1 and DNA polymerase beta. This effect was attenuated in the presence of NAD⁺, under conditions of poly(ADP-ribosylation).

Conclusion: Our results additionally confirm the currently relevant model for the regulation of the interactions of PARP1 and PARP2 with DNA. In particular, under ADP-ribosylation, autopoly(ADP-ribosylation) of these PARPs occurs that contributes to the dissociation of their complexes with the DNA/nucleosome, due to electrostatic repulsion between the DNA and the negatively charged polymer of ADP-ribose, which is covalently attached to PARP. The structural data could clarify the points of interaction and location of PARPs relative to each other or to nucleosome core and BER proteins during repair.

Key Words: nucleosome, DNA-repair, poly(ADP-ribose)polymerase1, poly(ADP-ribose)polymerase2.

This work was supported by RSF project № 17-74-20075

P-17

http://dx.doi.org/10.21103/IJBM.9.Suppl_1.P17

Structural and functional insights into eukaryotic translation reinitiation and ribosome recycling orchestrated by eIF2D and MCT-1/DENR

Desislava S. Makeeva¹, Elena A. Stolboushkina², Ivan B. Lomakin³, Sergey E. Dmitriev¹

¹Belozersky Institute of Physico-Chemical Biology, Lomonosov Moscow State University, Moscow, Russia; ²Institute of Protein Research, Russian Academy of Sciences, Pushchino, Russia; ³Department of Molecular Biophysics and Biochemistry, Yale University, New Haven, USA

The last stage of translation cycle is ribosome recycling which occurs after completed polypeptide is released. This step comprises dissociation of 60S ribosomal subunit, followed by tRNA and mRNA removal from the 40S-tRNA-mRNA post-termination complex. However, in some cases unrecycled 40S subunit is able to resume scanning on the same mRNA and initiate translation at the next start codon, thus resulting in translation reinitiation.

As previously shown in a reconstituted mammalian system, eukaryotic translation factor eIF2D and a heterodimer of two oncoproteins, MCT-1 and DENR, can operate with tRNA in the ribosomal P-site in two different modes, either stabilizing its binding to a non-canonical 48S initiation complex, or facilitating its removal from the post-termination 40S subunit followed by mRNA dissociation. However, the precise role of these proteins in living cells remained unclear.

Using in vitro translation systems prepared from *S.cerevisiae* mutant strains, we demonstrated that yeast orthologs of eIF2D, MCT-1 and DENR (TMA64, TMA20 and TMA22, respectively) prevent illegitimate reinitiation at the 3' untranslated regions of reporter mRNAs, and reduce reinitiation on mRNAs with uORF. Here we discuss how the recently solved X-ray and cryo-EM structures of the human MCT-1/DENR or eIF2D on the 40S ribosomal subunit provide mechanistic insights into this activity.

C-terminal regions of eIF2D and DENR contain SUI1 domain, which is also present in SUI1/eIF1, a factor controlling stringency of AUG recognition during translation initiation. Structural data indicate that, similarly to eIF1, the SUI1 domains of DENR and eIF2D are positioned in the P-site, modulating tRNA binding and codon-anticodon interaction. Other portions of the eIF2D or MCT-1/DENR molecules, including DUF1947 and PUA domains, provide an interface for tRNA CCA-end binding and occupy landing sites for canonical translation initiation factors eIF2 and eIF3 on the 40S subunit.

Based on these data, we proposed a model of how eIF2D (TMA64) and MCT-1/DENR (TMA20/TMA22) control translation reinitiation by forcing 40S recycling and preventing binding of eIF1, eIF2 and eIF3 to the post-termination 48S complex.

Key Words: protein synthesis, translation reinitiation and ribosome recycling, eIF2D/ligatin, MCTS1

This work was supported by the Russian Science Foundation (grant RSF 18-14-00291 to S.E.D.) and the Russian Foundation for Basic Research (grant RFBR 18-04-01331 to E.A.S.).

P-18

http://dx.doi.org/10.21103/IJBM.9.Suppl_1.P18

PARP1-induced structural rearrangements are enhanced in cisplatin-treated nucleosomes

Natalya Maluchenko¹, Alexey Feofanov^{1,2}, Mikhail Kirpichnikov^{1,2}, Vasily Studitsky^{1,3}, Nadezhda Gerasimova¹

¹Faculty of Biology, Lomonosov Moscow State University, Moscow, Russia; ²Shemyakin-Ovchinnikov Institute of Bioorganic Chemistry, Russian Academy of Sciences, Moscow, Russia; ³Fox Chase Cancer Center, Philadelphia, USA

Background: Cisplatin (Fig. 1) is a low molecular weight platinum-containing compound with a square planar geometry. It is widely used for the treatment of different cancers. Its mode of action is related to its ability to damage DNA through cross-linking of the adjacent purine bases followed by the appearance of different adducts (Fig. 1). The platinum-DNA adducts can induce local distortions of DNA and form micro-loops. Despite the fact that patients initially are responsive to cisplatin therapy, resistance to this drug develops later. The resistance is often associated with overexpression of poly(ADP-ribose)polymerase 1 (PARP1) in tumor cells. PARP1 acts as a repair enzyme and assists in cell survival after treatment with DNA-damaging agents. Numerous evidence indicate that a level of PARP1 expression and drug-resistance of tumors correlate. The present work is devoted to the study of the effect of cisplatin on PARP1-dependent structural rearrangements of chromatin.



Fig. 1. Experimental system. (a) Cisplatin binds to DNA, bends it and induces adduct formation. (b) The mononucleosomes used in our studies contained 20-bp extending DNA regions. Stars indicate positions of fluorescent Cy3/Cy5 labels.

Methods: Mononucleosomes were assembled from histone octamers and short DNA containing a nucleosome positioning sequence. To make nucleosomes suitable for structural studies, two single pairs of Cy3/Cy5 labels were introduced into a core or linker region of nucleosomal DNA (NI and NII, respectively, fig. b). Single particle Forster resonance energy transfer microscopy (spFRET-microscopy) was employed to examine structural rearrangements in NI and NII induced by cisplatin and PARP1. Measurements and data analysis were performed as described previously.

Results: spFRET-microscopy analysis of NI and NII treated with CYS10 (10 μM for 12 h) indicates that adduct formation does not affect DNA folding within a core region but changes conformation of DNA in the linker region of a nucleosome. Formation of complexes between PARP1 and nucleosomes affect the DNA structure both in the core and linker regions, increasing the distance between neighboring DNA gyres in the core region and decreasing a distance between DNA linkers. Thus, spFRET-microscopy data show that formation of complexes between PARP1 and nucleosomes pretreated with cisplatin is accompanied by the more pronounced structural rearrangements both in the core and linker regions of nucleosomes as compared to PARP1-nucleosome complexes.

Conclusion: PARP1-induced structural changes in nucleosomes likely facilitate access of the repair enzymes to nucleosomal DNA. The more efficient remodeling activity of PARP1 on cisplatin-modified nucleosomes could explain the more efficient DNA repair of cisplatin-induced lesions and high cisplatin resistance of cancer cells overexpressing PARP1 observed previously.

Key Words: Cisplatin, PARP1, nucleosomes, spFRET

Financial support by RFBR grant №17-00-00163 (17-00-00132, 17-00-00097) is acknowledged.

P-19

http://dx.doi.org/10.21103/IJBM.9.Suppl_1.P19

Cryo-EM structure of a new thiazole/oxazole-modified microcin – phasolicin – in complex with bacterial ribosome provides basis for species-specific activity of ribosome-targeting antibiotics

Dmitrii Y. Travin^{1,2}, Zoe Watson³, Mikhail Metelev^{1,2}, Fred Ward³, Ilya A. Osterman^{1,4}, Irina M. Khven^{4,5}, Marina Serebryakova⁴, Yury S. Polikanov^{6,7}

¹Center for Life Sciences, Skolkovo Institute of Science and Technology, Moscow, Russia; ²Institute of Gene Biology, Russian Academy of Science, Moscow, Russia; ³Department of Molecular and Cell Biology, University of California, Berkeley, USA; ⁴A.N. Belozersky Institute of Physico-Chemical Biology, Lomonosov Moscow State University, Moscow, Russia; ⁵Department of Bioengineering and Bioinformatics, Lomonosov Moscow State University, Moscow, Russia; ⁶Department of Biological Sciences, University of Illinois at Chicago, Chicago, Illinois, USA; ⁷Waksman Institute for Microbiology, Rutgers, the State University of New Jersey, Piscataway, USA

Background: Ribosomally synthesized and posttranslationally modified peptides (RiPPs) form a rapidly expanding class of natural products and serve as a source of new compounds with various biological activities. Linear azole-containing peptides (LAPs) comprise a relatively small heterogeneous subclass of RiPPs that exhibit extremely diverse mechanisms of action sharing many common structural features.

Results: Here we report the discovery of a new LAP biosynthetic gene cluster Pop5 in the genome of *Rhizobium* sp., which led to the identification of phasolicin (PHS) – an extensively modified ribosomally synthesized peptide exhibiting narrow-spectrum antibacterial activity against a set of bacterial species from Rhizobiales, symbiotic bacteria from the root nodules of various leguminous plants. PHS compound inhibits prokaryotic translation by binding to the 70S ribosome and obstructing nascent peptide exit tunnel through which an emerging protein exits the ribosome. We have also obtained cryo-EM structure of the *Escherichia coli* ribosome in complex with PHS that revealed a notably different mode of interaction with both the 23S rRNA and the ribosomal proteins uL4 and uL22 as compared with the recently published LAP klebsazolicin (KLB). Unlike KLB, PHS binds further away from the peptidyl transferase center where it interacts with the loops of proteins uL4 and uL22. Our microbiological data suggest that the sequence of the protein uL4 loop determines whether the PHS compound can bind to the ribosome and provides the basis for the species-specific activity of ribosome-targeting antibiotics.

Conclusions: PHS and its predicted homologs from genomes of other bacterial species expand the known diversity of LAPs, which potentially can be used as biocontrol agents for the needs of agriculture.

Key Words: Phasolicin, translation inhibitor, antibiotic, linear azole-containing peptides, RiPPs, *Rhizobium* natural products.

P-20

http://dx.doi.org/10.21103/IJBM.9.Suppl_1.P20

Linker histone H1: the interplay between chromatosome stability, oncomutations and post-translational modifications

Mikhail V. Bass, Grigoriy A. Armeev, Alexey K. Shaytan

Department of Bioengineering, School of Biology, Moscow State University, Moscow, Russia

Background: Variations in the sequence of linker histone (LH) H1 play an important role in the modulation of chromatin functioning. Meanwhile, an effect of LH variations on the chromatin structure remains unclear. The most common mutations of the core histones are located in their globular domains (GD) and many of them coincide with post-translational modifications (PTM) sites. It is known that five mutations in GD of *Drosophila* H1 can change LH position in the chromatosome from “off-dyad” to “on-dyad”. Given polymorphism of chromatosome structure, an investigation of the effect of different LH variants on the chromatosome structure is extremely relevant.

Methods: Amino acid sequences of human LH H1.2, H1.4, and H1.5 were obtained from HistoneDB database. For homology modeling, the crystal structure of the chromatosome was used (PDB ID 4qlc) as a template. Post-translational modifications in the globular domain of linker histone H1, listed in the UniProt database, were considered for analysis. In order to analyze potential driver mutations, oncomutations of LH that were reported in the COSMIC database more than once were analyzed. Using FoldX software based on an empirical force field we measured the difference in binding free energy between the two states (1):

$$\Delta\Delta G_{bind} = \Delta G_2 - \Delta G_1 \quad (1)$$

where and are the binding free energies for a complex with or without a mutation (or PTM), respectively. For PTMs that could not be handled by FoldX, the screening of their positions for potential steric constraints was done using UCSF Chimera by changing the torsion angles of the modified side chains.

Results: Using FoldX we have estimated binding energy differences for 45 missense oncomutations and 27 PTM of human LH H1.2, H1.4 and H1.5. Oncomutations S58F and S104F of LH H1.2 manifested significant binding energy changes (2.33 and 4.10 kcal/mol, respectively). These energies, however, are less than the experimentally measured free energy of dissociation of H1 in the presence of 0.2 M NaCl, which is 8.5 kcal/mol. Screening of PTM position allowed us to select variations of LH H1, which increase or decrease stability of the chromatosome.

Conclusion: We estimated the effect of PTM and oncomutations in GD of human LH on the chromatosome stability. PTM sites, in which additional positioning contacts between DNA and LH emerged, were determined. On the basis of the analysis, we can suggest that certain LH oncomutations may considerably change its binding affinity to nucleosome, potentially, affecting chromatin structure.

Key Words: nucleosome, chromatin, free energy calculations, histones

This work was supported by the Russian Science Foundation (project no. 19-74-30003).

P-21

http://dx.doi.org/10.21103/IJBM.9.Suppl_1.P21

The oligomeric state of base excision DNA repair proteins and their complexes explored by Dynamic light scattering

Inna A. Vasil'eva, Nina A. Moor, Rashid O. Anarbaev, Olga I. Lavrik
Institute of Chemical Biology and Fundamental Medicine, Siberian Branch of the Russian Academy of Sciences, Novosibirsk, Russia

Background: Base excision DNA repair (BER) is very efficient process that involves the action of many enzymes and accessory proteins to correct the most common DNA lesions usually induced by ionizing irradiation and oxidative stress. Coordination of BER depends on assembling protein participants into multicomponent dynamic "repairosome". Knowledge of the oligomeric states of protein complexes is useful for their structural studies. The primary aim of our work was to estimate the oligomeric states of enzymes and coordinating proteins of BER and of their complexes characterized previously by using fluorescence-based approach.

Methods: We employed dynamic light scattering (DLS) technique to measure the hydrodynamic sizes of several enzymes and proteins, DNA polymerase β (Pol β), apurinic/apyrimidinic endonuclease 1 (APE1), tyrosyl-DNA phosphodiesterase 1 (TDP1), X-ray repair cross-complementing protein 1 (XRCC1) and poly(ADP-ribose) polymerase 1 (PARP1), present alone or in the equimolar mixtures with each other. DLS measurements were performed in solution under true equilibrium conditions by using a Zetasizer Nano ZS instrument. Glutaraldehyde cross-linking was used to analyze the prevailing complexes in the proteins mixtures.

Results: The hydrodynamic radii of the protein particles determined from the volume weighted size distribution profiles have been used to estimate the oligomeric states of proteins and their complexes. All the proteins of different molecular weights and functions in BER have been proposed to form homodimers upon their self-association. The most probable oligomerization state of the binary complexes formed by PARP1 with various proteins is a heterotetramer (dimer of heterodimers). On the contrary, the oligomerization state of XRCC1 hetero-associated complexes has been shown to vary from the heterodimer (complex with APE1) to the heterotetramer (complexes with Pol β , TDP1 and PARP1). PARP1 was revealed to destabilize strong interaction between Pol β and XRCC1, suggesting modulation of the proteins association mode upon assembling higher order complexes.

Conclusion: Our study demonstrates for the first time applicability of the DLS technique for determination of the oligomeric states of various proteins and their complexes, when complemented with fluorescence-based and chemical cross-linking approaches.

Key Words: Base excision DNA repair complexes, dynamic light scattering, oligomeric state.

This work was supported by the RSF project 19-14-00107.

MOLECULAR ORGANIZATION OF CELLS AND ORGANELLES

P-22

http://dx.doi.org/10.21103/IJBM.9.Suppl_1.P22

The tannoglobule is a phenolic compounds compartment of the Maloideae (rosaceae) pericarp cells

Tamara K. Kumachova¹, Alexander S. Voronkov²

¹Timiryazev State University of Agriculture (Moscow Agriculture Academy), Moscow, Russia; ²K.A. Timiryazev Institute of Plant Physiology RAS, IPP RAS, Moscow, Russia

Background: In the Maloideae, pericarp cells were discovered, previously not described for this subfamily, the structural units of tannosome. Data on the tannosomes merge in the vacuoles to form tannoglobules has been obtained for the first time.

Methods: The samples were fixed in glutaraldehyde and subjected to a standard procedure of dehydration, contrast and pouring with some modifications. A JEM-1400 transmission electron microscope (JEOL, Japan) was used for the analysis of ultrathin sections.

Results: We were the first to observe tannosomes, structural units not detected in earlier studies of Maloideae, in the cells of the external zone of the pericarp. Electron microscopic studies showed that some chloroplasts of the subepidermal layer (hypodermal) cells contained electron-dense material that had the appearance of isolated small particles attached to the internal surface of the swollen thylakoid membrane or granular bead-like structures that protruded into the lumen. According to our observations, the tannosome is released from the chloroplast as a shuttle, regardless of the tannosome formation pathway. Tannosomes were sometimes scattered over the entire cytoplasm as small electron-dense membrane-enclosed structures similar to the endoplasmic reticulum (ER). This allowed the assumption that tannins were also synthesized in ER cisterns and subsequently transported to the vacuoles. These particles were subsequently merged in the vacuoles to form large tannin aggregates or tannoglobules. Our study revealed the variable morphology of tannin deposits in the vacuoles: they could be represented by coarse- or fine-grained electron-dense material, separate electron-dense bodies of oval or round shape (two to five or more per section), or isolated conglomerates or a continuous layer of flakes on the internal side of the tonoplast. The tannoglobules detected in the vacuoles of pericarp cells may represent one of the forms of the deposition of polyphenol compounds as reserve substances.

Conclusion: Thus, we have shown specific compartmental of polyphenolic substances, namely the formation of tannoglobules in the Maloideae pericarp cells. These formations can be a temporary storage place for these substances, playing an important adaptive and protective function.

Key Words: Tannosome, tannoglobules, polyphenolic substances, Maloideae.

P-23

http://dx.doi.org/10.21103/IJBM.9.Suppl_1.P23

Structural studies of DNA-Dps co-crystals formation

Andrey Moiseenko¹, Natalia Loiko^{2,3}, Ksenia Tereshkina³, Yana Danilova¹, Oleg Chertkov¹, Alexey V. Feofanov^{1,4}, Yurii Krupyanski³, Olga S. Sokolova¹

¹Faculty of Biology, Lomonosov Moscow State University, Moscow, Russia; ²FRC "Fundamentals of Biotechnology" RAS, Moscow, Russia; ³Semenov Institute of Chemical Physics, RAS, Moscow, Russia; ⁴Shemyakin-Ovchinnikov Institute of bioorganic chemistry, RAS, Moscow, Russia

Background: One of the universal mechanisms for the response of E.coli to stress is the increase of the synthesis of specific histone-like proteins that bind the DNA: Dps. As a result,

two-and three-dimensional crystalline arrays may be observed in the cytoplasm of starving cells.

Methods: The Dps protein was expressed in *E.coli*. A fluorescently labeled DNA template with a sequence of s603 (165 b.p) was obtained using a PCR/ Confocal laser scanning fluorescent images were recorded with an inverted LSM710-Confocor3 microscope (Zeiss, Germany). The stained grids were studied on an analytical transmission electron microscope JEM-2100 (JEOL, Japan) equipped with a LaB6 filament, with an accelerating voltage of 200 kV and low-dose conditions. The three-dimensional models of Dps crystals, and DNA-Dps co-crystals were constructed in the UCSF Chimera program package.

Results: Here, we determined the conditions to obtain very thin two-dimensional DNA-Dps co-crystals in vitro and studied their projection structures using electron microscopy. Analysis of the projection maps of the free Dps crystals revealed that they form two lattice types: hexagonal and rectangular. We used the fluorescently labeled 165 b.p. DNA fragment to prove that the DNA forms the co-crystals with Dps in vitro and to visualize the DNA's position. When comparing the structures of the co-crystals to the 2D crystals of free Dps, we observed extra-densities between Dps molecules that were 2 nm in diameter. Molecular modeling confirmed that DNA molecules may be located in the crevices between Dps molecules where positive-charged N-termini are exposed, or, alternatively, interact with the sides of the Dps molecules. We have also suggested a model for the DNA-Dps co-crystal dissolving in the presence of Mg²⁺ ions.

Conclusion: In conclusion, our findings indicate that both models of DNA interactions with Dps may exist in the course of the co-crystal formation: the model suggested by, apparently, describes the mature DNA-Dps co-crystal, while the model of alternating layers may represent the earlier stages of co-crystal dissolving and DNA release.

Key Words: Dps; two-dimensional crystals; Fourier transform; electron microscopy.

Fluorescent microscopy investigation was supported by Russian Science Foundation (19-74-30003). Electron microscopy was performed with the support of RFBR (19-04-00605). N.L., K.T., V.K. and Yu.K. thank the Ministry of Education and Science of Russia for the provided support within the frameworks of the state tasks for ICP RAS (0082- 2014-0001 and 0104-2019-0005).

P-24

http://dx.doi.org/10.21103/IJBM.9.Suppl_1.P24

Extracellular matrix secreted by stromal cells from soft tissues contain extracellular vesicles-like structures

Ekaterina S. Novoseletskaya^{1,2}, Georgy D. Sagaradze¹, Nataliya A. Basalova^{1,2}, Olga A. Grigorieva¹, A. Yu. Efimenko^{1,2}

¹Institute for Regenerative Medicine, Medical Research and Education Center, Lomonosov Moscow State University, Moscow, Russia; ²Faculty of Medicine, Lomonosov Moscow State University, Moscow, Russia

Background: In recent years the role of extracellular vesicles (EV) in various biological processes has been actively studied. Interest in this object is caused by the fact that EV, which are nanoscale bilipid spherical containers, can transfer between cells a wide range of substances from noncoding RNA, including microRNAs (Phinney et al., 2015), to entire receptors (Andaloussi

et al., 2013) and ion channels (Setti et al., 2015). In addition, the presence of EV in the composition of the extracellular matrix (ECM) of bone and cartilage is confirmed. ECM plays an important role in controlling cell behavior – viability, proliferation, migration and differentiation. Thus, the aim of this work was to evaluate the presence of EV in ECM secreted by stromal cells from soft tissues using electron microscopy.

Methods: We isolated human dermal fibroblasts and mouse pulmonary fibroblasts. Also, we used immortalized human mesenchymal stromal cells (MSC) derived from adipose tissue. The cells were cultured until formation of cell sheet with prominent deposition of ECM. After that, ECM was isolated by decellularization using incubation with CHAPS and then DNase I. Samples were transferred to glass and were conducted through standard sample preparation for electron microscopy.

Results: According to the obtained results, EV-like structures were found in all samples of ECM produced by stromal cells of different tissues. Also we investigate the cell sheet formation and dynamics of EV-like structures deposition in ECM. It was shown that EV-like structures were similar to migrasomes. Previously, we found that EV secreted by adipose-derived MSC could prevent the differentiation of fibroblasts into myofibroblasts (Basalova et al., 2018). We also confirmed that ECM produced by MSC and isolated by decellularization retained biological activity toward different types of cells (Kuznetsova et al., 2018).

Conclusion: In summary, we have isolated the ECM secreted by different types of stromal cells from soft tissues. The presence of EV-like structures in the composition of all the samples was shown. These data may indicate their possible participation in the functioning of organs.

Key Words: extracellular vesicles, extracellular matrix, stromal cells, soft tissue

This work was supported by Russian Scientific Foundation (grant agreement #19-75-30007).

P-25

http://dx.doi.org/10.21103/IJBM.9.Suppl_1.P25

Cryo-electron microscopy of extracellular vesicles from cerebrospinal fluid

Tatiana A. Shtam¹, Anton K. Emelyanov^{1,2}, Roman A. Kamyschinsky^{1,5}, Luiza A. Garaeva^{1,2}, Nikolay A. Verlov¹, Anastasia Kudrevatykh³, Gaspar Gavrilov⁴, Sofia N. Pchelina^{1,2,3}

¹Petersburg Nuclear Physics Institute named by B.P.Konstantinov of NRC «Kurchatov Institute», St. Petersburg, Russia; ²Pavlov First Saint Petersburg State Medical University, St. Petersburg, Russia; ³Institute of Experimental Medicine, St. Petersburg, Russia; ⁴S.M. Kirov Saint-Petersburg Military Medical Academy, St. Petersburg, Russia; ⁵National Research Center “Kurchatov Institute”, Moscow, Russia

Background: Extracellular vesicles (EVs) are membrane-enclosed vesicles which play important role for cell communication. EVs are found in many human biological fluids; contain proteins, nucleic acids and lipids. These vesicles deliver biological information to recipient cells thereby modulating their behaviors. In this way EVs are involved in the pathological development of many human disorders, including neurodegenerative diseases. Definition of the EV size and morphology is important for studying of their participation in the intercellular signaling pathways in pathology and normal state. Especially for understanding the role of EVs in the pathogenesis of brain, detailed characterization of

the vesicles from cerebrospinal fluid seems to be the most relevant.

Methods: In this study EVs purified from cerebrospinal fluid or plasma of patients with Parkinson's disease were characterized using cryo-electron microscopy (cryo-EM), nanoparticle tracking analysis (NTA) and flow cytometry.

Results: The size of the observed vesicles and the presence of protein exosomal marker on the membrane confirmed by NTA and flow cytometry, suggest that most of the vesicles were represented as exosomes. According to the NTA analysis the concentration EVs in the cerebrospinal fluid ($(6.1 \pm 4.9) \times 10^9$ particles/ml) is two orders of magnitude lower than that in blood plasma ($(19.8 \pm 14.9) \times 10^9$ particles/ml). Vesicles isolated from cerebrospinal fluid were examined in detail using cryo-EM. EVs of various sizes and morphology with lipid bilayer and vesicle internal structures were observed. More than 80 percent of the particles were classified as vesicles due to the clear presence of lipid bilayer membrane. The majority of vesicles was intact and had a round shape. Single (74.9 ± 27.24 nm), double (179.49 ± 105.29 nm) and multilayer vesicles (206.18 ± 78.3) were visualized. We found that multilayer vesicles were larger than the single vesicle ($p < 0.0001$). Vesicles were assigned into multilayer category when two or more vesicles were contained inside a larger one. Various combinations, having from two to six vesicles inside the one were also found.

Conclusion: Here, we described the characteristics of the vesicles from cerebrospinal fluid and found their variety suggesting that subpopulations of EVs with different and specific functions may exist.

Key Words: cryo-electron microscopy, cerebrospinal fluid, extracellular vesicles, Parkinson's disease.

Cryo-EM experiments were supported by the RSF (project 19-74-20146). All other experiments were supported by the RSF (project 17-75-20159).

P-26

http://dx.doi.org/10.21103/IJBM.9.Suppl_1.P26

Study of vimentin unit-length filaments aggregation in presence of different polymers

Anna V. Vakhrusheva¹, Pavel I. Semenyuk¹, Natalia V. Medvedeva², Alexander A. Minin², Olga S. Sokolova¹

¹Lomonosov Moscow State University, Moscow, Russian Federation;

²Institute of Protein Research of Russian Academy of Sciences, Moscow, Russian Federation

Background: Cell migration is one of the important processes, where cytoskeleton takes the main part. Vimentin intermediate filaments are also implicated in cell migration and adhesion, but their role is not clear yet. So, earlier we have investigated the influence of different vimentin forms (knocked out, with mutation that blocks filament formation on the stage of ULFs, and normal filaments) on the polarity determination in rat fibroblasts. Based on these results we have shown the principle role of vimentin even in the form of ULFs in determination of the cellular polarity and the directionality of cell migration. But ULFs are prone to aggregate, so in order to get their structure by electron microscopy we decided to investigate the influence of different polymers on prevention of ULFs aggregation.

Methods: To investigate the aggregation of ULFs we used the method of dynamic light scattering. The polymers such as dextran sulfate and heparin were mixed with filaments in different concentrations to prevent the aggregation.

Results: The ULFs assembly was conducted by adding of high salt concentration (160 mM NaCl). The process of aggregation was determined, mainly, at 37°C, and during various time periods - 15 minutes and 1 hour. The results revealed the start of aggregation after 15 minutes of incubation. The hydrodynamic diameters of aggregated ULFs were from 120 nm to 350 nm depending on the incubation time, while the approximate hydrodynamic diameter of single ULF is 70-80 nm. Addition of polymers, such as dextran sulfate and heparin at different concentrations, maintained the ULFs in separate mode during one-hour incubation at 37°C with hydrodynamic diameter of 80 nm.

Conclusion: Based on the obtained results we can conclude that both polymers, dextran sulfate and heparin, positively influence on ULFs separation and prevent their aggregation. Thus, this approach may help us for getting the single vimentin ULFs by electron microscopy in order to determine their structure.

Key words: ULF (unit-length filament), vimentin, aggregation, dynamic light scattering.

DLS experiments were supported by RSF grant (14-14-00234 to O.S.S) and protein purification by RFBR grant (17-04-01775 to A.A.M).

P-27

http://dx.doi.org/10.21103/IJBM.9.Suppl_1.P27

Computational modeling of tubulin protofilament relaxation during rapid freezing

Dmitrii S. Vinogradov¹, Evgeniy V. Ulyanov², J. Richard McIntosh³, Fazoil I. Ataullakhanov^{1,2}, Nikita B. Gudimchuk^{1,2}

¹Center for theoretical problems of physicochemical pharmacology, Moscow, Russia; ²Physics Department, Lomonosov Moscow State University, Moscow, Russia; ³MCD Biology Department, University of Colorado, Boulder, CO, USA

Background: Over the recent years, there has been a burst of ground-breaking studies, based on cryo-EM. They shed light on various intracellular structures, including microtubules (Alushin et al., 2014; Manka and Moores, 2018). Composed of 13 laterally stacked tubulin protofilaments, microtubules can exist in growth and shortening states, enabling them to search and capture chromosomes in mitosis. In our recent cryo electron tomography study we directly examined the shapes of protofilaments at the microtubule tips (McIntosh et al., 2018). We discovered an unexpected feature of tubulin protofilaments: they were highly curved at the tip, but progressively less curved as one moved closer to the microtubule lattice.

Methods: We have hypothesized that the gradient of curvature in protofilaments could be explained by their incomplete relaxation during rapid freezing. To test this idea, here we use Brownian dynamics method (ErmaK and McCammon, 1978). Protofilament is described as longitudinally bounded spheres, approximating tubulin monomers that can move only in the plane containing microtubule axis. Cooling rates achieve 10^6 - 10^7 K/s (Dubochet et al., 1988). Water viscosity increases in response to temperature drop according to published data (Dehaoui et al., 2015).

Results: We simulated fast freezing of soft and rigid protofilaments, having flexural stiffness coefficients of 35 and 174 kcal•mol⁻¹•rad⁻², respectively. At 10^6 K/s freezing rate both soft and rigid protofilaments had enough time to relax before cryo-immobilization, so that no gradient of curvature was predicted. When cooled at 10^7 K/s, rigid protofilaments again had enough time to fully relax. However, soft protofilaments displayed a

gradient of curvature, very similar to our experimental data. This suggests that in principle fast freezing could cause the gradient of curvature.

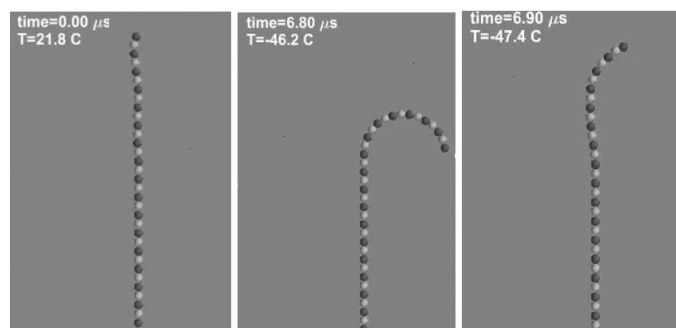


Fig. 1. Snapshots from protofilament freezing simulation. From left to right: initial straight state of protofilament, frozen protofilament with high flexural rigidity and frozen protofilament with low flexural rigidity. Cooling rate is 10^7 K/s.

Conclusion: Due to fast cooling, configurations of some large biomolecules, captured by cryo-EM, may represent snapshots of their incompletely relaxed states. Thus, additional using Brownian dynamics method can be helpful to correctly interpret cryo-EM data.

Key Words: microtubules, tubulin, cryo electron microscopy, freezing

This work was supported by Russian Science Foundation grant #17-74-20152 to N.G. The research was carried out using the equipment of the shared research facilities of HPC computing resources at Lomonosov Moscow State University.

STRUCTURE OF VIRUSES AND CHAPERONINS

P-28

http://dx.doi.org/10.21103/IJBM.9.Suppl_1.P28

Protocol of tick-borne encephalitis virus sample preparation for structural studies

Anton Y. Fedotov¹, Mikhail F. Vorovitch^{1,3}, Kseniya K. Tuchinskaya¹, Konstantin V. Grishin¹, Olga I. Konyushko¹, Dmitry I. Osolodkin^{1,2}, Aidar A. Ishmukhametov¹, Alexey M. Egorov^{1,2}

¹FSBSI "Chumakov FSC R&D IBP RAS", Moscow, Russia; ²Lomonosov Moscow State University, Moscow, Russia; ³Sechenov First Moscow State Medical University, Moscow, Russia

Background: Tick-borne encephalitis virus (TBEV), a member of genus *Flavivirus*, is an important human pathogen: up to 10,000 cases of TBE disease are registered in Europe and Asia annually. Inactivated vaccines are widely used to prevent the disease. The structure of viral particles forming the vaccine antigen was never studied in details sufficient to characterize them on the atomic level. Thorough characterization of the inactivated viral particles would allow their comparison with the native virus particles for the rational structure-based vaccine design. Such an information is important for understanding the virus neutralization and inactivation mechanisms, as well as for the comparison of the epitopes inducing the immunological response in the inactivated preparations and wild-type virions.

X-Ray Free Electron Lasers (XFEL) provide a unique opportunity to study the time-resolved solution structures of large macromolecular assemblies, such as viruses. In the

single particle approach, a suspension of the viral particles is injected into the X-ray beam with the help of electrospray. The method requires substantially high concentration of particles, homogeneity, absence of aggregates and large volume.

Methods: The prototype TBEV strain Sofjin was chosen as the model for developing the flavivirus sample preparation protocol for XFEL studies. Viral particles in the resulting samples were quantified by ELISA and RT-PCR. Negative staining electron microscopy and cryoelectron microscopy are the methods of choice for the quality control of flavivirus preparation. As flavivirus virions are enveloped, their preparation for electrospray injection requires a characterization of the particle rigidity.

Results: TBEV was grown using primary or continuous cell cultures. Several protocols, based on filtration, centrifugation, and chromatography, were applied to purify inactivated TBEV particles. The concentration of the sample obtained according to the optimized protocol was $\sim 10^{13}$ mL⁻¹.

Conclusion: The purification protocol based on the combination of tangential flow filtration and two steps of ultracentrifugation, one of them through the sucrose gradient, was the most efficient for obtaining high concentrated, non-aggregated virus suspension suitable for XFEL studies.

Key words: TBEV, structure, XFEL.

This work is supported by the Russian Foundation for Basic Research (grant no. 18-02-40026).

P-29

http://dx.doi.org/10.21103/IJBM.9.Suppl_1.P29

Quality control of tick-borne encephalitis virus samples using TEM and SAXS for XFEL studies

Valeriya R. Samygina^{1,2}, Evgeny B. Pichkur^{1,2,3}, Mikhail F. Vorovich⁴, Petr V. Konarev^{1,2}, Georgy S. Peters¹, Dmitry I. Osolodkin⁴, Aidar A. Ishmukhametov⁴, Alexey M. Egorov^{4,5}

¹NRC "Kurchatov Institute", Moscow, Russia; ²FSRC "Crystallography and Photonics", Moscow, Russia; ³B.P. Konstantinov Petersburg Nuclear Physics Institute of NRC "Kurchatov Institute", Gatchina, Russia; ⁴FSBSI "Chumakov FSC R&D IBP RAS", Moscow, Russia; ⁵Chemistry Department, M.V. Lomonosov Moscow State University, Moscow, Russia

Background: Tick-borne encephalitis virus (TBEV) from flavivirus family is an important human pathogen causing a wide range of symptoms from uncomplicated fevers to encephalitis and meningoencephalitis. XFEL studies can provide new insight into TBEV structure to further improve the vaccine design. Flaviviruses are promising objects for XFEL/SPB (single particle biology) experiments for several reasons: 1) their structural investigations have clinical significance; 2) symmetry of particles is an advantage for XFEL data processing; 3) particles size (~ 50 nm) is relatively large. XFEL is a cutting-edge method supposed to revolutionize structural biology by providing possibility to obtain 3D structures of biomolecules in their 'native state'. Although the determination of molecular structures at high resolution using the diffraction-before destruction approach with XFEL pulses is feasible in theory, there still remain many challenges for sample delivery, detector calibration and algorithm development for sample sorting. The method has special requirements regarding sample quantity and quality. Large volume, relatively high concentration, absence of aggregates and homogeneity of the sample are required.

Aggregates and broken particles cause problems during sample delivery and data processing. Preparation of TBEV samples at high concentration ($\sim 10^{13}$ - 10^{14}) without aggregates and with minimum amount of broken particles (which cannot be removed completely due to the TBEV structural heterogeneity) might be tricky and has to be controlled reliably. TEM negative staining technique is a common technique for characterizing viral suspensions, although it sometimes produces artifacts and has certain limitations.

Methods: Here we present an approach for the sample quality control which combines both negative staining TEM, cryoEM and small-angle X-ray scattering (SAXS).

Results: Negative staining TEM allows one to visualize TBEV particles while cryoEM and SAXS are employed to check sample in case of “aggregate-like” clusters finding. SAXS additionally gives an estimation of particles size volume distribution in at the same physical-chemical conditions as for XFEL experiment.

Conclusion: Combination of methods was significant for choice of sample preparation protocol. This hybrid approach makes an important contribution in successfulness of injection test at XFEL beamline. It can be useful for other virus samples evaluation for SPB experiment.

Key Words: flavivirus, cryoEM, SAXS

This work is supported by RFBR 18-02-40026.

P-30

http://dx.doi.org/10.21103/IJBM.9.Suppl_1.P30

Structure of bacteriophage SU10 from the family *Podoviridae*

Marta Šiborová¹, Tibor Füzik¹, Martin Benešik², Anders S. Nilson³, Pavel Plevka¹

¹Structural Virology, Central European Institute of Technology, Brno, Czech Republic; ²Laboratory of Microbial Molecular Diagnostics, Faculty of Science, Masaryk University, Czech Republic; ³Department of Molecular Biosciences, The Wenner-Gren Institute, Stockholm University, Stockholm, Sweden

Background: Bacteriophage SU10, from the family *Podoviridae*, infects a wide range of *E. coli* strains. The phage has 77kbp dsDNA genome, prolate capsid with the length of 135 nm and the diameter of 42 nm. Contrary to what was observed in most *Podoviridae* phages, bacteriophage SU10 has 27 nm long tail. Furthermore, the baseplate of SU10 changes conformation upon attachment to the host.

Methods: We used cryo-electron microscopy and localized single particle reconstruction techniques to determine the structure of capsid, portal, tail and base plate of SU10. Furthermore, we also characterized their conformational changes associated with cell-wall binding and genome ejection.

Results: Prolate capsid is formed by 11 pentons and 110 hexons of major capsid protein. Major capsid protein has HK97 fold. The dodecameric portal complex has prolonged crown-barrel, similar to that of phage P22. Three types of fibers, all present in six copies, decorate the phage particle. Collar fibers are connected to the neck protein. Long tail fibers connected to the upper tail protein are similar to that of phage T4 and short tail fibers are positioned on bottom part of the base plate.

Conclusion: Our studies of structural changes of tail and base plate extend the current knowledge of the mechanism of host recognition and genome delivery of bacteriophage SU10.

Key Words: bacteriophage, localized single particle reconstruction, *Podoviridae*, *E. coli*

P-31

http://dx.doi.org/10.21103/IJBM.9.Suppl_1.P31

Structure of *Pseudomonas aeruginosa* Luz-24-like phage U47

Evgeny Pichkur^{1,2,3}, Valery Novoseletsky⁴, Mikhail Shneider⁵, Anton Sedov⁵, Nina Sikilinda⁵, Konstantin Miroshnikov⁵, Olga Sokolova⁴

¹National Research Center “Kurchatov Institute”, Moscow, Russia; ²Petersburg Nuclear Physics Institute-National Research Center “Kurchatov Institute”, Gatchina, Russia; ³FSRC “Crystallography and Photonics”, Moscow, Russia; ⁴Lomonosov Moscow State University, Moscow, Russia; ⁵SIBCh RAS, Moscow, Russia

Background: Phage U47 belongs to the Luz24-virus genus of the *Podoviridae* family. Due to the effective mechanism of host metabolism suppression and an ability to penetrate bacterial biofilms Luz24-like *Pseudomonas aeruginosa* phages prospective for phage therapy applications. The relatively long tail of U47 makes it a promising model for structural studies of podoviruses. Yet, the structural information concerning adsorption complex of podoviruses, which is crucial for understanding of the infection process, is limited.

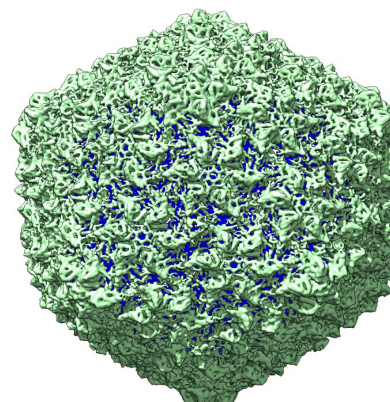


Fig. 1. Phage U47.

Methods: For the purification of the U47 phage, we used ultracentrifugation in a cesium gradient and further dialysis against buffer with low osmotic pressure. U47 solution was mixed 10:1 with 0.05% Tween 20. 3ul of the sample were applied onto the hydrophilized holey carbon support film (Quantifoil 1.2/1.3). A total of 6500 movies were collected using cryo-TEM Krios (Thermo-Fisher, USA) at acceleration voltage 300kV, pixel size 1.15Å, flux approx. 100 e/Å²s. Motion correction and CTF estimation was performed using Warp, particles were picked and processed in CryoSPARC and Relion 3.0. In spite of the absence of highly similar homologues molecular model of this protein was built with Modeller using HHpred for homology search. As templates served the structures of the major capsid proteins from bacteriophages Hk97 (pdb: 1OHG) and phi812K1-420 (pdb: 5LII). Structural model was fitted into the obtained cryo-EM density map.

Results: We have obtained the icosahedral reconstruction of the U47 phage capsid with a resolution of 4.5 ~ 6Å and the reconstruction of its tail with C6 symmetry. The elongated tail structure can be divided into 2-3 structural compartments (similar to the T7 phage; tail fibrils are visible that are attached to the distal tail protein; the tail possesses a distal spike, located

parallel to the long axis of the tail, similar to that of phages P22 and SF6. Also, the globular domain is clearly visible.

Conclusion: Here, we have, for the first time, reconstructed the capsid and tail of the *Paeruginosa* U47 phage and demonstrated that it possesses all the structural features of the Luz-24-like family. Further investigations should shed light to the specific adsorption complex of this phage.

Key words: phage, structure, molecular modeling, cryo-EM

This work was supported by RFBR # 19-14-00605 (cryo-EM data obtaining) and RSF #18-41-06001 (cryo-EM data processing). The authors would like to thank Sergey Nazarov for his helpful advice on sample preparation and data processing. The authors acknowledge the support and the use of resources of the Resource Center for Probe and Electron Microscopy at the NRC "Kurchatov Institute".

P-32

http://dx.doi.org/10.21103/IJBM.9.Suppl_1.P32

Viral chaperonins – new and intriguing group

Olga S. Sokolova¹, Tatiana Stanishneva-Konovalova¹, Wang Xi², Olga Shaburova³, Lidia P. Kurochkina¹

¹Lomonosov Moscow State University, Moscow, Russia; ²MSU-BIT University, Shenzhen, China; ³Mechnikov Research Institute of Vaccines and Sera, Moscow, Russia

Background: Chaperones can bind nascent or misfolded proteins and assist them in properly attaining their functional conformations to maintain the cellular protein homeostasis (Skjærven et al., 2015). According to gene family and structure, chaperonins are classified in two distantly related structural groups: Group I, found in bacteria and eukaryotic organelles, and Group II, expressed in Archaea and in eukaryotic cytosol.

Recently, putative GroEL-like chaperonins have been predicted in viruses of bacteria (bacteriophages). We have obtained, and characterized by various methods, including cryo-EM, two of the members of this group of proteins: gp (gene product) 146 from bacteriophage EL *Pseudomonas aeruginosa* (Kurochkina et al., 2012) and gp246 from bacteriophage OBP *Pseudomonas fluorescens* (Semenyuk et al., 2016).

All viral chaperonins are strikingly different in their architecture. While EL chaperonin acts as a double-ring structure, separating into two closed rings only in ADP-bound form (Molugu et al., 2016), the recombinant OBP chaperonin represents a single heptameric ring. In this form, it can adopt various conformational states, representing different steps in its ATPase cycle. It is not excluded that the OBP chaperonin acts as a heptamer, which is consistent with previous findings that the single-ring mutant of GroEL represents an independent folding unit (Erbse et al., 1999; Chatellier et al., 2000).

Most recently described by us the new viral chaperonin, gp228 from bacteriophage AR9 *Bacillus subtilis*, was investigated by single particle EM. To our surprise, it seems to possess the structural features of both, OBP and EL, viral chaperonins. The AR9 chaperonin particles were distributed into two subpopulations, representing open single-ring and closed double-ring structures. These features may suggest the new mechanism of viral chaperonins functioning.

Conclusion: Unique and diverse structural and functional features of viral chaperonins imply that they might be considered as the new group.

Key Words: single particle cryo-electron microscopy, structure, viral chaperonin

This work was supported by RFBR grants (19-04-00605 to O.S.S.) and (18-04-01281 to L.P.K.).

APPLICATIONS OF CRYO-EM IN MEDICINE

P-33

http://dx.doi.org/10.21103/IJBM.9.Suppl_1.P33

Changes in the structure of amyloid alpha-synuclein aggregates under the action of cinnamic acid derivatives

Kseniya V. Barinova¹, Mariia V. Medvedeva², Aleksandra K. Melnikova², Alexander S. Erofeev³, Peter V. Gorelkin³, Vasily S. Kolmogorov³, Vladimir I. Muronetz^{1,2}

¹Belozersky Institute of Physico-Chemical Biology, Lomonosov Moscow State University, Moscow, Russia; ²Faculty of Bioengineering and Bioinformatics, Lomonosov Moscow State University, Moscow, Russia; ³National University of Science and Technology «MISIS», Moscow, Russia

Background: Alpha-synuclein is the main amyloid protein involved in the development of Parkinson's disease and other synucleinopathies. The aim of our work was to investigate the possibility of preventing alpha-synuclein amyloid aggregation using soluble curcumin analogues, known as effective antiaggregants. For this purpose, cinnamic acid derivatives were used as such analogues – ferulic (3-methoxy-4-hydroxycinnamic acid), 3-methoxy-4-acetamidoxycinnamic, and 3,4-dimethoxycinnamic acid (3,4-DMCA).

Methods: Alpha-synuclein amyloid transformation was studied in the presence of different cinnamic acid derivatives by the use of ThT fluorescence, seeding assays, resistance to proteolysis by proteinase K, circular dichroism, scanning ion conductance microscopy, and also in a cellular assay using a neuroblastoma cell line.

Results: Alpha-synuclein monomers are known to form amyloid fibrils in vitro at acidic pH values or at neutral pH values in the presence of the already formed fibrils of this protein, used as seeds. It was shown that the addition of all three compounds prevents the formation of fibrillar structures by alpha-synuclein. The structure of alpha synuclein fibrils formed by incubating protein monomers at pH 4.0 was investigated using scanning ion conductance microscopy. Under these conditions, large aggregates are formed, with a maximum thickness of 2.5 µm and a length of several tens of microns. In the presence of ferulic acid, the aggregates have the spherical shape and their thickness does not exceed 1.2 µm, while their diameter is several microns. In the presence of 3-methoxy-4-acetamidoxycinnamic acid, formed aggregates are slightly larger and their thickness is about 1.5 µm. 3,4-DMCA demonstrated the smallest effect, however, even in this case, the formation of extended amyloid fibrils is prevented.

Conclusion: The results show that soluble cinnamic acid derivatives, which are naturally occurring compounds found in coffee beans and other plant products, can be used to prevent pathological amyloid transformation of alpha-synuclein.

Key Words: (up to 4) alpha-synuclein, cinnamic acid derivatives

This work was supported by the Russian Foundation for Basic research (grant 19-34-80004).

P-34

http://dx.doi.org/10.21103/IJBM.9.Suppl_1.P34

The Regulation of Amyloid Proteins Aggregation by Adjacent domains

Anastasia V. Grizel¹, Anastasiia V. Maitova¹, Andrey Zelinsky¹, Aleksandr A. Rubel¹, Yuri O. Chernoff^{1,2}

¹Staint Petersburg State University, Saint Petersburg, Russia;

²Georgia Institute of Technology, Atlanta, USA

Background: Amyloids – cross-beta fibrous protein polymers. They are associated with a variety of diseases, including Alzheimer's disease (Aβ peptide aggregation).

Almost all amyloidogenic proteins contain additional domains that regulate their aggregation. Despite the important role of domains adjacent to amyloidogenic regions in the regulation of their properties, the mechanism of their effect on the aggregation has not been well studied.

Methods: We have carried out a comparative analysis of the amyloids formation by proteins containing the predicted amyloidogenic regions and their fragments consisting only of amyloidogenic sequences. The obtained results have compared with data on the structures of domains adjacent to amyloidogenic regions. Moreover, the effect of various sequences (structured (fluorescent proteins)), unstructured (the M domain of the yeast Sup35 protein (Sup35M)), amyloidogenic (Sup35 N domain (Sup35N)) on Aβ aggregation is studied. We use a special yeast screening model, SDD-AGE, fluorescence microscopy and electron microscopy (C-DAG).

Results: We tested the ability NF-YC protein form amyloid aggregates. The full-length NF-YC does not form amyloid aggregates, while the amyloidogenic fragment aggregates. The crystal structure of NF-YC shows the amyloidogenic region adjoins the alpha-helical domain, which prevents the formation of amyloid aggregates.

Amyloid aggregation leads to disruption of the functioning of adjacent domains. The Aβ aggregation in the Aβ-eYFP leads to a drastic decrease in eYFP fluorescence. The effect depends on the fluorescent protein type (eCFP or eYFP) and on the level of protein production.

The Aβ fusion to prion domain of the Sup35 protein (Sup35N-Aβ) promotes its aggregation and allows to aggregate under conditions where Sup35 does not aggregate. However, the addition of sequences to both sides of the Aβ (Sup35N-Aβ-YFP) inhibits formation of amyloid aggregates, leading to the formation of non-amyloid-type assemblies instead (biocondensates). Introduction of the linker (Sup35M) between Aβ and YFP (Sup35N-Aβ-Sup35M-YFP) restores its ability to amyloid aggregation.

Conclusion: Thus, mode of amyloid regions aggregation depends on the nature and location of adjacent sequences. We hypothesize the proximity to large structured domains disrupts amyloid formation aggregation due to steric hindrance, and in some case, promotes formation of alternative assemblies - bicondensates.

Key words: Amyloids, biocondensates, Aβ, Sup35

This work was supported by grant 18-74-00041 from RSF. The authors acknowledge the SPbSU Resource Centers "Chromas", "Molecular and Cell Technologies" and "Biobank" for technical support.

P-35

http://dx.doi.org/10.21103/IJBM.9.Suppl_1.P35

Unusual spiral structures, formed by glycosylated casein in the presence of thioflavin T

Vladimir I. Muronetz^{1,2}, Ivan A. Zanyatkin¹, Yulia Y. Stroylova^{1,2}

¹Belozersky Institute of Physico-Chemical Biology, Lomonosov Moscow State University, Moscow, Russia; ²Faculty of Bioengineering and Bioinformatics, Lomonosov Moscow State University, Moscow, Russia

Background: Information about the stimulation by glycation of the amyloid transformation of proteins, including beta-casein, is not well defined. On the one hand, it is possible to detect signs characteristic of amyloid structures (primarily changes in the fluorescence of thioflavin T (ThT) by various indirect methods, and on the other hand, using direct methods, primarily electron microscopy, it is not possible to reveal characteristic beta-casein amyloid fibrils. In the present work, we investigated the thermal aggregation of glycosylated beta-casein, paying particular attention to the effect of ThT on the formation of various aggregates, including unusual spiral structures, first discovered in this work.

Methods: Glycosylated beta-casein transformation was studied by the use of ThT fluorescence, fluorescence microscopy and transmission electron microscopy.

Results: This study reports an appearance of unusual spiral-like structures in aggregates formed by glycosylated beta-casein in the presence of ThT. Different incubation conditions – glycation agent, temperature, pH, incubation time and concentration of protein and modifier were characterized, but only glycation by 0.2 M glucose for 2 days at 37°C leads to formation of spiral structures. The beta-casein content of these structures was confirmed by ninhydrin reaction, as well as immunohistochemical staining of spiral aggregates. Interaction of glycosylated beta-casein with ThT leads to a 3.5-fold increase in the intensity of its fluorescence, which is about 2 times less than for dye, bound to beta-sheet structures of amyloid proteins. ThT affects the size of the particles formed by glycosylated beta-casein and also stimulates heat-induced aggregation not only for glucose modification but also with a relatively rapid modification by methylglyoxal. Reduction with sodium cyanoborohydride has no significant effect on the ability of ThT to interact with beta-casein and alter its properties.

Conclusion: The results suggest that such interactions of ThT molecule with glycosylated proteins should be taken into account while using it as an indicator for amyloid structures and as a potential agent for prevention and treatment of amyloidosis.

Key Words: beta-casein, glycation, thioflavin T, amyloid structure

This work was supported by the Russian Science Foundation (project No. 16-14-10027).

P-36

http://dx.doi.org/10.21103/IJBM.9.Suppl_1.P36

HBc4M2e virus-like particles for influenza A vaccine development: a CryoEM study

Alexey V. Shvetsov^{1,2}, Evgeny B. Pichkur^{1,3,5}, Tatiana A. Shtam¹, Vladimir V. Egorov^{1,4}, Liudmila M. Tsybalova⁴, Liudmila A. Stepanova⁴, Aram A. Shaldzhyan^{1,4}, Yana A. Zabrodskaya^{1,2,4}

¹NRC «Kurchatov Institute» - PNPI, Gatchina, Russia; ²Peter the Great St. Petersburg Polytechnic University, Saint-Petersburg, Russia; ³NRC «Kurchatov Institute», Moscow, Russia; ⁴Smorodintsev Research Institute of Influenza, Saint-Petersburg, Russia; ⁵FSRC "Crystallography and Photonics", Moscow, Russia

Background: Currently, various virus-like particles (VLPs) are widely used in antiviral vaccines design, including Hepatitis B virus core antigen (HBc)-based VLPs (Blokina et al. 2013 doi:10.1016/j.virol.2012.09.014). In this work, a structure of HBc-based VLP with the antigenic insert corresponding to the highly conserved region of the M2E protein antigen of the influenza (fourfold repetition) was characterized. This study is essential for optimization of antigenic insertion sequence and increasing the effectiveness of an existing universal flu vaccine.

Methods: Cryo-EM data was collected using cryo-TEM Krios (Thermo-Fisher, USA) at 300kV using DED Falcon II. Dataset was processed using Relion (Scheres et al. 2012 doi:10.1016/j.jsb.2012.09.006, Scheres et al. 2012 doi:10.1016/j.jmb.2011.11.010) and CisTEM (Grant et al. 2018 doi:10.7554/elife.35383). Refinement of the full-atom structure of electron density maps was carried out using the Phenix (Adams et al. 2010 doi:10.1107/S0907444909052925, Grant et al. 2018 doi:10.7554/elife.35383) and Gromacs (Abraham et al. 2015 doi:10.1016/j.softx.2015.06.001) software packages using the Gromacs densit module (Igaev et al. 2019 doi:10.7554/elife.43542).

Results: It was found that HBc4M2E VLPs have icosahedral symmetry and, like HBc VLPs, can form structures with symmetry T = 3 and T = 4 (180 monomers and 240 monomers, respectively). It was noteworthy that, in contrast to HBc VLPs in which particles with T = 4 symmetry predominate (about 80%), particles with T = 3 symmetry (about 70%) predominate in HBc4M2E VLPs. In this case a fragment of M2E repeats situated in the HBc antigenic loop are located on the outer surface of the VLP.

Conclusion: Thus, as a result of CryoEM-based study, the structures peculiar to virus-like particles carrying the antigen of influenza A virus were characterized. Results obtained allow us to optimize number of M2E repetitions and primary structure of HBc antigenic insert for further universal flu vaccine development.

Key words: vaccine design, structure, cryo-EM, virus-like particles.

This work was supported by grant #19-74-20146 by RSCF. The authors acknowledge the support and the use of resources of the Resource Center for Probe and Electron Microscopy at the NRC "Kurchatov Institute". The authors acknowledge the support and the use of computing resources of the Federal Collective Usage Center "Complex for Simulation and Data Processing for Mega-Science Facilities."

P-37

http://dx.doi.org/10.21103/IJBM.9.Suppl_1.P37

Ultrastructural differential-diagnostic criteria for renal oncocytoma and chromophobe renal cell carcinoma

Elena Smirnova, Irina Bukaeva, Vera Delektorskaya, Svetlana Bezhanova, Alena Puchkova

N. N. Blokhin Russian Cancer Research Center, Ministry of Health of Russia, Moscow, Russia

Background: The differential diagnosis between renal oncocytoma (RO) and chromophobe renal cell carcinoma (chRCC) is clinically significant because of their different biological behavior: the former widely accepted as a benign neoplasm and the latter largely considered as malignant tumor with potential for metastatic spread. The light microscopy differentiation of RO and chRCC may be problematic due to the overlapping morphology among these neoplasms and further investigations are needed to define the correct diagnosis. The aim of this study was to investigate the ultrastructural peculiarities of RO and chRCC and to examine the value of electron microscopy in differentiating between these neoplasms.

Methods: Fifteen histological confirmed cases of RO and 16 cases of chRCC were examined by electron microscopy. Ultrathin sections were used for observation under a JEM-1200EX (II) transmission electron microscopy.

Results: Ultrastructurally, RO consisted of large clear cells. Nuclei were generally round with smooth margin. Chromatin was finely dispersed, the nucleoli were predominantly centrally located. The cytoplasm was densely packed with numerous mitochondria with lamellar cristae. ChRCC consisted of solid growth pattern of polygonal cells with prominent cell membrane and separated by thin-walled blood vessels. The tumor cell nuclei were polygonal, often with invaginations. Small clumps of condensed chromatin were detected. In the cytoplasm large amounts of glycogen were observed. Mitochondria were polymorphic, showing tubulo-vesicular cristae, part of those were ring-shaped.

Tumor cells of chRCC showed unique feature such as presence of numerous cytoplasmic microvesicles along with mitochondria displaying tubulo-vesicular cristae.

Conclusion: Ultrastructural examination of mitochondria is the helpful approach in the diagnosis of RO and chRCC: RO showed mitochondria with lamellar cristae while chRCC exhibited mitochondria with tubulo-vesicular cristae. Thus, electron microscopy provides the important information for the differential diagnosis between RO and chRCC, for the estimation of grade malignancy and also for the choice of the appropriate therapy of these tumors.

Key words: oncocytoma, chromophobe renal cell carcinoma, electron microscopy.

P-38

http://dx.doi.org/10.21103/IJBM.9.Suppl_1.P38

Comparative Study of the Structure of Amyloid Fibrils Formed From Lysozyme and Beta-2-microglobulin

Anna I. Sulatskaya¹, Maksim I. Sulatsky¹, Eugene B. Pichkur², Irina M. Kuznetsova¹, Konstantin K. Turoverov^{1,3}

¹Institute of Cytology of the Russian Academy of Science, St. Petersburg, Russia; ²National Research Center «Kurchatov Institute», Moscow, Russia; ³Peter the Great St. Petersburg Polytechnic University, St. Petersburg, Russia

Background: The accumulation of amyloid fibrils in tissues and organs is a marker of a large number of diseases, such as Alzheimer's, Parkinson's, prion diseases, etc. Recent studies showed that the structure of these protein aggregates can affect their cytotoxicity. The aim of this work was a comparative study of the fibrils formed from lysozyme

and beta-2-microglobulin, which are the cause of systemic lysozyme and hemodialysis amyloidosis, respectively.

Methods: We used a wide range of physicochemical approaches: cryo-electron microscopy to visualize tested objects, a number of spectroscopic approaches to study photophysical properties and secondary structure of aggregates, as well as absorption, steady-state and time-resolved fluorescence spectroscopy to characterize their interaction with a specific fluorescent probe thioflavin T. Tested solutions were prepared by equilibrium microdialysis technique.

Results: We showed that amyloids formed from lysozyme and beta-2-microglobulin are unbranched fibers up to 1000 nm long. Lysozyme fibrils are thinner and tend to laterally interact with each other to form beams. Evaluation of the samples secondary structure indicated a lower proportion of beta-sheet structure (forming the core of the fibrils), and a greater proportion of disordered structure (which can participate in the interaction of fibrils with each other) for lysozyme amyloids. Furthermore, we found mode of thioflavin T binding to lysozyme fibrils (which is absent in beta-2-microglobulin fibrils) that according to earlier hypotheses is due to the interaction of the dye with fibrillar clots.

Conclusion: Our results indicate that despite the similar morphology of amyloids formed from lysozyme and beta-2-microglobulin, the secondary structure of these fibers differs markedly. Observed features of lysozyme fibrils structure can cause their tendency to interact with each other and form clusters, which can increase their stability and resistance to the effects of various external factors, such as proteolytic degradation or chaperones, due to the reduced availability of some fibers areas inside the bundle. The results of the work can be used for further studies aimed to identifying the relationship between the structure of amyloids and their cytotoxicity.

Key words: lysozyme, beta-2-microglobulin, amyloid fibrils, structural features.

This work was supported by grant from Russian Science Foundation No. 18-74-10100. Work of M. Sulatsky was awarded by the RF President Fellowship No. SP-3291.2019.4 (studies by the time-resolved spectroscopy).

NEW METHODS OF SAMPLE PREPARATION AND DATA PROCESSING FOR CRYO-ELECTRON MICROSCOPY

P-39

http://dx.doi.org/10.21103/IJBM.9.Suppl_1.P39

Novel Perspectives for CLEM Techniques in Multiparametric Morphology Protocols

Oleg V. Gradov

N.N. Semenov Institute of Chemical Physics, Russian Academy of Sciences, Moscow, Russia

Background: It is well known that CLEM techniques are very informative SEM strategies and approaches based on the fluorescence dyes and pigments as labels and electron microscopy contrast agents in some cases. Despite this fact, the general problem is the impossibility of target-label detection of most physical properties of cells or tissues, which can be visualized using different techniques of standard optical microscopy, because some most important optical microscopy techniques (such as polarizing microscopy, interference-phase contrast, DIC, etc.) and in situ electron microscopy techniques

(environmental scanning electron microscopies with different gaseous atmospheres, ballistic electron microscopy, 4D strobe-electron microscopy, etc.) have not been combined within the CLEM's ideology. In the framework of this problem, our group joined the initiative R&D program on correlated light and electron microscopy development. Our initiative mission was previously focused on the development of databases and knowledge bases for annotations of the possible CLEM approaches without a fluorescence labeling (in situ using ESEM-like systems and in cryo-mode).

Methods: Some novel techniques of electron microscopy for biomedical and physicochemical applications were developed using TRIZ database background and novel techniques of combinatorial rapid prototyping and optimization (know how). For example, it is possible to create some exotic CLEM-microscopes, such as: Laser Holographic CLEM; Second-Harmonic Imaging CLEM (SHI-CLEM); Interference Reflection CLEM (IRM-CLEM); CLEM Microinterferometry using Linnik Interferometer (without chromatic dispersion or other optical aberrations); Single Plane Illumination CLEM (SPIM-CLEM); Nomarski or Pluto Differential Interference Contrast CLEMs (DIC-CLEMs); Phase Contrast and Anoptral Phase Contrast CLEM; Diffraction Imaging CLEM (DICLEM); Rheinberg Illumination CLEM; Hoffmann's Modulation Contrast CLEM; Photo-Activated Localization CLEM (PAL-CLEM or FPALCLEM); Total Internal Reflection Fluorescence CLEM (TIRF-CLEM); Multiplane/Multifocal Plane CLEM (CLEMUM).

Results: In our work the database of such not implemented yet, but rather possible and computed (in our program) variants is described. Some of them were realized in hardware and some of them have a technical documentation pull providing prerequisites for multiphysical (COMSOL MULTIPHYSICS assisted) modeling within CAD-CAM-CAE approaches. Among the conventional staining techniques, it is possible to apply the dispersion staining methods in CLEM (both for electron microscopy and for optical one).

Conclusion: Novel techniques for correlation light and electron microscopy (CLEM) are proposed and annotated in this brief communication.

Key Words: CLEM, ESEM, CAD-CAM-CAE, MULTIPHYSICS.

This work was supported by FASO (project 0082-2018-0006, registration code AAAA-A18-118020890097-1).

P-40

http://dx.doi.org/10.21103/IJBM.9.Suppl_1.P40

Computational evaluation of binding of heme-focused library to cholesterol-metabolizing P450 enzymes from *Mycobacterium tuberculosis*

Egor Marin¹, Sergey Bukhdruker¹, Natallia Strushkevich², Valentin Borshchevskiy¹

¹Laboratory for Advanced Studies of Membrane Proteins, Moscow Institute of Physics and Technology, Moscow, Russia;

²Institute of Bioorganic Chemistry, National Academy of Sciences of Belarus, Minsk, Belarus

Background: Tuberculosis (TB), caused by pathogenic bacteria *Mycobacterium tuberculosis* (MTb), is known to be among top-10 causes of death worldwide. In 2019, WHO mentioned drug-resistance with special focus on drug-resistant TB as one of the top-10 threats to the global health. Hence, there is need for novel antimycobacterial drugs.

Methods: Recently, structures of several P450 enzymes from MTb CYP125 and CYP142), capable to conversion of cholest-4-en-3-one to its 25-26-dihydroxy product, have been determined. They are also known to be important for bacterial growth in vitro. Current work is focused on structure-based drug design (SBDD) targeting these enzymes. Using available structures and open data, we analyze the ability of existing computational algorithms to predict binding of fragment-like heterocyclic compounds from experimentally tested library to the enzyme.

Results: We find that apo structures of all three enzymes have the most promising capabilities in terms of both overall discriminating ability (ROC AUC) and top-10% enrichment.

Conclusion: Obtained results establish a blueprint for both structure-based and fragment-based drug design of novel therapeutics against Mycobacterium tuberculosis.

Key Words: Mycobacterium tuberculosis, structure-based drug design

This work was supported by Belarusian Republican Foundation for Fundamental Research X18P-098 and Russian Science Foundation, grant no. 16-15-00309.

P-41

http://dx.doi.org/10.21103/IJBM.9.Suppl_1.P41

Cryo-electron tomography and 3D analysis of detonation nanodiamonds hydrosols

Alexey A. Mikhutkin¹, Roman A. Kamyshinsky^{1,2}, Nikita M. Kuznetsov¹, Sergey N. Chvalun¹, Alexander L. Vasiliev^{1,2}

¹National Research Center "Kurchatov Institute", Moscow, Russia;

²Shubnikov Institute of Crystallography of FSRC "Crystallography and Photonics" RAS, Moscow, Russia

Background: Hydrosols of nanodiamonds prepared from detonation synthesis of carbon-containing explosives find applications in biomedicine, development of novel liquid heat carriers and magnetic liquids. Thus, study of their rheological properties in various liquid media is of great importance. Two unusual rheological features of detonation nanodiamonds (DNDs) hydrosols have been recently revealed: the sharp increase in viscosity and the phase sol-gel transition at a relatively low filler concentration. These features have been explained using the model based on network formation from the chains of faceted DND particles linked together due to the electrostatic interaction of the facets. The 3D spatial distribution, connectivity and agglomeration of the DND particles together with fractal analysis can explain the rheological properties of the hydrosols under the study.

Methods: The specimens were hydrosols of disaggregated DNDs with positive and negative electrokinetic ζ -potential in the concentration range between 1 and 7 wt%. Cryo-Electron Tomography on Titan Krios 60-300 TEM/STEM (FEI, USA) was used for 3D study of DNDs hydrosols at nano- and microscale.

Results: The 3D models of positive and negative ζ -potential DNDs were obtained (example is shown in Fig. 1) and the 3D spatial distribution of DNDs was revealed. It demonstrates the formation of extended fractal structures and chains formed by individual faceted nanodiamond particles. The skeletonization procedure was applied in order to understand the connectivity of objects and percolation. In case of DNDs with positive ζ -potential tomography data demonstrate the formation of a

percolation network. However, such network does not form in hydrosols of DNDs with negative ζ -potential. This explains the differences in the rheological behavior at low concentrations of samples with different sign of ζ -potential. The 2D and 3D fractal dimensions were calculated for the mass-fractal and fractal surface. The fractal dimensions, which were estimated from the cryo-electron tomography, are in good correlation with the results of small angle X-ray scattering.

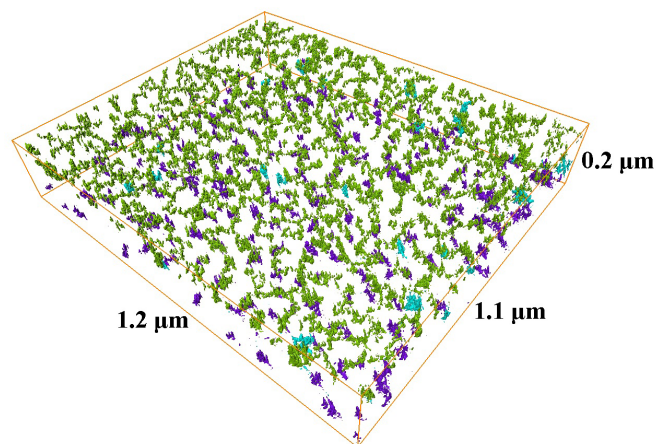


Fig. 1. Cryo-electron tomography 3D model for 1 wt% nanodiamonds hydrosol with positive ζ -potential.

Conclusion: The results of 3D reconstruction and analysis based on cryo-electron tomography data allow to explain observed features of the rheological behavior associated with DNDs agglomeration and chain formation.

Key words: 3D reconstruction and analysis, cryo-electron tomography, nanodiamonds hydrosols, fractal analysis

The detonation nanodiamonds hydrosols were kindly provided by Prof. A. Ya. Vul' and coworkers from Laboratory Physics for Cluster Structures of Ioffe Institute. This work was partially supported by Russian Foundation for Basic Researches, project 18-29-19117 mk.

COMPLEX AND EMERGING TECHNIQUES IN STRUCTURAL BIOLOGY

P-42

http://dx.doi.org/10.21103/IJBM.9.Suppl_1.P42

DSC-investigations of lipid's membrane that imitated of the animal's biomembrane under biological active substances actions

Olga M. Alekseeva¹, Anna V. Kremetsova¹, Aleksey V. Krivandin¹, Yury A. Kim²

¹Emanuel Institute of Biochemical Physics, Russian Academy of Sciences; ²Institute of Cell Biophysics, Russian Academy of Sciences

Background: To investigate the effect of biological active substances (BAS) on the structural organization of animal biomembranes, DSC (adiabatic differential scanning microcalorimetry) and SAXS (small-angle X-ray scattering) methods may be used. The DSC method of melting individual synthetic phospholipids, which are formed into multilamellar liposomes, demonstrates the organization manner of phospholipid microdomains. Multilamellar liposomes are a simple and stable model that imitates organelle membranes and their location in regards to other organelles or the outer

cellular membrane. Using the SAXS method allows to measure the type of bilayer packing in multilamellar liposomes, which contain a mix of natural phospholipids, and the thickness of this bilayer.

Methods: The solutions and suspensions of BAS: melamine salt of bis (oximethyl) phosphinic acid (Melafen) and β -4-oxy-(3,5-ditretbutyl-4-oxiphenyl)potassium propionate (Fenozan) and its hydrophilic and hydrophobic derivatives, were prepared step by step by mixing a solution of ethanol-aqua concentrated samples of BAS. The emulsions of phospholipid multilamellar liposomes were formed from dimyristoilphosphatidylcholine (DMPC) or from egg lecithin. The formation was conducted from thin films, when the DMPC- chlorophorm solution was dried under argon. And after that, using the layer-by-layer hydration method, with the temperature being higher than that for lipid phase transition, many bilayers formed multilamellar liposomes.

Results: Microcalorimetry research identified one peak of structural thermo-induced transition into microdomain organization in membranes, throughout the whole thickness of multilamellar liposomes. The influence of biological active substances - melamine salt of bis (oximethyl) phosphinic acid (Melafen) and β -4-oxy-(3,5-ditretbutyl-4-oxiphenyl)potassium propionate (Fenozan) and its hydrophilic and hydrophobic derivatives, greatly changed the thermodynamic parameters of DMPC liposomes. That indicated the reorganizations of lipid microdomains in membranes. But, using the SAXS method, it has been shown that the hydrophilic substance Melafen does not change of bilayers thickness and the order of their packing in multilamellar liposomes. For these investigations of bilayer thickness and the order of bilayer packing in multilamellar liposomes, a mix of natural lipids – egg lecithin – was used.

Conclusion: These liposomes were formed by a similar method, as for DMPC liposomes were. We can confirm that Melafen and Fenozan's influence on model membranes organization differs and had several variations on different membrane organization levels. These facts may be used for further understanding of the lipid's role in response of the animal cellular biomembrane to the impact of exogenous substances.

Key Words: phospholipids, multilamellar liposomes, biology active substances, DSC

P-43

http://dx.doi.org/10.21103/IJBM.9.Suppl_1.P43

Approximating protein alpha-helices with cylinders for free electron lasers diffraction experiments

Grigory A. Armeev¹, Mikhail A. Lozhnikov², Valery N. Novoseletsky¹, Aleksandr V. Kudriavtsev¹, Alexey K. Shaytan¹, Georgy M. Kobelkov², Konstantin V. Shaitan¹

¹Faculty of Biology, Lomonosov Moscow State University, Moscow, Russia; ²Faculty of Mathematics and Mechanics, Lomonosov Moscow State University, Moscow, Russia

Background: Free electron lasers open up new exciting possibilities for protein structure studies. Extremely high brilliance allows obtaining diffractograms from microcrystals, single particles (such as viruses) and, theoretically, even protein molecules. However, the analysis of these kind of data is significantly hampered by a small number of scattered photons,

as well as the random orientation of the particles in the X-ray beam. For this reason, it is necessary to develop new approaches to the analysis of experimental data from such experiments. Here, we paid attention to the possibility of coarsening protein alpha helices models to simplify such analysis.

Methods: To calculate the diffractograms from electron density maps of protein alpha helices and model cylinders, we used the Condor software. Model experiments were carried out under conditions similar to those in setup for measuring diffraction from single particles in the European XFEL (6A wavelength, 500 nm focus, the distance to the detector - 70 cm and 10 cm for a wide angle, the detector is 20x20 cm). The electron density maps of protein alpha helices were calculated using the Chimera software (1 Å resolution). Model electron density of cylinders was further smoothed with the Gaussian filter with a 3 Å core.

Results: The obtained scattering patterns of model cylinders on small-angles are very similar to the scattering patterns of alpha-helices, which changes upon going to large scattering angles. The amino acid composition of alpha helices affects the character of diffraction patterns, which can be accounted for by selecting the effective radius of the model cylinders.

Conclusion: We have shown that protein alpha-helices can be described by cylindrical models with an effective radius, depending on the amino acid composition. These results can be used in the future to build simple geometric models that satisfy the experimental diffractograms for coarse interpretation of protein structures.

Key Words: X-ray laser, diffraction pattern, alpha-helices

This work was supported by the Russian Foundation for Basic Research No. 18-02-40010.

P-44

http://dx.doi.org/10.21103/IJBM.9.Suppl_1.P44

Dimer structure of highly thermostable archaeal beta-galactosidase revealed by Cryo-EM

Alexander A. Cheblov¹, Evgeny B. Pichkur^{1,2,4}, Yuri V. Kil², Vladimir R. Sergeev^{2,3}, Georgy N. Rychkov^{2,3}

¹Petersburg Nuclear Physics Institute named by B.P.Konstantinov of National Research Center "Kurchatov Institute", Gatchina, Russia; ²National Research Center "Kurchatov Institute", Moscow, Russia; ³Peter the Great Saint-Petersburg Polytechnic University, St. Petersburg, Russia; ⁴FSRC "Crystallography and Photonics", Moscow, Russia

Background: Studies on beta-galactosidases (EC3.2.1.23) are of a great value for the optimization of industry production of low-lactose or lactose-free dairy products. A new 975 amino acid Da- β -gal (proposed to be a GH35 family member) from hyperthermophilic archaeon *Desulfurococcus amylolyticus* possesses high thermoactivity and thermal stability at temperatures closed to 100°C.

Methods: Negative staining TEM with 1% uranyl acetate was performed for sample characterization prior to the cryo-EM studies. Preliminary Cryo-EM dataset was collected using Titan Krios (Thermo-Fisher, USA) equipped with the direct electron detector Falcon II at 300kV accelerating voltage. Movie stacks were preprocessed using Warp. All further processing steps were performed in CryoSPARC and Relion 3.0. Constructed full-atom model of dimer formed by similar mesophilic beta-galactosidase from *Trichoderma reesei* (Tr- β -gal), PDB entry

3OGV, was refined by molecular dynamics (MD) simulations in explicit water box with periodic boundary conditions in Amber16 (ff14SB, TIP3P, PME, 1 atm, 300K, 100 ns).

Results: The Da- β -gal enzyme, expressed in *Escherichia coli* cells and purified to homogeneity by column chromatographies, was subjected to negative contrast microscopy and Cryo-EM. Analysis of electron density distributions in collected set of 30K appropriately classified individual particle images allowed us to solve the structure of the enzyme at 7 Å resolution. The symmetry of obtained structure has revealed that in utilized buffer conditions the enzyme exists as a dimeric form. MD simulations of Tr- β -gal hypothetical dimer have shown stability of the complex along 100 ns trajectory. As estimated from the model the protomer of Tr- β -gal buries about 7.5% of solvent accessible surface area into dimer interface.

Conclusion: The preliminary CryoEM data in concert with molecular modeling identifies dimeric quaternary structure of a 111-kDa Da- β -gal that can be assumed as a structural basis for high temperature stability of the enzyme.

Key words: beta-galactosidase, protein 3D structure, thermostable enzymes, cryo-EM

This work was supported by the Russian Science Foundation under grant 19-74-20146. The authors acknowledge the support and the use of resources of the Resource Center for Probe and Electron Microscopy at the NRC "Kurchatov Institute".

P-45

http://dx.doi.org/10.21103/IJBM.9.Suppl_1.P45

Structural studies of multispecific Antibody/Antigen complexes by cryo-EM

David Fernandez-Martinez^{1,2}, Eazhisai Kandiah¹, Magali Mathieu², Gordon Leonard¹

¹Structural Biology Group, European Synchrotron Radiation Facility, Grenoble, France; ²Sanofi R&D, IDD, Center de Recherche Vitry-sur-Seine, Vitry-sur-Seine Cedex, France

Background: Multispecific antibodies are artificially engineered molecules designed to bind simultaneously to several (different) antigens. Potential advantages of generating viable multispecific antibodies include the identification of malignant cells coupled with the concurrent recruitment of immune cells and the blocking of complex viral escape mechanisms. The cross-over dual-variable immunoglobulin (CODV-Ig) has been proposed as a universal bispecific therapeutic format. Its unique antigen-binding fragment (Fab) architecture provides pM affinities for ligands, no positional effect in target binding and a stable self-supporting structure. However, the three-dimensional arrangement of the constant and antigen-binding fragments in the CODV-Ig format may play a role in its in vivo effects. To further understand the structure and function of multispecific antibodies based on the CODV-Ig format high-resolution structural information is required. Towards this, we use cryo-electron microscopy (cryo-EM).

Methods: We purified CODV-Ig both in an unbound state and in complex with a single antigen and validated sample quality using SDS-PAGE, Small Angle X-Ray Scattering (SAXS) and negative-stain electron microscopy (NSEM; Tecnai T12 and F20 microscopes at IBS, Grenoble). Data

of sufficient quality for image analysis was obtained using a Titan Krios microscope (ESRF, Grenoble) equipped with a Quantum LS energy filter and K2 Summit direct electron detector.

Results: NSEM of CODV-Ig resulted in low-resolution structural models and suggested a preferential orientation of the antibody under negative-stain conditions. Close-to-optimal vitrification conditions for CODV-Ig and antibody-antigen complexes have been identified. Efforts are in progress to reduce the antibody's propensity to aggregation and aversion to conventional cryo-EM supports. Nevertheless, image processing of both CODV-Ig alone and in complex with antigens suggests very high flexibility and conformational heterogeneity.

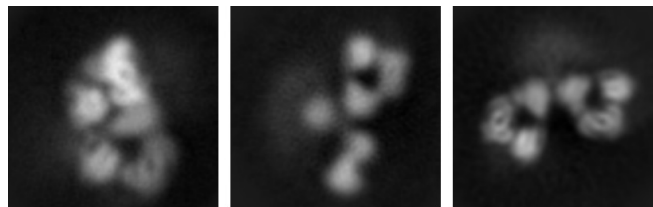


Fig. 1. Representative classes from 2D classifications of an antigen-bound CODV-Ig cryo-EM sample. Ghost-like densities, a result of heterogeneous signal averaging, suggest great conformational heterogeneity.

Conclusion: Particle heterogeneity may require additional data to be collected, in order to have sufficient signal that will lead to well-defined classes. An additional strategy may involve efforts to immobilize the molecules as to obtain fewer and better-defined classes.

Key words: Antibody, Cryo-EM, Image Processing

This work was supported by a doctoral grant under the CIFRE convention.

P-46

http://dx.doi.org/10.21103/IJBM.9.Suppl_1.P46

Role of hexamerin in regulation of pupa development in holometabolous insects

Mária Gondová¹, Lucie Valentová¹, Tibor Füzik¹, Dominik Hřebík¹, Antonín Přidal², Pavel Plevka¹

¹Structural virology, Central European Institute of Technology, Masaryk University, Brno, Czech Republic; ²Department of Zoology, Fishery, Hydrobiology, and Apidology, Faculty of Agronomy, Mendel University, Brno, Czech Republic

Background: Hexamerins are the most abundant proteins in the haemolymph of larvae and pupae of honeybee (*Apis mellifera*) and red flour beetle (*Tribolium castaneum*). They serve as a source of aminoacids for development in non-feeding pupal stage. Furthermore, they act as juvenile hormone-binding proteins, however, the details of this interaction remain unknown.

Methods: We have isolated hexamerins from honeybee and tribolium pupae and solved their structures by X-ray crystallography and cryoelectron microscopy, respectively.

Results: The structure of honeybee and tribolium hexamerins were resolved to 2.0 Å and 3.2 Å resolution, respectively. They are composed of six identical subunits with sizes around 70 kDa and possess 3 2 symmetry. The honeybee hexamerin structure

revealed that each subunit contains an enclosed hydrophobic cavity occupied by one molecule of putative juvenile hormone. Electron density map of tribolium hexamerin was not of sufficient quality to observe juvenile hormone molecules, however we were able to identify hydrophobic cavity similar to that in honeybee hexamerin.

Conclusion: We hypothesize that proteolytic digestion of hexamerin leads to release of juvenile hormone. Therefore, the consumption of hexamerin is linked to level of free juvenile hormone in haemolymph, affecting the development of pupa. Since both, honeybee and tribolium hexamerins possess similar hydrophobic cavities, possibly occupied by juvenile hormone, we propose this mechanism to be conserved among holometabolous insects.

Key Words: hexamerin, juvenile hormone, honeybee, tribolium

P-47

http://dx.doi.org/10.21103/IJBM.9.Suppl_1.P47

Recognition of single particle's diffraction images generated in X-ray free electron laser experiments

Mikhail A. Lozhnikov¹, Georgiy M. Kobelkov¹, Grigoriy A. Armeev², Aleksandr V. Kudriavtsev², Valery N. Novoseletsky², Alexey K. Shaytan², Konstantin V. Shaitan²

¹*Faculty of Mechanics and Mathematics, Lomonosov Moscow State University, Moscow, Russia;* ²*Faculty of Biology, Lomonosov Moscow State University, Moscow, Russia*

Background: X-ray free electron lasers (XFEL) proved to be powerful instruments for solving the problem of structural analysis of biological objects and studying its functional structural dynamics. The combination of huge intensity and short flashing time leads to unique results. On the one hand the molecule tears up under Coulomb's forces caused by the flash. On the other hand the molecule leaves a diffraction image before destruction. XFELs are widely used in traditional X-ray diffraction analysis for the purpose of obtaining the 3D structure of crystals.

Methods: The paper proposes an algorithm for obtaining molecule's 3D structure. Suppose we have a finite set of different molecular structures. The goal of the paper is to obtain the 3D structure by its diffraction image. Each corresponding molecule can be approximated by a number of simple solids like cylinders, spheres, tori. The diffraction images of these solids including a set of them are defined by an explicit formula. Thus, the problem of 3D reconstruction comes to the problem of multi class image classification which is suggested to be solved by means of convolutional neural networks (CNN). CNN is a widely known example of supervised learning i.e. it requires a training dataset with labels. The training dataset is suggested to be generated by means of direct simulation.

Results: The proposed method allows to classify the corresponding molecules into up to 50 disjoint classes. It shows the accuracy about 80% on the testing dataset.

Conclusion: Many interesting biological objects (including alpha helices, viruses, DNA molecules, etc.) can be approximated by means of a combination of solids. This approach allows to solve the problem of obtaining the 3D space structure of the corresponding objects.

Key Words: structural biology, x-ray lasers, image recognition, neural networks

This work was supported by the Russian Foundation for Basic Research No. 18-02-40010.

P-48

http://dx.doi.org/10.21103/IJBM.9.Suppl_1.P48

Injectable self-assembled surfactant-clay hydrogel

Vyacheslav S. Molchanov¹, Marina A. Efremova¹, Tatiana Yu. Kiseleva¹, Anton S. Orekhov², Natalia A. Arkharova³, Olga E. Philippova¹

¹*Lomonosov Moscow State University, Moscow, Russia;* ²*National Research Centre "Kurchatov Institute", Moscow, Russia;* ³*Federal Scientific Research Centre "Crystallography and Photonics", Moscow, Russia*

Background: Soft nanocomposite hydrogels can be based either on polymer network or on self-assembled network of wormlike surfactant micelles (WLMs). To provide additional functionality to the matrix the hydrogels can contain delivery vehicle components, for instance, nanoclay tactoids, which make them very promising for drug delivery and tissue engineering applications.

Injectable systems represent an evergrowing class of nanomaterials possessing a unique combination of physical and chemical properties. For the injection applications, the hydrogels should demonstrate a shear-thinning behavior and a fast recovery of the initial state, when the deformation is no longer applied. Such hydrogels can be used as control delivery systems, since they can be delivered in a minimally invasive manner, because their final form and shape are defined by the space, into which they are injected.

Methods: Cryo electron microscopy experiments were performed to study network structure. To measure the gap between the clay platelets, X-ray diffraction analysis was carried out. The influence of organoclay on the mechanical properties of mixed WLMs of surfactants was studied by rheometry. The oscillation recovery tests were carried out both at small and high stress amplitudes to study breaking and recovery of the nanocomposite WLM network.

Results: The present study is devoted to soft nanocomposite based on network of WLMs composed of biocompatible zwitterionic and anionic surfactants with embedded plate-like bentonite nanoclay particles. It is shown that nanoparticles enhance significantly the rheological properties of WLM hydrogel acting as physical cross-links between micellar chains. It was explained by the formation of micelle-nanoparticle junctions as a result of binding of the WLMs end-caps to the layer of surfactant adsorbed on the particle surface.

The studied network possesses gel-like properties. In particular, its rheological properties demonstrated plateau modulus, low values of loss factor. At the same time, under high deformation, the micellar chains was disrupted, which induced a much more pronounced drop of viscosity than the disruption of physical cross-links in polymer gels. The disrupted micellar chains were completely recovered due to restoration of non-covalent bonds between surfactant molecules within the micelle.

Conclusion: It was demonstrated that the prepared nanocomposite hydrogels possess promising properties for injection applications.

Key words: injectable hydrogel, nanoclay, wormlike micelles

This work was supported by the Russian Science Foundation (project № 17-13-01535).

P-49

http://dx.doi.org/10.21103/IJBM.9.Suppl_1.P49

Determination of relative positions of two helices in two-helical proteins basing on X-ray diffraction data with the use of convolutional neural networks

Valery Novoseletsky, Mikhail Lozhnikov, Grigory Armeev, Alexandr Kudriavtsev, Alexey Shaytan, Georgy Kobelkov, Konstantin Shaitan

Lomonosov Moscow State University, Moscow, Russia

Background: Protein structure determination using X-ray free-electron laser (XFEL) includes analysis and merging a large number of snapshot diffraction patterns. Convolutional neural networks are widely used to solve numerous computer vision problems, e.g. image classification, and can be used for diffraction pattern analysis. But the task of protein structure determination with the use of CNNs only is not yet solved.

Methods: We collected a number of predominantly alpha-helical protein structures from PDB and analyzed their geometry. Relatively straight helices were left unchanged while curved ones were split into helices of smaller length. Finally, 88 two-helical protein structures were selected with the length of helices from 5 to 38 residues (7 to 57Å). For every structure radii, lengths and relative position and orientation of helices were calculated.

Diffraction patterns were calculated by means of straight modeling. Every structure was approximated as a pair of cylinders of given length and radius and then its diffraction image was calculated with the explicit formula:

$$I(\vec{R}) \approx \frac{A_0^2}{R^2} \left| \int_V \exp(-i(\vec{k} - \vec{k}_0)\vec{r}) d\vec{r} \right|^2,$$

where $I(R)$ is intensity generated on the point of detector with radius-vector R , V is the volume of structure, A_0 is an amplitude of w-ray wave, \vec{k}_0 is a vector of initial wave, \vec{k} is a vector of scattered wave.

The obtained collection of diffraction patterns was used to train and test the convolutional neural network (CNN). A number of convolutional layers is used to extract features from input images. Then, a dense layer is used to solve a multi-class classification problem. In order to obtain learnable parameters, we have to solve the minimization problem of the cross-entropy loss function.

Results: Preliminary length and radius of helices with given sequence could be obtained from molecular modeling. Taking this into account, our model demonstrates a possibility to classify helix pairs into up to 50 disjoint classes.

Conclusion: CNNs could be successively used for the purpose of classification of two-helical idealized protein structures. This could be used for preliminary analysis of protein conformation. Our further efforts will be directed towards enlarging the number of classes and expanding our approach to more complex structures.

Key Words: X-ray crystallography, diffraction pattern, alpha-helices, convolutional neural networks

This work was supported by the Russian Foundation for Basic Research No. 18-02-40010.

P-50

http://dx.doi.org/10.21103/IJBM.9.Suppl_1.P50

On the features of X-ray laser diffraction on certain elements of macromolecular structures

Konstantin V. Shaitan

Department of Biology, Lomonosov Moscow State University, Moscow, Russia

Background: The possibility of using free electron X-ray lasers for solving problems of structural biology in single particle experimental mode is discussed. In the first Born approximation analytical expressions for the amplitudes and intensities of X-ray diffraction on cylinders, balls, hemispheres and tori in various combinations and orientations are obtained. The characteristic diffraction patterns from these geometric bodies are analyzed. The modeling of elements of the secondary structure of biopolymers (for example, alpha-helices, characteristic DNA packs, some viruses, etc.) is discussed by a certain set of these geometric bodies with the corresponding parameters.

Methods: As an example (due to space constraints and because of the reason below), we present the solution of the scattering equation in the Born approximation for the amplitude of diffraction on a hemisphere with a uniformly distributed density. Note, that the solution of a similar problem for a sphere (ball) is well known but it is difficult to find the analytical results for hemispheres and many other geometric bodies. The solution for a sphere (ball) can be obtained from the next integral

$$A(\vec{s}) \sim \int_0^r r^2 dr \int_0^\pi J_0(s_{xy} r \sin \theta) \exp[-irs_z \cos \theta] \sin \theta d\theta = \frac{1}{3} (\sin sr - sr \cos sr) \quad (1)$$

The calculation of the integral of type (1) for a hemisphere turns out to be much more complicated. Available reference books give this integral or integrals to which it can be reduced with errors.

Results: We present the correct value of the integral, which is expressed in terms of Bessel function and Lommel function $U_0(x, y)$ of two arguments

$$A(\vec{s}) \sim \rho \int_0^r r^2 dr \int_0^{\pi/2} J_0(s_{xy} r \sin \theta) \exp[-irs_z \cos \theta] \sin \theta d\theta = \frac{1}{3} \{ (\sin sr - sr \cos sr) + i(\cos sr + sr \sin sr - 1 + \frac{s^2 r}{s_{xy}} J_1(s_{xy} r) - 2 \int_0^r r U_0[r(s - s_z), rs_{xy}] dr) \} \quad (2)$$

Here we have introduced the standard notation for the modulus of the scattering vector

$$s = \frac{4\pi}{\lambda} \sin \frac{\theta}{2} = \sqrt{s_x^2 + s_y^2} \quad (3)$$

and introduced the notation sz for the projection of the scattering vector on the axis of symmetry of the hemisphere. Considering the corresponding integrals, one can also obtain a useful relation for Lommel function

$$U_0[\vec{a} - \vec{x}, y] + U_0[\vec{a} + \vec{x}, y] = \cos \vec{a} \cdot \vec{y} J_0(y); \quad x^2 + y^2 = a^2 \quad (4)$$

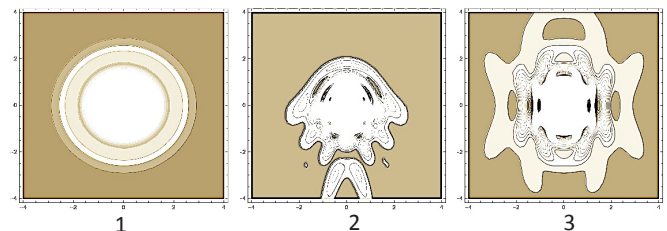


Fig.1. Diffraction on a hemisphere ($r=7$, $\lambda=2$). 1 - the axis of symmetry of the ball is parallel to the incident beam, 2 - is rotated by an angle of 45° , 3 - is perpendicular to the incident beam.

Conclusion: Using (4) it is easy to obtain a formula for the scattering amplitude of a ball made up of two halves with different densities. Fig.1.1 demonstrates the pattern which is typical for uniform ball at any orientation angle as well. But in the case of the hemisphere (and heterogeneous balls) the diffraction patterns form some characteristic features depend on the orientation angles.

Key Words: XFEL, X-ray diffraction, single particle, Bessel and Lommel functions

This work was supported by Russian Foundation for Basic Research (RFBR, 18-02-40010).

Author Index**A**

Agard, David OR-16
 Afanasyev, Pavel OR-12
 Afonina, Zhanna P-13, P-14
 Alekseeva, Olga M. P-42
 Anarbaev, Rashid O. P-21
 Arkharova, Natalia A. P-48
 Armeev, Grigoriy A. OR-19, OR-23,
 P-20, P-43, P-47, P-49
 Ataulakhanov, Fazoil I. P-27
 Atherton, Joseph OR-8

B

Bagrov, Dmitry OR-20, OR-24, P-11
 Barinova, Kseniya V. P-33
 Basalova, Nataliya A. P-24
 Bass, Mikhail V. P-20
 Baymukhametov, Timur N. OR-21,
 P-13, P-14
 Belousova, Ekaterina A. P-16
 Benešik, Martin P-30
 Berkut, Atonina A. OR-1
 Bezhanova, Svetlana P-37
 Blum, Thorsten B. OR-8
 Bogyo, Matthew OR-12
 Bogdanov, Alexey A. P-10
 Borshchevskiy, Valentin P-4, P-6, P-9,
 P-40
 Boyko, Konstantin M. OR-21
 Bozdaganyan, Marine E. P-11
 Buchta, David OR-10
 Bukhdruker, Sergey P-40
 Bukaeva, Irina P-37
 Bulkley, David OR-16
 Buslaev, Pavel P-2

C

Cheblokov, Alexander A. P-44
 Chen, Wenbo P-12
 Chertkov, Oleg P-23
 Chernoff, Yuri O. P-34
 Cheng, Yifan OR-16
 Chesnokov, Yuri M. OR-21, OR-22,
 P-13, P-14
 Chupin, Vladimir V. P-8
 Chugunov, Anton O. OR-1
 Chvalun, Sergey N. P-41
 Colbasevici, Alexandr P-11
 Cramer, Patrick OR-2

D

da Fonseca, Paula C.A. - OR-12
 Dadinova, Liubov OR-22
 Danilova, Yana P-23
 Delektorskaya, Vera P-37

Dmitriev, Sergey E. P-17
 Dodonova, Svetlana OR-2
 Dulimov, Ruslan OR-24

E

Egorov, Alexey M. P-28, P-29
 Egorov, Vladimir V. P-36
 Efremova, Marina A. P-48
 Efimenko, A.Yu. P-24
 Erofeev, Alexander S. P-33
 Emelyanov, Anton K. P-25
 Evtushenko, Evgeniy OR-20

F

Fedorov, Vladimir OR-5
 Fedotov, Anton Y. P-28
 Feofanov, Alexey P-18, P-23
 Fernandez-Martinez, David P-45
 Fibriansah, Guntur OR-9
 Füzik, Tibor OR-10, P-30, P-46

G

Garaeva, Alisa OR-13
 Garaeva, Luiza A. P-25
 Gati, Cornelius OR-13
 Gavrilov, Gaspar P-25
 Gerasimova, Nadezhda P-18
 Glukhov, Grigory P-3
 Gondová, Mária P-46
 Gordon, Leonard P-45
 Gorelkin, Peter V. P-33
 Gradov, Oleg V. P-39
 Grigorieva, Olga A. P-24
 Grizel, Anastasia V. P-34
 Grishin, Konstantin V. P-28
 Gudimchuk, Nikita B. OR-5, P-27
 Guskov, Albert OR-13
 Gushchin, Ivan P-2
 Gusach, Anastasiia P-4, P-5, P-6

H

Hons, Michael OR-21
 Holzer, Amihai OR-25
 Hrebík, Dominik P-46

I

Ilyinsky, Nickolay P-9
 Ishmukhametov, Aidar A. P-28, P-29

K

Kacher, Julia - P-3
 Kamyshevsky, Roman OR-22, P-7, P-25,
 P-41
 Kandiah, Eaazhisai P-45
 Kasatsky, Pavel OR-4, P-15
 Khorn, Polina A. P-5, P-9
 Kholina, Ekaterina OR-5

Khodyreva, Svetlana N. P-16
 Khven, Irina M. P-19
 Khusainov, Iskander OR-15
 Kil, Yuri V. P-44
 Kim, Yuri A. P-42
 Kiseleva, Tatiana Yu. P-48
 Kireev, Igor I. OR-6
 Kirpichnikov, Mikhail P-18
 Kobelkov, Georgy M. 23, P-43, P-47,
 P-49
 Kolesnikov, Egor S. P-5
 Kolmogorov, Vasily S. P-33
 Konevega, Andrey OR-4, P-15
 Konarev, Petr V. P-29
 Konyushko, Olga I. P-28
 Kostyuchenko, Victor A. OR-9
 Kovalchuk, Michail V. OR-21
 Kovalenko, Ilya B. OR-5
 Kremetsova, Anna V. P-42
 Krivandin, Aleksey V. P-42
 Krupyanskii, Yuri OR-7, P-23
 Kudriavtsev, Aleksandr V. OR-23,
 P-43, P-47, P-49
 Kudrevatykh, Anastasia P-25
 Kudryashev, Mikhail P-12
 Kulbatskii, Dmitrii S. OR-1, P-7
 Kumachova, Tamara K. P-22
 Kurochkina, Lidia OR-11, P-32
 Kutuzov, Mikhail M. P-16
 Kuzmichev, Pavel K. P-8, P-9
 Kuznetsova, Irina M. P-38
 Kuznetsov, Nikita M. P-41

L

Lavrik, Olga I. P-16, P-21
 Lipkin, Alexey V. OR-21
 Loiko, Natalia OR-7, P-23
 Lok, Shee-Mei Lok OR-9
 Lomakin, Ivan B. P-17
 Lozhnikov, Mikhail A. OR-23, P-43,
 P-47, P-49
 Luginina, Aleksandra P-4, P-5, P-6
 Lushchekina, Sofya V. OR-21
 Lyabin, Dmitry N. P-13
 Lyukmanova, Ekaterina N. OR-1, P-7

M

Magali, Mathieu P-45
 Maitova, Anastasiia V. P-34
 Makeeva, Desislava S. P-17
 Maksimova, Elena OR-4
 Maluchenko, Natalya P-18
 Marin, Egor P-40
 Maslov, Ivan P-9
 McIntosh, J. Richard P-27
 Medvedeva, Natalia V. P-26
 Medvedeva, Mariia V. P-33
 Melnikova, Aleksandra K. P-33

Metlev, Mikhail P-19
 Mikhailov, Anatolii E. P-8
 Mikirtumov, Vasiliy I. P-7
 Mikhutkin, Alexey A. P-41
 Minin, Alexander A. P-26
 Miroshnikov, Konstantin P-31
 Mishin, Alexey P-4, P-5, P-6
 Moiseenko, Andrey OR-7, P-23
 Molchanov, Vyacheslav S. P-48
 Moores, Carolyn A. OR-8
 Moor, Nina A. P-21
 Mosslehy, Wageiha P-11
 Mozhaev, Andrey OR-22
 Mukhamedova, Liya OR-10
 Mulkidjanian, Armen Y. P-11
 Muronetz, Vladimir I. P-33, P-35
 Myasnikov, Alexander OR-4, OR-16, P-15
 Myshkin, Mikhail Yu. OR-1

N

Ng, Thiam-Seng OR-9
 Nikishin, Igor OR-24
 Nilson, Anders S. P-30
 Novitskaia, Olga P-2
 Novoseletsky, Valery N. OR-23, P-31, P-43, P-47, P-49
 Novoseletskaya, Ekaterina S. P-24
 Nurdinova, Aizada P-9

O

Olieric, Natacha OR-8
 Orekhov, Anton OR-22, P-48
 Orekhov, Philipp S. OR-5, P-11
 Orlova, Elena OR-17
 Osolodkin, Dmitry I. P-28, P-29
 Osterman, Ilya A. P-15, P-19

P

Paleskava, Alena OR-4, P-15
 Paramonov, Alexander S. OR-1
 Paulino, Cristina OR-13
 Pchelina, Sofia N. P-25
 Peters, Georgy S. P-29
 Petrovskaya, Lada E. P-8
 Philippova, Olga E. P-48
 Pichkur, Evgeny OR-4, OR-11, P-15, P-29, P-31, P-36, P-38, P-44
 Plekhova, Natalia G. OR-18
 Plevka, Pavel OR-10, P-30, P-46
 Popov, Vladimir O. OR-21
 Polikanov, Yury OR-4, P-15, P-19
 Popinako, A.V. P-1

Pozdnyakov, Ilya A. P-10
 Přidal, Antonín P-46
 Prota, Andrea E. OR-8
 Puchkova, Alena P-37
 Pustovalov, Evgeniy V. OR-18

R

Rubel, Aleksandr A. P-34
 Rychkov, Georgy N. P-44

S

Sagaradze, Georgy D. P-24
 Safronova, Nadezhda P-9
 Samygina, Valeriya R. P-29
 Schneidman-Duhovny, Dina OR-25
 Schröder, Gunnar F. OR-14
 Sedov, Anton P-31
 Sejwal, Kushal OR-8
 Semina, Svetlana OR-20
 Semenyuk, Pavel I. OR-11, P-26
 Sergeev, Vladimir R. P-44
 Serebryakova, Marina P-19
 Shaburova, Olga P-32
 Shaldzhyan, Aram A. P-36
 Shaytan, Alexey K. OR-19, OR-23, P-20, P-43, P-47, P-49
 Shaitan, Konstantin V. OR-23, P-11, P-43, P-47, P-49, P-50
 Sharma, Ashwani OR-8
 Shenkarev, Zakhar O. OR-1, P-7
 Shirokov, Vladimir A. P-13
 Shneider, Mikhail P-31
 Shtam, Tatiana A. P-25, P-36
 Shtykova, Eleonora OR-22
 Shvetsov, Alexey V. P-36
 Sikilinda, Nina P-31
 Šiborová, Marta P-30
 Skryabin, Gleb OR-24
 Slotboom, Dirk OR-13
 Smirnova, Elena P-37
 Sokolova, Olga OR-7, OR-11, P-3, P-7, P-23, P-26, P-31, P-32
 Soloviov, Dmitro V. P-8
 Sosnovskaya, Sophia Yu. OR-6
 Stanishneva-Konovalova, Tatiana B. OR-11, P-32
 Steinmetz, Michel O. OR-8
 Stepanova, Liudmila A. P-36
 Stolboushkina, Elena A. P-17
 Strelkova, Olga S. OR-6
 Stroylova, Yulia Y. P-35
 Strushkevich, Natallia P-40
 Studitsky, Vasily P-18
 Sulatskaya, Anna I. P-38

Sulatsky, Maksim I. P-38

T

Tchevkina, Elena OR-24
 Tereshkina, Kseniya OR-7, P-23
 Terterov, Ivan N. P-10
 Travin, Dmitrii Y. P-19
 Tsarev, Andrey V. P-7
 Tsybalova, Liudmila M. P-36
 Tuchinskaya, Kseniya K. P-28
 Turoverov, Konstantin K. P-38

U

Ulyanov, Evgeniy V. P-27
 Usachev, Konstantin OR-15

V

Vakhrusheva, Anna V. OR-23, P-26
 Valentová, Lucie P-46
 Validov, Shamil OR-15
 Vassilevski, Alexander A. OR-1
 Vasiliev, Alexander L. OR-22, P-13, P-14, P-41
 Vasil'eva, Inna A. P-21
 Verlov, Nikolay A. P-25
 Vinogradova, Daria OR-4
 Vinogradov, Dmitrii S. P-27
 Vnukova, Anna OR-20
 Voronkov, Alexander S. P-22
 Vorovitch, Mikhail F. P-28, P-29
 Voskoboynikova, Natalia P-11

W

Ward, Fred P-19
 Watson, Zoe P-19

X

Xi, Wang P-32

Y

Yablokov, Eugene O. P-7
 Yoo, Euna OR-12
 Yusupov, Marat OR-15

Z

Zakirov, Amir N. OR-6
 Zabrodskaya, Yana A. P-36
 Zanyatkin, Ivan A. P-35
 Zharkov, Dmitry O. OR-3
 Zhang, Shuijun OR-9
 Zelinsky, Andrey P-34
 Zhironkina, Oxana A. OR-6